Sample Preparation for Point-of-Care Nucleic Acid Amplification Testing of Bloodborne Viruses

Andrew T. Bender

A dissertation

submitted in partial fulfillment of the

requirements for the degree of

Doctor of Philosophy

University of Washington

2020

Reading Committee:

Jonathan D. Posner, Chair

Jae-Hyun Chung

Paul Drain

Program Authorized to Offer Degree:

Mechanical Engineering

University of Washington

Abstract

Sample Preparation for Point-of-Care Nucleic Acid Amplification Testing of Bloodborne Viruses

Andrew T. Bender

Chair of the Supervisory Committee:

Professor Jonathan D. Posner

Department of Mechanical Engineering

Nucleic acid amplification tests (NAATs) provide high diagnostic accuracy for infectious diseases and quantitative results for monitoring viral infections. The majority of NAATs require complex equipment, cold chain dependent reagents, and skilled technicians to perform tests. This largely confines NAATs to centralized laboratories and can significantly delay appropriate patient care. Low-cost, point-of-care (POC) NAATs are especially needed in low- and middle-income countries (LMICs) for the detection of bloodborne infectious diseases, such as HIV, hepatitis B, hepatitis C, dengue, Zika, and Ebola viruses. The work presented in this dissertation describes novel sample preparation approaches for use in POC diagnostics for bloodborne pathogens. I developed paper-based isotachophoresis (ITP) systems for integrated on-chip detection and specialized nucleic acid purification of DNA and RNA. I also developed chemistries for inactivating endogenous blood RNases and lysing viral envelopes, and I paired these chemistries with ITP for detecting HIV from human serum. My sample preparation methods use low-cost materials and reagents, and ITP uses an electric field to automate nucleic acid purification, reducing manual user steps. Ultimately, I believe this work may be used to develop POC NAATs for bloodborne pathogens in a low-cost format with minimal protocol complexity.

TABLE OF CONTENTS

LIST OF FIGURES

LIST OF TABLES

Chapter 1. INTRODUCTION

1.1 POINT-OF-CARE MOLECULAR DIAGNOSTICS

Propelled by the advent of the polymerase chain reaction (PCR), nucleic acid amplification tests (NATs) have become the gold-standard for the accurate diagnosis of many infectious diseases.[1–3] NAATs have been developed for numerous diseases due to their high diagnostic sensitivity and specificity, rapid time to result, and multiplexing strategies.[4,5] NAATs are also employed by clinicians to quantify the viral load for several infectious diseases (*e.g.* HIV-1, Hepatitis B, Hepatitis C), providing crucial information for evaluating patient treatment plans.[6–8] The majority of NAATs are performed in upper or mid-tier laboratories because they require complex protocols, cold chain dependent reagents, delicate instrumentation, reliable electrical power, qualified laboratory staff, and appropriate infrastructure to host equipment and materials. Laboratory-based NAATs necessitate significant logistics around specimen collection, transport, batched testing, and the return of results to clinicians and patients. In low resource settings, this often results in delayed diagnoses that can negate patient management benefits.[9] The challenges associated with laboratory-based NAATs have prompted the development of simple, affordable, and rapid point-of-care (POC) NAATs that can facilitate diagnosis and treatment in a single clinic visit.[10,11] POC NAATs are especially needed in low resource settings where laboratory testing is limited and rapid testing is crucial for improved treatment (*e.g.* mitigating loss to follow-up which can lead to treatment failure and spread of disease).[12,13]

The World Health Organization developed the ASSURED design criteria (Affordable, Sensitive, Specific, User-friendly, Rapid and robust, Equipment-free, and Delivered) for POC diagnostics that describes the required qualities that adequately address the needs of patients in

developing countries where infectious disease prevalence remains high.[14] Significant challenges remain in the development of POC NAATs that perform sample-to-answer analysis with clinical specimens while meeting the ASSURED criteria. Towards this goal, several POC NAAT platforms are now commercially available including the m-PIMA (Abbott Diagnostics), cobas Liat (Roche Diagnostics), and GeneXpert (Cepheid).[15] These platforms offer a range of diagnostic tests for infectious diseases of global significance including HIV, influenza, and tuberculosis and several have been CLIA-waived.[16–18]

These commercial POC NAATs provide diagnostic results through automating the three operational steps of NATs; namely, sample preparation, nucleic acid amplification, and detection of amplification. These commercial platforms employ mechanical systems for fluidic manipulation and precision heating that increase platform complexity, raising overall testing costs and introducing electrical power demands. The development of low-cost, rapid, and instrument-free POC NAATs for bloodborne viruses has been particularly slow due to the heightened challenge of processing blood samples, which have more extensive sample preparation requirements than most respiratory samples (e.g. saliva, nasal swabs, throat swabs, etc.). Research and innovation are still needed to lower the cost of capital equipment, perform quantitative tests, and reduce the complexity and costs of POC NAATs for bloodborne viruses in low- and middle-income countries (LMICs).

1.2 Sample Preparation Steps for Blood Specimens

A primary roadblock for simplifying POC NAATs for bloodborne viruses is sample preparation, which requires purifying viral nucleic acids from the salts, proteins, cellular debris, and nucleases present in blood.[19] Endogenous blood ribonucleases (RNases) are particularly problematic because they are exceptionally stable enzymes and capable of rapidly degrading free

RNA in blood on the order of seconds.[20,21] Permanently inactivating blood RNases is a challenge because they have been shown to tolerate pH extremes, weak denaturing solutions, and heat denaturation at temperatures up to 90 °C.[22–24] Lysis is necessary to release viral nucleic acids from the viral envelope and nucleocapsid proteins. When targeting an RNA virus, free RNA released during lysis may be degraded if blood RNases are not fully immobilized. Viral nucleic acid in the lysate requires purification to remove inhibitors in the sample that hinder downstream detection assays.

The most widely-used method for sample preparation in NAATs for bloodborne viruses is solid phase extraction (SPE).[25] This technique employs a lysis buffer that fully denatures all proteins present in a blood with high concentrations of chaotropic salts, specifically 4 to 6 M guanidinium chloride or guanidinium thiocyanate.[26] The highly chaotropic conditions lyse open pathogens and inactivate all nucleases present in the sample. The guanidinium-based lysis buffer is paired with a silica column that adsorbs nucleic acids before subsequent elution.[25] SPE adequately protects RNA from degradation and returns a high yield, yet several washing steps and/or buffer exchanges are required to remove guanidinium, phenol, chloroform, and alcohols before downstream assays.[27] For example, a gold standard product for viral RNA extraction is the QIAamp Viral RNA Mini Kit (Qiagen), and it requires 6 manual pipetting steps and 5 centrifugations, totaling 30 minutes to an hour of hands-on time – according to the product handbook. Automation of these processes necessitates centrifuges, pumps, or robotics which requires complicated engineering designs and expensive components.[28] This approach faces a practical barrier to lowering the overall platform costs of molecular testing in blood samples, which has prompted researchers to find new sample preparation approaches for POC use.

1.3 Amplification and Detection of Nucleic Acids

Following extraction of target nucleic acids, laboratory NAATs often use polymerase chain reaction (PCR) to amplify nucleic acids. This technique can be difficult to implement at the point-of-care due to the need for highly purified nucleic acids and energy-intensive thermocycling equipment that typically cannot tolerate the environmental extremes in many resource limited settings (e.g. dust, high humidity, high temperature).[29] In the last two decades, several isothermal nucleic acid amplification methods (*e.g.* iSDA, HDA, LAMP, RPA) have been developed to amplify nucleic acids at a single reaction temperature and are more tolerant to inhibitors than traditional PCR.[30–34] Isothermal amplification has been explored for POC NAATs using simple resistive heaters, water baths, or chemical heaters.[35,36] Recombinase Polymerase Amplification (RPA) is a promising isothermal amplification strategy that is ideal for use in POC NAATs due to its sensitivity (<10 copies/rxn), specificity, speed (<20 minutes), low constant incubation temperature (25–43 °C), tolerance to inhibitors, and reagent stability at ambient temperatures.[37,38] RPA amplicon detection can be performed using either endpoint techniques, such as gel electrophoresis, or by measuring fluorescence in real-time. Fluorescence detection of RPA involves a sequence-specific probe which creates a signal only after hybridizing to the target nucleic acid sequence and being cleaved by an exonuxclease.[33] Real-time fluorescence monitoring of RPA requires moderately complex instrumentation, yet it can provide semi-quantitative information to assess severity of disease infection.[39]

1.4 Isotachophoresis as a Sample Preparation Tool

In this dissertation, I investigate a promising electrokinetic technique called isotachophoresis (ITP) for use in simplifying sample preparation for POC NAATs.

Isotachophoresis (from the Greek, “ísos” meaning “equal” and “takhos” meaning “speed”) is an electrophoretic separation and concentration technique carried out in a discontinuous buffer system. The buffer system is comprised of a high conductivity leading electrolyte (LE) and low conductivity trailing electrolyte (TE). Upon application of a voltage bias across the system, the LE forms the front zone while the TE forms the rear zone. Analytes focus at the interface of the two zones. In most systems, a common counterion is present across all zones to control the pH during electromigration.[40]

The theoretical bases for isotachophoresis were pioneered in the late 1800s and early 1900s by Walther Nernst, Friedrich Kohlrausch, and James Kendall.[41–43] The first analytical use of isotachophoresis (ITP) came in 1953 when L.G. Longsworth separated ionic earth metal species and several organic acids, while coining the terms “leading” and “trailing” electrolytes.[40] After several other advancements in the field, the late 20th century saw a multitude of fundamental studies emerge describing the theory, experimental methodology, and analytical applications that form the foundation of modern ITP research. One prominent study by Petr Boček provided an extensive list of electrophoretic mobilities and dissociation constants measured via capillary ITP.[44] This paper is useful resource for selecting leading and trailing electrolytes with mobilities that bracket the analyte.

In the mid 2000s, Valentina N. Kondratova published the first studies using ITP to isolate nucleic acids from complex samples. Several experimental setups were explored, including ITP through standard agarose gels and cellulose acetate membranes.[45,46] The most successful substrate for ITP reported by this group was a 0.1% agarose gel within 2 – 3 mm diameter plastic tubing.[47] The plastic tubing simplifies the excision of separated DNA within the gel as the tubing can easily be cut. This technique handles a large volume of sample (0.5 – 1 mL) with a finite injection ITP

system and focuses 93% of DNA in a concentrated band after 2 – 3 hours. There are several detractors that limit the utility of this ITP setup as a diagnostic tool. While this system processed large sample volumes, significant sample pre-treatment was performed to simplify the ITP separation. The authors used plasma and serum samples spiked with DNA. However, they performed overnight deproteinization using proteinase K and sodium dodecyl sulfate (SDS), followed by overnight dialysis to desalt the samples. Following isotachophoretic separation, the authors then heat-inactivated the proteinase K present in the ITP plug. Additional post-treatment would be needed to remove the anionic surfactant SDS, a potent PCR inhibitor, before any downstream nucleic acid amplification assays.

Although limited for diagnostic use, Kondratova's work paved the way for future ITP studies in the sample preparation field. Starting in 2009, Juan Santiago's group published a flurry of papers on the purification of DNA and RNA from complex samples. These studies focused on ITP systems in microfluidic chips, which featured highly efficient analyte accumulation and concentration. Notably, they reported on an injection molded ITP chip that processes 25 μL of sample, yet they dilute by 10-fold before processing with ITP. Therefore the 25 μL sample contains 2.5 μL of clinical specimen. This chip processes whole blood and consistently extracts 76% to 86% of input DNA from blood lysate, and extracted DNA can be amplified via PCR.[48] This research group also compiled and further refined much of the theoretical background on ITP concerning electroosmotic flow, analyte stacking ratio, analyte accumulation, separation time, and other transport phenomena.[49–52]

Recently, ITP extractions in paper-based devices has emerged as a promising approach for use in low-cost diagnostics. Paper-based ITP formats are well-suited for POC diagnostic applications due to their reduced operational complexity, low material costs, ease of buffer control,

and capacity for large sample volumes.[53] Several studies have utilized ITP in paper substrates to extract and preconcentrate fluorescent dyes and DNA in pure buffer, but these reports did not use complex samples.[53–55] This dissertation describes novel advances in paper-based ITP systems for use in DNA and RNA extractions from blood samples and for integrating nucleic acid extraction, amplification, and detection on-chip.

1.5 Rationale for POC Molecular Testing for Bloodborne Viruses

This section investigates several prominent viral infections and their unmet needs for point-of-care molecular testing. These viruses are all bloodborne infections and many share inherent attributes, such as genomic diversity, short genomes, envelope or capsid structure, and low virion concentration. Therefore, these infections share technical challenges that have slowed the development of rapid yet low-cost molecular tests.

1.5.1 *Clinical need and technical challenges of HIV viral load testing*

The HIV/AIDS pandemic continues to increase in prevalence and remains among the leading causes of death, especially in low- and middle-income countries (LMICs). Of the over 35 million people living with HIV, 20 million are receiving antiretroviral therapy (ART) to suppress the viral infection and prevent its spread. Studies have shown successful virological suppression results in lower mortality rates[56] and negligible risk of sexual transmission to HIV-negative partners.[57] The Joint United Nations Programme of HIV/AIDS (UNAIDS) launched the 90-90-90 initiative to quell the growing global health ramifications of the pandemic. These ambitious efforts aim to reach the following targets by 2020: (1) 90% of all people living with HIV know their HIV

status, (2) 90% of all people with diagnosed HIV infection will receive sustained antiretroviral therapy, (3) 90% of all people receiving antiretroviral therapy will have viral suppression.

This campaign has set significant pressure on global HIV diagnostic efforts, as well as providing greater access to HIV viral load monitoring. HIV viral load monitoring is needed for health care providers to assess if ART is achieving viral suppression. Viral load testing for HIV-positive patients is recommended at least twice a year, which sets the global need for tests at over 40 million per year. The majority of these tests are needed in LMICs where, commonly, dried blood spots are sent to large central laboratories for processing, often delaying test results for several weeks. Delays lead to worse patient outcomes due to loss to follow-up and continued spread of disease. Point-of-care viral load testing is needed to address this shortcoming in the HIV care cascade. While several commercial platforms have recently hit the market (e.g. Abbott's *m-PIMA*, Cepheid's *GeneXpert*, Diagnostics for the Real World's *SAMBA*), these systems require further innovation to reduce testing costs, reduce time-to-result, simplify required steps for test operators, improve accuracy across HIV clades, and alleviate the reliance on a dependable power grid.

The entire process of HIV molecular testing – from sample collection to amplification and detection – presents significant technical challenges, especially considering the ambitious design criteria outlined in a target product profile from Drain et al. An ideal POC HIV viral load test should be simple enough for minimally trained technicians to operate, return results in less than 30 minutes, robustly operate without dedicated electrical power, process a 200 μL finger or heel stick whole blood sample, and quantify within 0.3 $\log_{10}$ copies/mL. Drain et al. recommend a target LoD of 200 copies per mL of plasma while the WHO recommends an LoD of 1,000 copies per mL of plasma. In working towards these targets, test developers will continue to compromise in

certain areas where they deem acceptable. For example, in lieu of providing fully quantitative results, the commercial *SAMBA* test provides semi-quantitative results by using its LoD as a cutoff for viral suppression. Therefore, a negative test result indicates ART treatment is achieving successful viral suppression.

Molecular testing for HIV has stringent requirements for sample preparation. For patients with partial viral suppression, HIV virions are present in blood at very low concentrations (10^3 to 10^5 cp/mL). Capillary blood provides low sample volumes (75–200 μL), furthering reducing the number of detectable viral RNA in a sample. For this reason, all aspects of the diagnostic procedure must minimize losses of target RNA. A crucial sample preparation step is thoroughly lysing the HIV virion, which degrades the lipid and protein viral envelope that encapsulates RNA strands. Lysis can be achieved by heating, detergents, enzymes, or chaotropic salts.[58,59] Lysis protocols should also deactivate RNases which rapidly degrade foreign RNA.[20] After virion lysis, efficient isolation of highly purified HIV RNA is required as even trace amounts of inhibitors can significantly affect performance of quantitative amplification. Solid phase, silica-based extraction methods are used in gold standard tests,[25] and have been translated into POC microfluidic or paper-based formats.[60,61] Silica-based extraction requires exchanges of wash and elution buffers, a concept difficult to automate in simple POC devices. Several single-step nucleic acid purification strategies have emerged in paper-based devices, such as chitosan-coated membranes[62] and electrophoretic separation of nucleic acids from blood.[63] Despite these recent advancements in sample preparation techniques, automating HIV lysis and RNA extraction from blood samples remains a formidable challenge.

Real-time PCR has long been the staple of nucleic acid amplification testing (NAT), including most of the current gold standard viral load tests.[64] PCR assays are difficult to implement

in POC devices due to the significant power demands of thermocycling and the need for highly purified nucleic acids. Other options may include isothermal amplification techniques, such as loop-mediated isothermal amplification (LAMP),[65,66] helicase dependent amplification,[67] and recombinase polymerase amplification.[68] Isothermal assays do not require thermal cycling, and therefore have reduced power demands and require less time for amplification. While isothermal methods are convenient for POC implementation, few assays have demonstrated reliable quantitative results.[69,70] For researchers developing HIV VL isothermal amplification assays, the primary challenge remains demonstrating quantitative accuracy comparable to real-time PCR across wide ranging viral loads (10^3 – 10^6 cp/mL) and subtypes.

While not unique to POC testing, NAAT for HIV is also complicated by the virus' high rate of mutation, recombinant forms and different clades associated within regions of high prevalence.[64] NAATs can account for sequence diversity with degenerate primers,[71] long primers capable of tolerating mismatches,[68] and targeting highly conserved regions of the HIV genome.[72] Still, the HIV sequence diversity can impact the performance of an assay, especially when applied to a variety of subtypes.[73]

When it comes to readout, quantitative NAATs most commonly use fluorescence-based methods to detect amplification, while LFA-based detection methods can provide semi-quantitative results.[74] Additional strategies have targeted reverse transcriptase activity[75] or optically sense virus particles.[76]

1.5.2 *Unmet testing needs for other bloodborne viruses*

HIV viral load testing at the POC is a focus for researchers in industry and academia alike. This stems from sustained governmental funding for HIV research (such as the President's Emergency Plan for AIDS Relief (PEPFAR) and the Global Fund) and high public awareness of

the HIV pandemic. However, there are several other prominent viral infections that affect millions globally, all with unmet clinical testing needs and similar diagnostic challenges to HIV. Here I describe the global health effects, POC testing needs, and technical diagnostic hurdles of hepatitis B, hepatitis C, dengue virus, Zika virus, and Ebola virus.

1.5.2.1 Hepatitis

Viral hepatitis has been a major public health issue for decades yet is commonly overlooked by populations across the globe. The CDC and America Liver Foundation have referred to hepatitis as the Silent Epidemic due to the low public awareness. In fact, an estimated 257 million people are living with chronic hepatitis B (HBV) yet only 9% know they are infected. 71 million people are living with chronic hepatitis C (HCV) with only 20% diagnosed with the condition. HBV and HCV are leading causes of chronic liver disease, resulting in an estimated 1.34 million deaths per year. This global mortality rate is higher than that of both tuberculosis and HIV, and it continues to increase every year.[77]

Chronic HBV infections have continued to climb globally despite the arrival of a highly effective HBV vaccine in 2001.[77] As with HIV, there are antiviral drugs available to treat and suppress HBV infections. These medications are once-a-day oral pills (e.g. tenofovir), and proper adherence to the treatment slows the progression of cirrhosis and liver cancer and leads to improved long-term survival.[78] In 2015, of over 250 million HBV infections, 1.7 million people (less than 1%) were on treatment.[77] The WHO published a comprehensive Global Hepatitis Report in 2017 that set a goal of providing treatment to over 80% of people diagnosed with HBV.[77] With this target comes a greatly expanded need for point-of-care testing. In low resource settings, rapid diagnostic testing for HBV surface antigens is currently used for diagnosis. POC NAATs for HBV are needed to measure the viral load. This testing is required upon initial diagnosis to assess the

severity of the infection and in regular clinic visits to monitor treatment effectiveness.[79] Depending on several demographic factors, the WHO recommends HBV treatment for patients with viral loads higher than 10^4 cp/mL of serum.[79,80] Efforts to expand the number of HBV-positive people receiving treatment has increased the demand for inexpensive, rapid NAATs for HBV DNA. There are no appropriate commercial POC NAATs for HBV viral load monitoring that address this need. The hepatitis B virus is a partially double-stranded DNA virus protected by an outer lipid envelope and a nucleocapsid protein coat. Its genome is a circular DNA structure with an approximate length of 3,200 nucleotides. In contrast to other DNA viruses, HBV is genetically diverse due to an intermediate RNA stage in the replication cycle. Reverse transcription of the viral DNA is prone to frequent mutations, and reverse transcriptase does not have error correction activity.[81] HBV has at least eight different genotypes (genotypes A-H), which presents difficulties for nucleic acid amplification assays when targeting conserved regions of the HBV genome.[82]

From a molecular testing perspective, HBV is strikingly similar to HIV. Both HBV and HIV (1) are bloodborne viruses, (2) are protected by an envelope and capsid, (3) have relatively short genomes, (4) are genetically diverse, (5) have unmet clinical need for POC viral load testing, and (6) require similar testing LoDs (10^3 to 10^4 cp/mL). Further, the mechanisms of transmission are similar, which has resulted in common coinfections of HBV and HIV especially among injection-drug users. Kourtis et al. estimate there may be 3 to 6 million people worldwide living with HBV-HIV coinfection, mostly in low-resource settings (see Figure 1-1).[83] Considering these shared attributes, molecular testing for HBV and HIV present nearly identical challenges for sample preparation, amplification assays, and detection assays. The recent developments toward POC platforms for HIV viral load monitoring may easily translate to HBV testing. POC viral load monitoring platforms should also consider multiplexing for HBV-HIV coinfection.

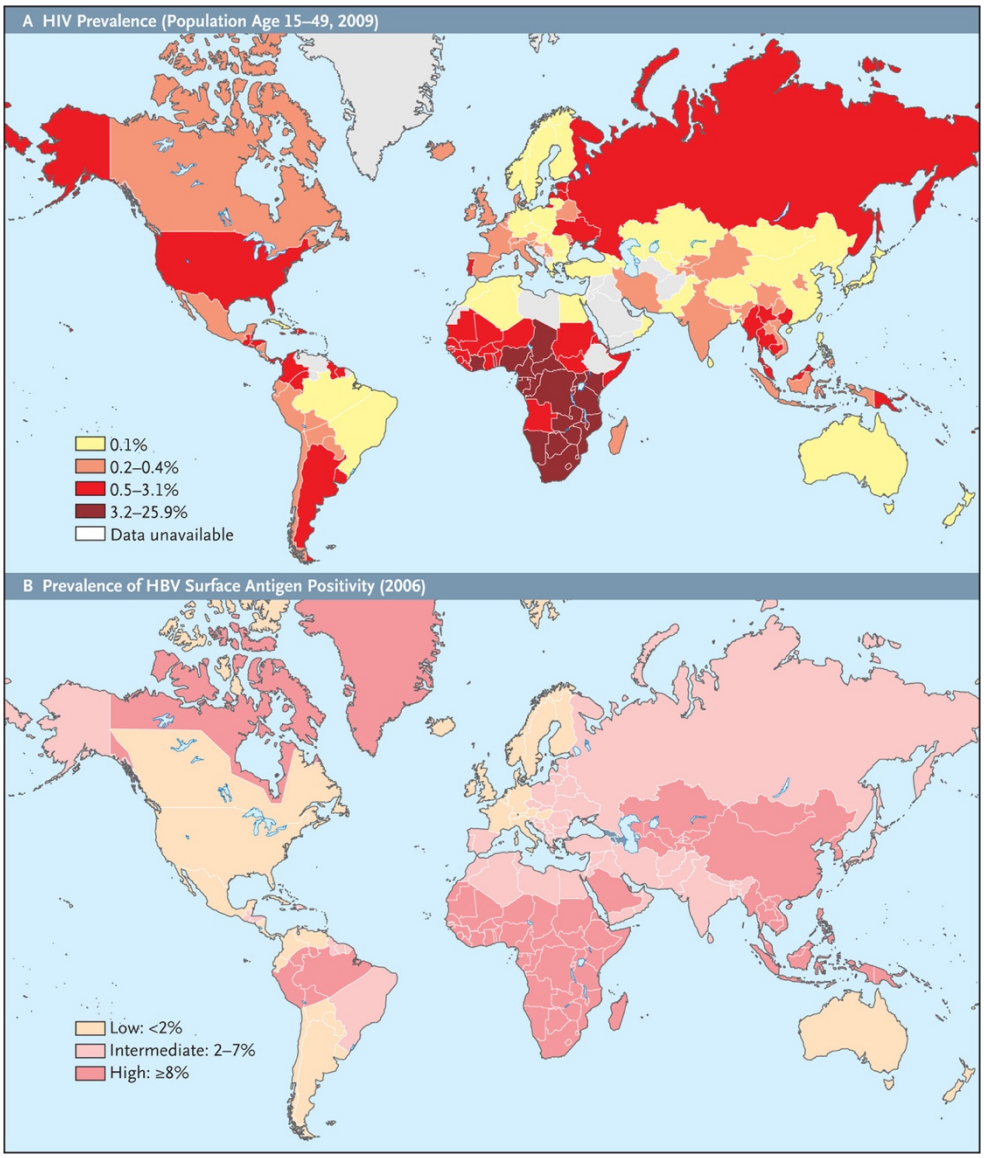

Figure 1-1. Worldwide prevalence map of HIV-1 and HBV infection. HIV data are from the United Nations Children's Fund, the World Health Organization, and (in the case of province-level data for China) the China Centers for Disease Control. Data on HBV are from the U.S. Centers for Disease Control and Prevention.[83]

In 2015, of the estimated 71 million people living with HCV (about 1% of the world population), 1.1 million received treatment.[77] There is no vaccine available to prevent HCV contraction. Expanded screening and treatment programs for HCV are of increased importance

since the introduction of direct acting antiviral (DAA) regimens which offer cure rates greater than 90% after 12 weeks of treatment.[84] Access to DAAs has recently expanded to LMIC countries where a full course of HCV medication costs US$100 to $250.[85] This has sparked interest in development of improved rapid diagnostic tests as well as quantitative or qualitative POC HCV RNA tests.

Researchers from Médecins Sans Frontières published a target product profile to guide the development of new rapid tests for HCV.[86] The goals of new tests are twofold: (1) diagnose active HCV viraemic infection and provide baseline viremia assessment and (2) confirm cure of HCV upon completion of DAA treatment. While a quantitative HCV RNA test is ideal, a qualitative test with an LoD between 1,000 to 3,000 IU/mL has high clinical utility towards these goals.[86] As shown in Figure 1-2, rapid antibody tests may not be useful for determining the state of the infection (e.g. cured versus not cured, elevated viremia, or reinfection status).[87] Among a list of ambitious targets, the target product profile recommends a maximum of 2 user steps with the preferred sample being capillary blood. Several tests have emerged that are moving closer to meeting these criteria. The Cepheid Xpert HCV Viral Load assay is the only CE-IVD certified for decentralized HCV testing.[88] Recent publications on the GeneDrive POC HCV test[88] and HCV Quant assay[89] show promising results toward satisfying the TPP criteria. As with many POC molecular testing platforms, additional research and development is needed to improve performance metrics and reduce the complexity and resource requirements for HCV RNA testing.

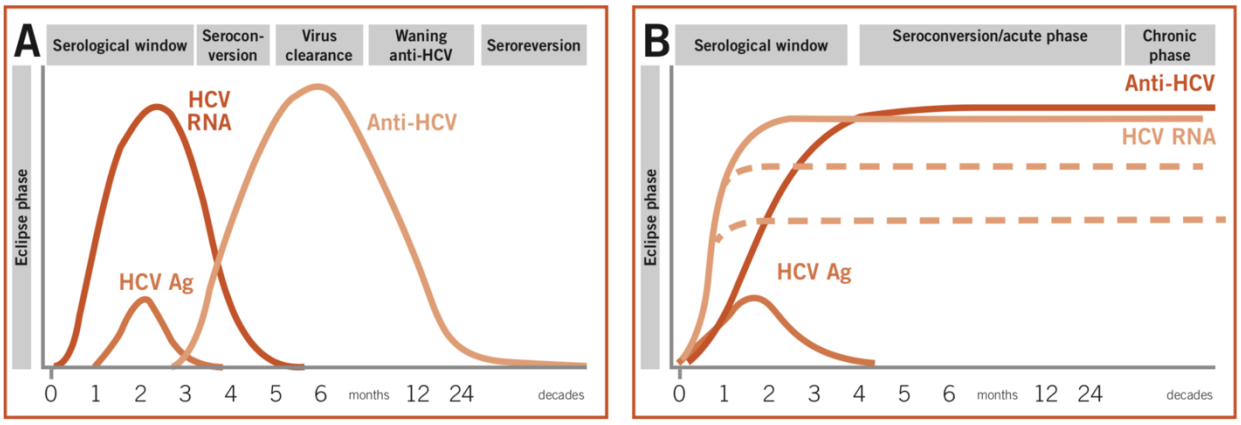

Figure 1-2. Approximate time windows of virological and immunological biomarkers for HCV. (A) For cases of self-resolving HCV, detection using anti-HCV antibodies result in false-positive results between 6 to 24 months after infection. (B) Chronic HCV infection results in elevated antibodies and HCV RNA for sustained periods.[79]

HCV is a single-stranded RNA virus with a genome 9,600 nucleotides in length. It is enveloped by a lipid and glycoprotein membrane with a protein capsid surrounding the viral RNA. As with HIV, it requires reverse transcription for viral replication which introduces mutations into the genome. HCV is highly genetically diverse, with six genotypes and several subtypes within each genotype. HCV has >30% nucleotide differentiation across genotypes.[90] HCV is nearly identical to HIV in genomic type (RNA virus), genomic length, virus structure, and relevant concentrations in blood – making HCV and HIV perfect analogs in diagnostic test development.

1.5.2.2 Dengue virus

In a seminal 2013 paper on the dengue disease burden, the authors estimate approximately 390 million dengue infections occur each year. Approximately 96 million of these are symptomatic cases.[91] Dengue is a viral infection transmitted to humans via *Aedes* mosquitoes, isolating disease outbreaks to tropical regions with high rainfall, temperatures, and high population densities. The WHO published a Global Strategy for Dengue Prevention and Control, and it emphasizes the

importance of expanding diagnostic testing in order to detect viral dengue during the initial stages of the infection. There are no vaccines or antiviral therapeutics for dengue, but mortality rates are reduced to less than 1% by implementing timely diagnosis and clinical management of the infection.[92] The CDC and WHO recommend detection of early stage dengue infection (first 5 days of symptoms) using nucleic acid-based testing.[93,94] Dengue is a single-stranded RNA with an 11,000-nucleotide genome. It is protected by an envelope rich with glycoproteins and a nucleocapsid. Dengue virus is present at relatively high concentrations within the first 5 days of symptoms. A study by Bai et al found that within the first 3 days of onset of symptoms, the median viral load was 8.29×10^5 cp/mL. For the following 3 days, the median viral load was 4.33×10^3 cp/mL.[95]

1.5.2.3 Zika virus

Zika virus garnered international attention after a 2015 outbreak in Brazil. Zika is transmitted between humans through infected female mosquitoes. Zika has emerged as a significant public health risk due to growing evidence that it causes fetal abnormalities, microcephaly, neurological complications, and autoimmune disorders.[96] Since its emergence, researchers have focused on developing effective vaccines, treatments, and diagnostics to fight its health threats. Similar to dengue virus, NAAT is the gold-standard for diagnosis within the first 14 days after the onset of symptoms.[97] From 2015 to 2017, 14 laboratory-based molecular assays for Zika virus were approved by the U.S. FDA.[98] Low-cost, rapid molecular testing is still needed to provide timely detection of zika virus at the point of need. There is no existing target product profile for POC Zika diagnostics, but the limit of detection requirements may not be stringent as the mean viral titer within the first 7 days of symptoms is approximately 9.9×10^4 cp/mL.[98] Zika

is an enveloped single stranded RNA virus with a 10,000-nucleotide genome protected by a nucleocapsid.

1.5.2.4 Ebola virus

The 2014/2015 Ebola outbreak in west Africa resulted in over 27,000 reported cases and over 11,000 reported deaths, a startling mortality rate for an infectious disease.[99] This deadly epidemic of the Ebola virus disease elicited an international response to improve existing diagnostic methods.[100] The main utility for nucleic acid-based testing comes during the acute illness phase, immediately after symptom onset. Elevated viral titers (>10^7 cp/mL) is associated with significantly higher mortality rates.[101] Nucleic acid testing is preferable to other diagnostic techniques because lysis buffers instantly inactivates virions in infectious blood samples. Field diagnose is critical for governmental and organizational agencies carrying out disaster response. Rapid testing for Ebola virus allows for real-time tracking of disease spread and confirmation of deaths caused by Ebola virus disease.[100] The Ebola virus is an enveloped RNA virus with a genome 19,000 nucleotides long. Its structure is somewhat unique; the virions are tubular with lengths up to 10 times longer than the diameters.

1.6 Research Objectives

The previous sections have outlined the need for sample preparation approaches for POC NAATs that may be implemented in low-cost tests for low- and middle-income countries (LMICs). I detailed the need for improved POC HIV viral load tests, as well as the clinical testing need for several other prominent bloodborne viruses with similar technical challenges to HIV. The objective of my dissertation is to develop a sample preparation method for point-of-care detection of bloodborne viruses in low-cost, disposable, and non-instrumented tests.

In order to address this objective, I have developed a research plan which will address the following technical challenges:

1. Identify a chemistry for inactivating blood RNases that is compatible for use in point-of-care nucleic acid tests.
2. Develop a paper-based isotachophoresis system for extracting viral DNA and RNA from human serum.
3. Implement an HIV detection method from serum with integrated RNase inactivation, viral lysis, protein digestion, isotachophoretic RNA extraction, and reverse transcription recombinase polymerase amplification (RT-RPA)
4. Integrate extraction, amplification, and detection of nucleic acids leveraging paper-based ITP.

Chapter 2. METHODS FOR INACTIVATING BLOOD RNASES

2.1 INTRODUCTION

There are widespread efforts from academic and commercial research laboratories to decentralize molecular testing for prominent bloodborne RNA viruses (i.e. HIV, hepatitis C, Ebola, Zika, and dengue) in order to provide rapid diagnostic results to medical clinics in low and middle income countries (LMICs).[102] Development of effective POC NAATs is challenging due to the technical complexities of detecting RNA from blood samples. While blood carries many infectious pathogens and useful biomarkers, it complicates the sample preparation of viral RNA due to its high concentration of endogenous ribonucleases (RNases) that are highly active and extraordinarily stable.

Human blood hosts an assortment of RNases that rapidly degrade exogeneous RNA as part of a natural defense system from infectious nucleic acids.[103] Notably, Tsui *et al.* found that free RNA incubated with blood plasma for only 15 seconds was degraded such that 99% of the RNA could not be amplified via RT-PCR.[20] RNases are among the most stable enzymes known to microbiologists, making them difficult to inactivate.[21] RNase A has been widely studied for decades, and some have posited that its compact structure, controlled by persistent disulfide bonds, lends increased protection from denaturation.[104,105] RNases are generally stable in pH extremes and weak denaturing solutions.[24] Heat inactivation of RNase A is reversible for short incubations up to 90 °C.[22,23] Further, human blood serum RNases are diverse in size, structure, and function.[106,107] Completely inactivating a wide range of endogenous RNases with differing stability poses a challenge for POC NATs.

Commercial NAATs targeting RNA biomarkers in blood samples commonly use lysis buffers that inactivate RNases in order to protect RNA from degradation.[27] The typical chemistry

fully denatures all proteins present in a sample with high concentrations of chaotropic salts, specifically 4 to 6 M guanidinium chloride or guanidinium thiocyanate.[26] Guanidinium-based lysis buffers can be paired with a silica column that adsorbs nucleic acids before subsequent elution, otherwise known as solid-phase extraction (SPE).[25] Qiagen DNA and RNA purification kits are the gold standard for conducting SPE in laboratory settings.[108] SPE adequately protects RNA from degradation and returns a high yield, making it the predominant sample preparation technique in blood-based NATs.[27] Another widely-used RNA purification protocol developed by Chomczynski and Sacchi uses guanidinium-based lysis and phenol-chloroform extraction.[109] Several washing steps and/or buffer exchanges are required to remove guanidinium, phenol, chloroform, and alcohols before downstream assays, and automation of these processes necessitates centrifuges, pumps, or robotics which complicates its use in POC devices.[28]

There are ongoing research efforts to circumvent SPE or other cumbersome nucleic acid purification techniques (e.g. phenol extraction) to simplify POC NATs. Electrokinetic techniques, which leverage the negatively-charged phosphate backbone of nucleic acids, have proven effective in extracting nucleic acids from a wide range of complex samples in microchips and paper-based devices that are well-suited for POC applications.[63,110–112] An alternate approach is to eliminate nucleic acid purification and amplify targets directly from crude lysates (*e.g.* blood, urine, or saliva). Amplifying crude lysates has been enabled by a combination of novel additives and mutant forms of PCR polymerases with increased tolerance to traditional inhibitors, including whole blood, sputum, and stool.[113,114] For example, the Phusion Blood Direct PCR Kit claims polymerase activity is retained even in the presence of up to 40% whole blood, according to the product bulletin. This “direct PCR” method has been applied to pathogenic nucleic acids targets in whole blood and serum.[115–117] Recent isothermal amplification assays have exhibited excellent tolerance

of crude samples and have many features congruous with point-of-care use.[118,119] The sample preparation strategies I have reviewed here have not been employed to detect RNA viruses in blood and may not be effective because of endogenous RNases and the potential for RNA target degradation. For tests that detect RNA in blood, methods must be used to inactivate RNases in lysates so that target RNA is protected from degradation.

In the absence of guanidinium, many sample preparation protocols employ the use of enzymes and surfactants, such as proteinase K, pronase, Triton X, Tween, and sodium dodecyl sulfate (SDS).[120] The lytic mechanisms and properties of these reagents are reported elsewhere,[121–123] yet their utility for nuclease control in complex samples is not well characterized. Proteases irreversibly break down proteins by cleaving specific peptide bonds.[21] Nonionic surfactants (*e.g.* Triton X and Tween) disrupt viral envelopes or cellular membranes and solubilize proteins. SDS is a powerful anionic surfactant that at high concentrations denatures proteins by disturbing the noncovalent bonds which provide secondary protein structure.[122] Proteases and surfactants act in different ways to alter proteins and their native configurations. As such, they have been shown to remove RNase activity in samples such as HeLa and neuroblastoma cell cultures.[124,125] I found the majority of studies on RNase inactivation techniques used samples with low concentrations of pancreatic RNase.[126–129] This is useful for identifying potential inhibiting reagents, yet human serum and other complex biological samples often contain high concentrations of salts, proteins, cells, and diverse RNases of varied structure. RNase inhibiting conditions are not necessarily universal across samples, so additional study is needed to identify chemistries that effectively inactivate diverse RNases in human serum, without the use of highly concentrated guanidinium.

In this chapter, I investigate the effects of several prominent proteases and chemicals on RNase activity in human blood serum. The most common method for RNase detection is extended

incubation of an RNA substrate with a test solution followed by gel electrophoresis to identify possible degradation.[130] This technique is laborious and not amenable to high throughput experimentation, so I selected a commercially available RNA substrate that emits fluorescence when cleaved by an RNase enzyme. This RNase activity assay allows for numerous parallel experiments on a microwell plate and generates real-time data of the activity over a 30-minute incubation time. I report on the performance of proteinase K, nonionic detergents, SDS, DTT, and other additives on inactivating RNases in human serum. I show denaturing SDS concentrations must be combined with either proteinase K or DTT for irreversible and complete RNase inactivation in serum. My findings provide valuable information for researchers looking for alternative strategies to guanidinium-based lysis and nuclease removal. I identify several novel RNase inactivation protocols in this chapter that may be compatible with ITP-based RNA extraction from blood lysates.

2.2 Materials and Methods

2.2.1 *Sample and Reagents*

I define samples as volumes of pooled serum, individual serum, plasma, or RNase A that are tested for RNase activity. Pooled serum is sterile-filtered from clotted whole blood of male donors with AB blood type (H6914, Sigma-Aldrich, St. Louis, MO). Individual serum was unfiltered and recovered from the whole blood of five different donors (BioIVT, Hicksville, NY). Donors included both males and females, different races, and ranged in age from 18 to 70, as detailed in Table 2-1. I obtained plasma from whole blood of a 23-year-old female donor pretreated with K_2EDTA anticoagulant (BioIVT). I centrifuged 1 mL of whole blood at 3,000 g for 10 minutes and removed the plasma supernatant with a pipette. The stock solution of RNase A (2250G, Thermo Fisher Scientific, Waltham, MA) at 30 units per liter (U/L) was diluted in DEPC-

treated water (AM9906, Thermo) prior to testing. The manufacturer approximated fifty units of RNase A equivalent to one Kunitz unit.[131]

Select experiments used serum pretreated by proteinase K (AM2546, Thermo) with or without additives. I incubated these samples for 1 hour in a water bath at 50 °C. After incubation, I immediately tested the samples for RNase activity. All reagents used in this study are certified RNase-free by the manufacturers. Reagents include dithiothreitol (D9779, Sigma), guanidinium chloride (G3272, Sigma), PRONASE (537088, Sigma), trypsin (T5266, Sigma), Sodium dodecyl sulfate (71725, Sigma), Triton X-100 (T8787, Sigma), Poly (A) (27-4110, GE Healthcare, Chicago, IL), Vanadyl ribonucleoside complexes (94742, Sigma), and Qiagen AVL viral lysis buffer (19073, Qiagen, Hilden, Germany). Working solutions were diluted with DEPC-treated water.

Table 2-1. Descriptions of blood samples. I obtained whole blood and individual serum samples from BioIVT and gender, age, and race of donors were provided by the supplier. I obtained pooled (male) serum from Sigma Aldrich.

Sample	Supplier	Gender	Age	Race	Notes
Whole blood	BioIVT	Female	23	Black	K2EDTA Vacutainer
Serum, pooled	Sigma Aldrich	Male	n/a	n/a	sterile-filtered
Serum, donor #1	BioIVT	Male	34	Black	
Serum, donor #2	BioIVT	Male	18	Hispanic	
Serum, donor #3	BioIVT	Male	66	Hispanic	
Serum, donor #4	BioIVT	Male	70	Caucasian	
Serum, donor #5	BioIVT	Female	37	Caucasian	

2.2.2 *RNase Detection Assay*

I employed the RNaseAlert Substrate Detection System (Integrated DNA Technology, Coralville, IA) for testing RNase activity in samples. The detection method relies on short RNA oligonucleotides with fluorophores (fluorescein) and quenchers on either end. In their native form, the RNA substrates are quenched and do not fluoresce. As illustrated in Figure 2-1, RNase cleaves the RNA substrates which separates the fluorophores from the quenchers and emits fluorescence. The intensity of the fluorescence is measured in real-time using a fluorometer, providing temporal data that indicate the rate of RNase activity. I chose human serum as the primary sample in this study because it carries the five known human blood RNases.[107] Whole blood contains red blood cells rich with hemoglobin that has high absorbance at the emission wavelengths of fluorescein. Unless significantly diluted, I observed that hemoglobin absorbance obscured the fluorescence signal from the RNaseAlert assay. Human serum is similar to plasma except that it has fibrinogen and clotting factors removed, making it easier to store and manipulate in laboratory settings.

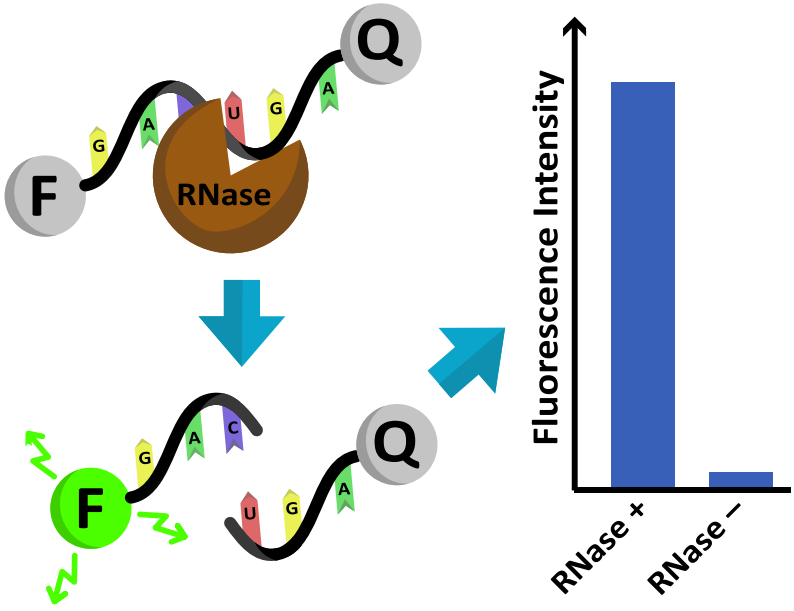

Figure 2-1. Illustration of the mechanism of the RNaseAlert assay used to test for RNase activity in serum and RNase samples. The short single-stranded RNA substrate is bookended with a

fluorescein molecule and quencher. When the sugar-phosphate backbone is cleaved by an RNase, the fluorescein is spatially separated from the quencher, allowing for fluorescence.

The manufacturer's recommended protocol for the RNaseAlert assay allows for some flexibility depending on application. Here, I supplement the recommended protocol and provide the necessary specifications to replicate my work. I prepared the RNaseAlert experiments in a lidded 96-well plate with black walls and clear bottom (3603, Corning Incorporated, Corning, NY). The total assay volume in each well was 100 µL. I first pipetted 10 µL of RNaseAlert substrate and 10 µL of 10X RNaseAlert buffer into each well. I then added 60 µL of water or reagents at the specified concentrations. When running experiments in parallel, it is crucial to simultaneously add samples to the wells so the incubation time with RNA oligonucleotides is equal. Towards this end, I used a 12-channel pipette to concurrently add 20 µL of samples to each well. The plate was immediately loaded into a plate reader (SpectraMax iD3, Molecular Devices, San Jose, CA). The excitation and emission wavelengths were 485 nm and 535 nm, respectively. The PMT gain was set to "low" with an exposure of 140 ms. The heating block in the plate reader was set to 37 °C. The instrument agitated the plate and measured the fluorescence in the wells every 2 min over a 30 min incubation time. For each set of data presented in this chapter, I present a positive control of RNase A (1.5 U/L). The maximum fluorescence of this positive control is used to normalize the fluorescence values of each data set.

2.3 Results and Discussion

2.3.1 *Differences in RNase activity of serum and plasma samples*

My goal was to compare the performance of common lytic chemicals and enzymes on inactivating serum RNases and shed light on the complex mechanisms of RNA degradation in

serum. I first compared RNase activity in human plasma and a variety of serum samples, both pooled and individual donors. Figure 2-2A shows normalized fluorescence intensities from RNase activity assays of serum and plasma samples over a 30-minute incubation period. All data is normalized by the maximum average fluorescence of the RNase A (1.5 U/L) controls run in triplicate. In the RNase controls, fluorescence rapidly increases after adding RNase A samples to the wells containing RNA substrate. After 10 to 15 minutes of incubation, the fluorescence signal plateaus, indicating that all available RNA substrate was cleaved. I observe that, with samples containing RNase activity, the initial fluorescence value at t=0 is substantially higher than respective value of the negative control. This is due to the short delay required to load the microplate into the reader and begin data acquisition, over which the RNA substrate in the assay begins to degrade. The serum and plasma experiments increased in fluorescence at differing rates, yet they all appear to plateau near a normalized fluorescence value of 0.75, notably lower than the RNase control. I attribute this lower plateau to two different sources. First, serum has some absorbance over the emission spectrum of fluorescein, which results in a decrease in measured fluorescence intensity. I support this hypothesis in Figure 2-3. Second, serum is highly proteinaceous, and it has been documented that non-specific RNA-protein complexes are common in biological systems.[132] These complexes between serum proteins and the assay's RNA substrate may sequester a portion of the substrate, resulting in less total fluorescence.

I observe that there are differences in the fluorescence curves between the individual serum samples. This indicates that RNase activity differs between blood donors. There are documented differences in blood RNase activity, but this has primarily been observed in patients with certain conditions, such as pancreatic cancer.[133] The pooled serum exhibited the lowest RNase levels, which may be due to the particular collection technique. I chose to use pooled serum as the primary

sample in this study because it is similar in RNase activity to plasma and other serum samples. This pooled serum is also commercially available so others may replicate my results.

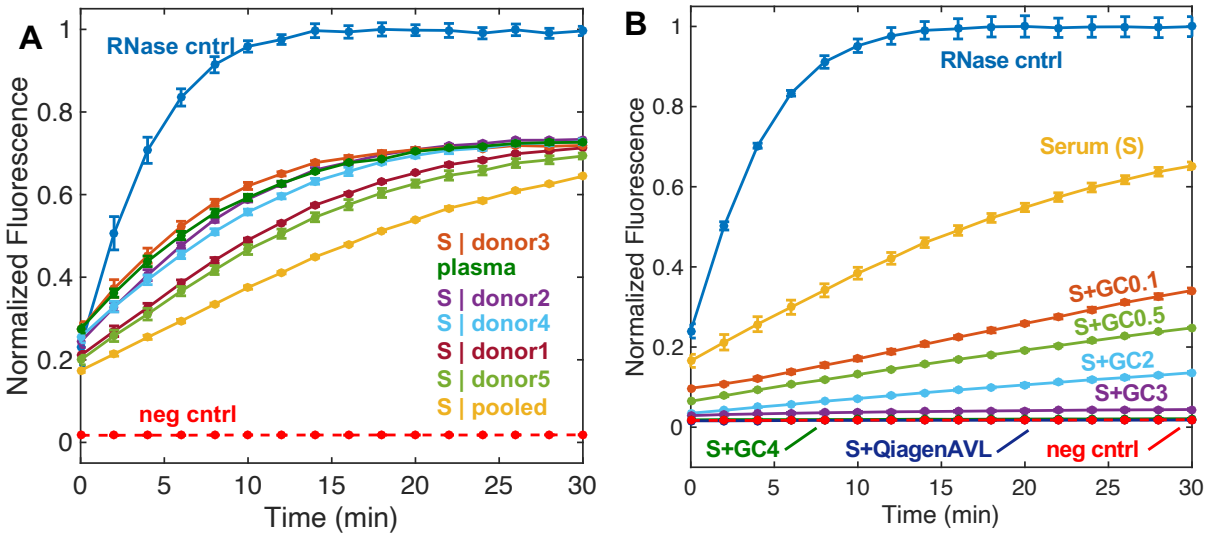

Figure 2-2. (A) RNase activity in pooled serum, serum from five individual donors, and plasma from a donor. Samples were simultaneously added to a 96 well plate with RNaseAlert substrate and fluorescence intensity was measured in 2-minute increments over a 30-minute incubation. (B) Effect of guanidinium chloride (0.1 M to 4M) on serum RNase activity. Serum with no GuHCl is presented for comparison. The positive controls are RNase A (1.5 U/L), and the negative controls are RNase-free water. The 's+GC4' and 's+QiagenAVL' data are indistinguishable from the negative controls. RNase A (1.5 U/L) is the positive control and its mean maximum fluorescence intensity is used to normalize all data points. The negative control is RNase-free water added to the RNaseAlert assay. All data plotted are averaged triplicates (N=3) with error bars of one standard deviation around the mean. Data points where no error bars are visible have errors too small to plot.

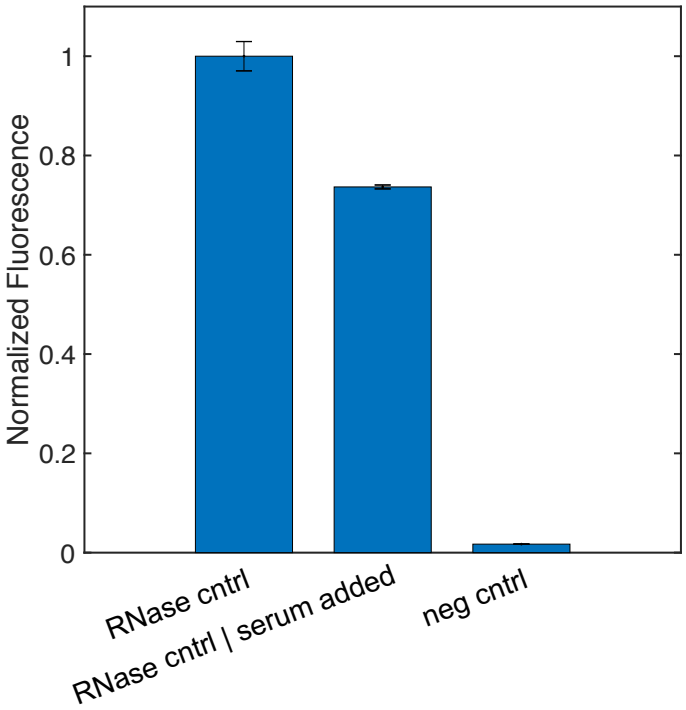

Figure 2-3. Reduction in fluorescence from the RNaseAlert assay after the addition of human serum. I plot the endpoint fluorescence of a 30-minute RNaseAlert assay after a sample of RNase A (1.5 U/L) has completely degraded the target substrate, labeled 'RNase cntrl'. This is contrasted with the endpoint fluorescence after human serum is spiked into control. The serum reduces the intensity of the fluorescence signal emanating from the sample.

2.3.2 *Guanidinium-mediated RNase immobilization*

Guanidinium is the most common chemical used in RNA purifications and considered the gold-standard for inactivating diverse RNases.[134] It is commonly used at concentrations between 4 to 6 M to denature proteins.[25,26] I investigated the effects of guanidinium on inactivating serum RNases as a comparison benchmark and if lower concentrations may be used. Figure 2-2B plots the fluorescence from the RNase detection assays of serum treated with guanidinium chloride at 100 mM to 4 M. Lower concentrations of guanidinium reduce the activity of endogenous serum RNases, but complete inactivation is achieved at a minimum of 4 M concentration. I found that guanidinium chloride completely eliminated serum RNase activity at 4 M and only partially

reduced activity at lower concentrations. This finding is in agreement with a recent study observing partial unfolding or an "expanded form" of RNase HI at low concentrations of guanidinium and extensive protein unfolding of the hydrophobic core at concentrations of 3 to 4 M.[135] Guanidinium must be purified away from RNA or significantly diluted before adding to PCR or other amplification assays. PCR can tolerate guanidinium up to approximately 50 mM;[136] therefore a blood lysate at 4 M guanidinium chloride would need to be diluted 80-fold in order to enable PCR amplification. A lysate dilution of this magnitude is not preferred for POC NAATs because it drastically dilutes the analyte concentration, negatively affecting the limit of detection of the test. Dilution also may allow blood RNases to renature and regain activity. A widely used commercial lysis buffer for immobilizing RNases in blood samples is the Qiagen viral lysis buffer (AVL buffer), composed of guanidinium thiocyanate and a detergent. As seen in Figure 2-2B, I see that this buffer is also highly effective at eliminating activity of serum RNases.

2.3.3 *Effects of nonionic surfactants*

I first tested Triton X-100 for RNase inactivation properties. Nonionic surfactants, such as Triton X-100, are well-suited for simple sample preparation strategies because they do not inhibit PCR or other amplification assays, even at high concentrations.[137] Therefore, there is no need for onerous purification methods to remove the surfactant. Nonionic surfactants solubilize proteins rather than fully denaturing them, so enzyme activity may be retained in the presence of even high concentrations of surfactant.[122] I explored the effect of Triton X-100 on RNase activity, as plotted in Figure 2-4A. All concentrations of Triton X-100, ranging from 0.1% to 2% w/v, increased the rate of RNA degradation in serum when compared to an untreated sample. I observed this same effect with Tween-20, another common nonionic surfactant (see Figure 2-5). A possible explanation is that nonionic surfactants directly interact with RNases and increase their activity,

which has been observed for other enzymes in molecular biology.[138] Figure 2-4B plots the activity of RNase A in the presence of Triton X-100. There are no distinguishable differences in the slopes of the fluorescence curves of the detection assay, suggesting Triton X-100 does not significantly affect RNase activity.

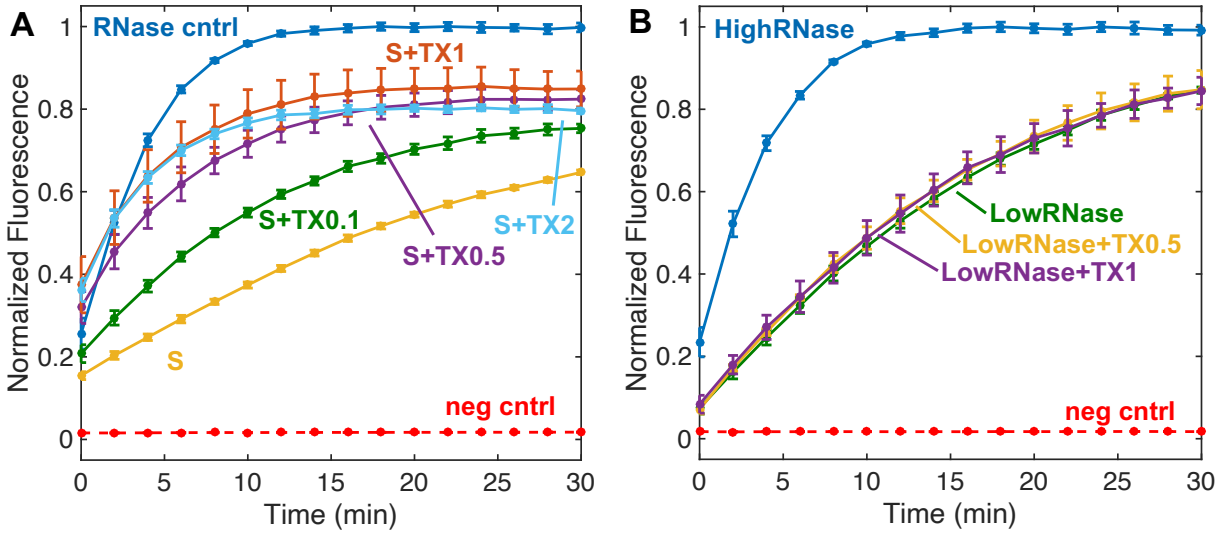

Figure 2-4. (A) RNase activity of untreated serum (S) versus serum treated with Triton X-100 (0.1% to 2% w/v). (B) Effect of Triton X-100 on the activity of RNase A. The 'HighRNase' sample is the typical RNase A control (1.5U/L). The 'LowRNase' samples with and without Triton X-100 all contain 0.3U/L RNase A. Either 0.5% or 1% w/v Triton X-100 was added to RNase A.

I hypothesize that this surfactant-induced increase in RNase activity in serum may be a result of the disruption of protective protein-RNA complexes. Immunoglobulin G (IgG) is present in high concentrations in serum, and Sidstedt *et al.* observed that IgG readily binds to ssDNA, which is similar in chemical structure to ssRNA.[139] Nonspecific ribonucleoprotein complexes have not specifically been studied in human serum, but free RNA is likely bound by multiple proteins in biological matrices, such as serum.[132] Ribonucleoprotein complexes create a protection from RNase degradation.[140] Surfactants disrupt the hydrophobic interactions of ribonucleoprotein complexes and free the RNA, making it more susceptible for degradation. I hypothesize that Triton

X-100 prevents the formation of complexes between RNA substrate and serum proteins, allowing for rapid degradation of free RNA via serum RNases. Similarly, I found nondenaturing concentrations (specifically less than 0.3%) of the anionic surfactant, SDS, accelerate RNA degradation in serum. I suspect this is due to the same mechanism observed with Triton X-100.

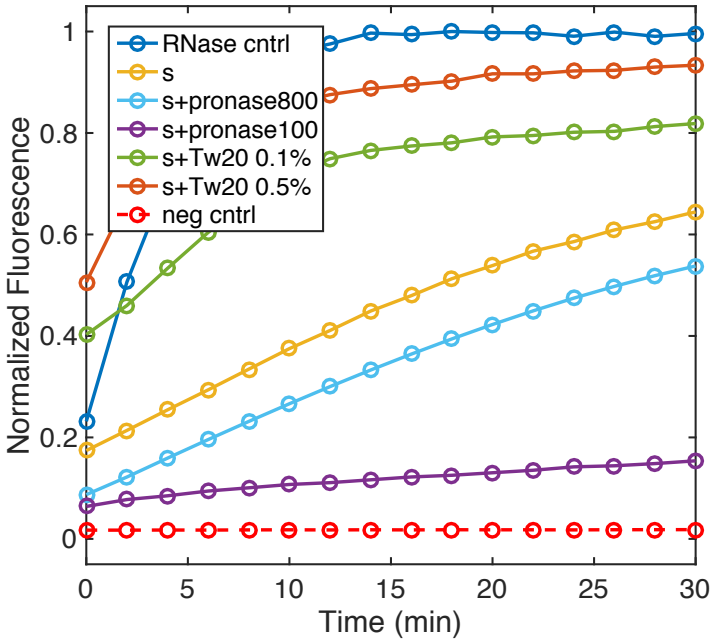

Figure 2-5. RNase activity in serum samples in the presence of Tween 20 or pretreated with pronase. Samples (N=1) were simultaneously added to a 96-well plate with RNaseAlert substrate and fluorescence intensity was measured in 2-minute increments over a 30-minute incubation. There is a short delay between adding samples to the microplate and loading it into the plate reader, which results in some experiments with initial fluorescence values significantly greater than the negative control. RNase activity in serum in the presence of nonionic surfactant, Tween 20, is higher than that of serum with no surfactant. Activity is greater in samples at 0.5% w/v Tween 20 than at 0.1%, as observed with Triton X-100. I also measured RNase activity of serum pretreated with the protease cocktail, pronase, for 1 hour at 50 °C. As with proteinase K, digestions at higher protease concentrations resulted in serum samples with increased RNase activity. RNase A (1.5 U/L) is the positive control and its maximum fluorescence intensity is used to normalize all data points. The negative control is RNase-free water added to the RNaseAlert assay.

2.3.4 *Protease-mediated RNase removal*

Proteinase K is a broad-spectrum serine protease that has been used for decades in DNA and RNA preparations to remove nucleases from biological samples.[124] I examined the ability of proteinase K to inactivate serum RNases. I tested samples of serum that were pretreated with proteinase K for 1 hour at 50 °C, as advised in the product manual. The concentrations of proteinase K during the pretreatments ranged from 5 to 1000 µg/mL. Figure 2-6A reports the normalized real-time fluorescence values of each digested serum sample over the 30-min RNaseAlert assay, and Figure 2-6B plots the endpoint fluorescence to highlight the relationship between proteinase K in the digestions and resulting RNase activity. I observe increases in fluorescence in all serum samples compared to that of negative controls, indicating proteinase K is unable to fully deactivate serum RNases. I confirmed that the proteinase K stock was free of RNase activity with a proteinase K-only control. There appears to be an optimum concentration of proteinase K at 50 µg/mL to protect RNA, as illustrated in Figure 2-6B. Incubations at high concentrations of proteinase K lead to extensive degradation of the RNA substrate, even when compared to untreated serum.

In my investigation of protease-mediated RNase inactivation, the data revealed two curious findings: (1) proteinase K does not inactivate all serum RNases and (2) higher concentrations of protease result in more severe RNA degradation in serum. In addition to proteinase K, I found serum RNases were not removed by other broad-spectrum proteases, including pronase and trypsin (see Figure 2-5). I also could not inactivate serum RNases with an extended 24-hour proteinase K digestion. High concentrations of proteases result in more thorough digestion of proteins in a sample. This suggests that serum RNases are resistant to proteolysis. I hypothesize that extensive degradation of serum proteins may remove protective ribonucleoprotein complexes, leading to

more rapid RNA degradation in the sample. Another possible explanation for the adverse effects of high proteinase K concentrations is that proteinase K may actually activate some endogenous RNases. A study from Simpson *et al.* found that endogenous RNase activity was activated by proteinase K in mitochondrial extracts from *Leishmania tarentolae*, a eukaryotic protozoan parasite.[141] This finding has not been observed in serum RNases.

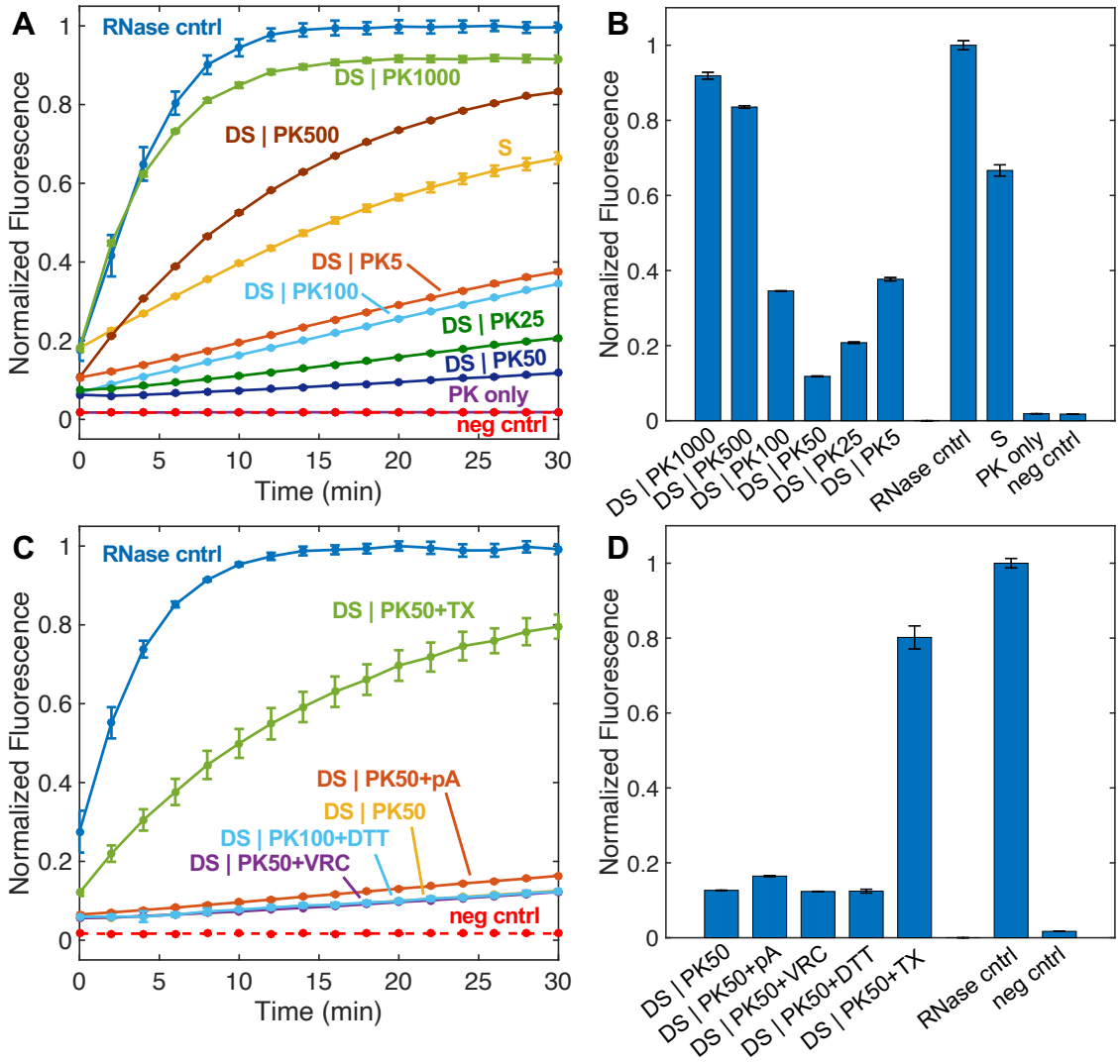

Figure 2-6. (A) Inactivation of serum RNases via proteinase K (5 µg/mL to 1000 µg/mL). Serum samples are pretreated with proteinase K for 1 hour at 50°C and resulting digested serum (DS) is tested with the RNaseAlert assay. I plot the real-time fluorescence from the assay during a 30-minute incubation with the substrate. (B) Respective endpoint fluorescence values are provided to

highlight the optimal proteinase K concentration for RNA protection in serum digestions. I present a positive control with RNase A (1.5 U/L) and negative control with nuclease-free water. (C,D) RNase activity in serum pretreated with proteinase K as well as various additives. Additives tested include 0.5 µg/µL poly(A) (pA) carrier RNA, 2 mM ribonucleoside vanadyl complex (VRC), 5 mM dithiothreitol (DTT), and 0.5% w/v Triton X-100 (TX).

There are a number of additives that are known to inhibit RNase activity or improve the proteolytic performance of proteinase K. I explore several prominent additives by digesting serum with 50 µg/mL proteinase K in the presence of 0.5 µg/µL poly(A), 2 mM vanadyl ribonucleoside complex (VRC), 10 mM dithiothreitol (DTT), or 0.5% w/v Triton X-100. Poly(A) serves as sacrificial carrier RNA that slows the degradation of RNaseAlert RNA substrate, and VRC is a well-known RNase inhibitor. DTT is a disulfide bond reducer which helps unravel protein structures, making peptide bonds more susceptible to proteases. Triton X-100 similarly relaxes protein structures by weakening hydrophobic effects. Respective additive concentrations are typical values for inhibiting RNases or aiding proteinase K. Figure 2-6C plots real-time fluorescence over a 30-minute assay measuring RNase activity in the samples, with respective endpoint fluorescence displayed in Figure 2-6D. Data indicate proteolyic digestion to remove serum RNases is not significantly impacted by the selected additives, with the exception of Triton X-100.

I further explored the efficacy of protease-mediated RNase inactivation with RNase A samples. I either pretreated RNase A with proteinase K for a one-hour incubation or combined both enzymes at the initiation of the RNaseAlert assay. Figure 2-7A shows pretreated RNase A samples have no detectable ribonucleic degradation. I observe that when proteinase K and RNase A (1.5 U/L) are added at the initiation of the detection assay, RNase is eliminated within 10 minutes. 500 µg/mL proteinase K degrades RNase A more rapidly than 50 µg/mL proteinase K. I

highlight that proteinase K easily digests RNase A but is not able to remove endogenous RNases in serum. It has been noted in other studies that protease digestion efficiency varies widely across proteins. This may be due to differences in disulfide bonds, specific folds, glycosylation, or a combination thereof.[142] There may be certain serum RNases with structures resilient to proteases.

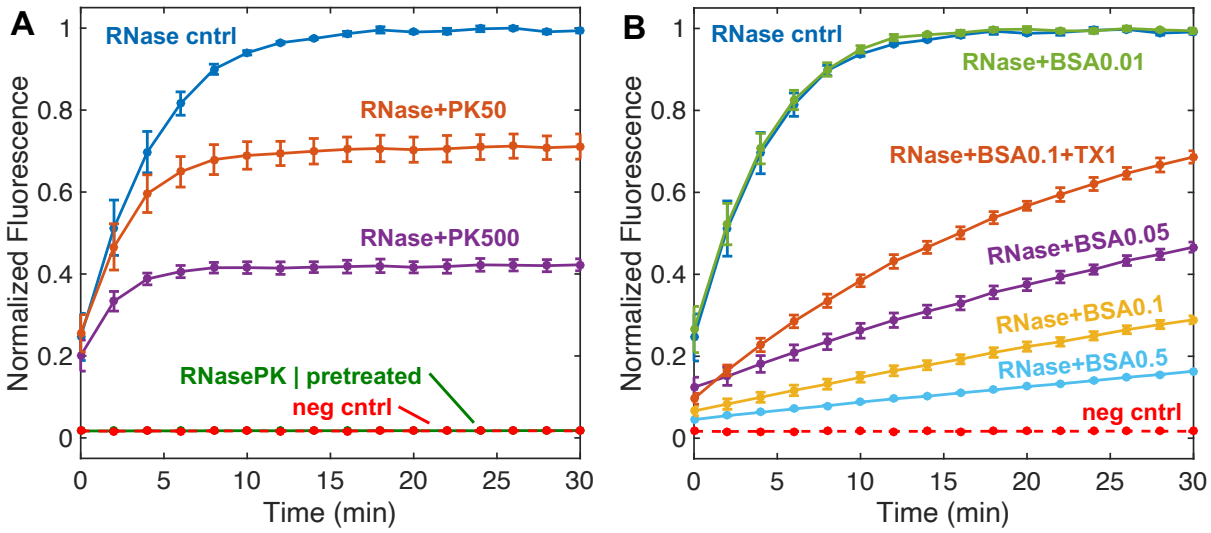

Figure 2-7. (A) Effect of proteinase K on RNase A activity. I monitored the RNase A activity in real-time over a 30-minute period. For the 'RNase+PK500' (1.5 U/L RNase A and 500 µg/mL proteinase K) and 'RNase+PK50' (1.5 U/L RNase A and 50 µg/mL proteinase K) experiments, proteinase K and RNase A were not incubated together prior to the 0-minute mark of incubation. The other data set shown is RNase A (1.5 U/L) pretreated with proteinase K (50 µg/mL) for 1 hour at 50°C before adding to the RNaseAlert assay. This data is indistinguishable from the negative control. (B) Shielding effect of bovine serum albumin (BSA) on RNase A. RNase A (1.5 U/L) activity was tested in the presence of BSA at various concentrations (0.5% to 0.01% w/v).

In Figure 2-7B, I explore the effects of nonspecific proteins on shielding RNA from degradation. Increasing concentrations of bovine serum albumin (BSA) drastically reduce RNA degradation from RNase A. The minimum concentration of BSA needed for noticeable RNA protection was 0.05% w/v. It is notable that the highest concentration I tested is 0.5% w/v or 5

mg/mL. Human serum albumin in blood is typically between 35 to 50 mg/mL.[143] Human serum albumin (66 kDa) and BSA (66 kDa) are similar in chemical makeup and function. Therefore, it is reasonable to assume that human serum albumin plays a role in protecting exogenous RNA from degradation by serum RNases. This supports the theory that nonspecific complexes between proteins and RNA slow degradation. While this finding does not address RNase inactivation, it frames a strategy that may be leveraged to protect RNA in samples with limited RNases, such as cell lysates or heavily diluted serum or blood. BSA is advantageous for RNA preservation because it is compatible with downstream nucleic acid amplification techniques, unlike other RNA preservation reagents such as VRCs. Only commercial BSA preparations that are confirmed to be RNase-free should be used with RNA samples. I found multiple commercial BSA products purified using the traditional heat shock fractionation method had significant RNase activity (see Figure 2-8). There may be other proteins besides BSA that provide RNA protection in complex samples, including single-stranded binding proteins which may have a higher affinity for exogenous RNA. Further study of the interplay between serum proteins, RNA, and surfactants could employ an electrophoretic mobility shift assay with carefully selected running buffer to mimic binding conditions in serum.[144]

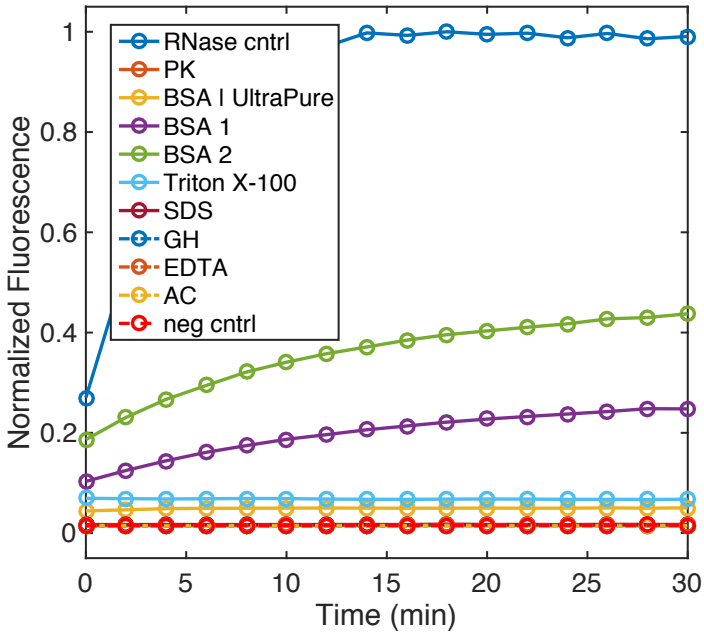

Figure 2-8. RNase activity of the stock solutions of reagents used in this work. Here I see if any reagents I employed may have activity measurable via the RNaseAlert assay. Reagents tested include 200 µg/mL proteinase K, 50 mg/mL UltraPure BSA (Thermo Fisher), 50 mg/mL BSA 1 (B4287, Sigma Aldrich), 50 mg/mL BSA 2 (A7030, Sigma), 0.5% w/v Triton X-100, 0.5% w/v SDS, 500 mM guanidine hydrochloride, 25 mM EDTA, and 100 mM ammonium chloride. Two different BSA products from Sigma Aldrich possess noticeable RNase activity. The UltraPure BSA has an elevated baseline fluorescence, but no noticeable increase in fluorescence over the incubation, indicating minimal or nonexistent RNase activity. Triton X-100 has no RNase activity but does emit some fluorescence at the same wavelength as the fluorophore in the RNaseAlert assay.

2.3.5 *Other methods for RNase immobilization*

A 2012 research article and 2015 patent describe a technique for irreversibly inactivating serum RNases with a combination of DTT, Triton X-100, poly(A) carrier RNA, and high basicity.[145,146] The pH of the sample is elevated to approximately 12 which theoretically accelerates the DTT-mediated disulfide bond reduction of RNases. The authors use Triton X-100 (1%) and poly(A) (0.4 mg/mL) to accelerate RNase inactivation and reduce degradation of target

RNA, respectively. The authors claim that, with these conditions, short incubation times of less than 5 minutes are needed. This is important because RNA is unstable in extended incubations at high pH. I replicated this protocol in our research group's laboratory with a 5-minute incubation and found that it did not eliminate serum RNase activity, as measured by the RNaseAlert assay. Figure 2-9 shows that serum treated with the aforementioned method rapidly degrades the RNA substrate. I present a control experiment in which the method was carried out on RNase-free water instead of human serum, and this resulted in data that is consistent with the negative control.

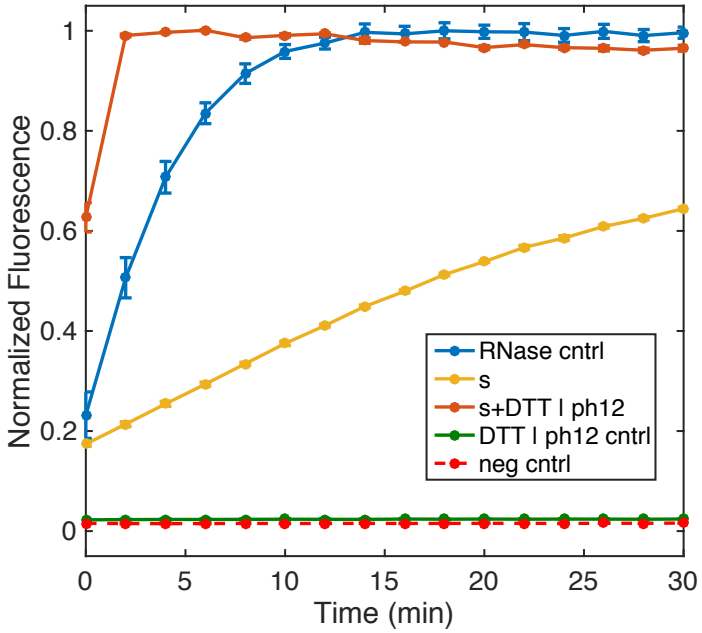

Figure 2-9. DTT-mediated inactivation of serum RNases accelerated by highly basic conditions. Human serum treated with DTT, Triton X-100, and poly(A) carrier RNA at pH 12 was tested with the RNaseAlert assay. I treated RNase-free water at these same conditions and observe that its fluorescence does not increase over the RNaseAlert incubation period. An RNase A control, untreated serum control, and negative control are provided for comparison.

Curtis et al. detected HIV-1 RNA in whole blood and plasma lysed with a 37.5 mM ammonium chloride buffer.[147,148] They demonstrated nucleic acid extraction may be avoided in their assay by directly adding blood lysate to an RT-LAMP reaction for detection. The authors do

not discuss difficulties with HIV RNA degradation in the lysate, which is surprising as ammonium chloride is not a known RNase inhibitor. In Figure 2-10, I plot measured RNase activity in serum in the presence of ammonium chloride. I observed that ammonium chloride slightly reduces serum RNase activity, but high concentrations of ammonium chloride were not able to completely eliminate activity. For reference, the concentration of ammonium chloride in a typical red blood cell lysis buffer is 150 mM. I expect the sensitivity of the HIV assay from Curtis *et al.* suffered due to RNase-mediated analyte loss.

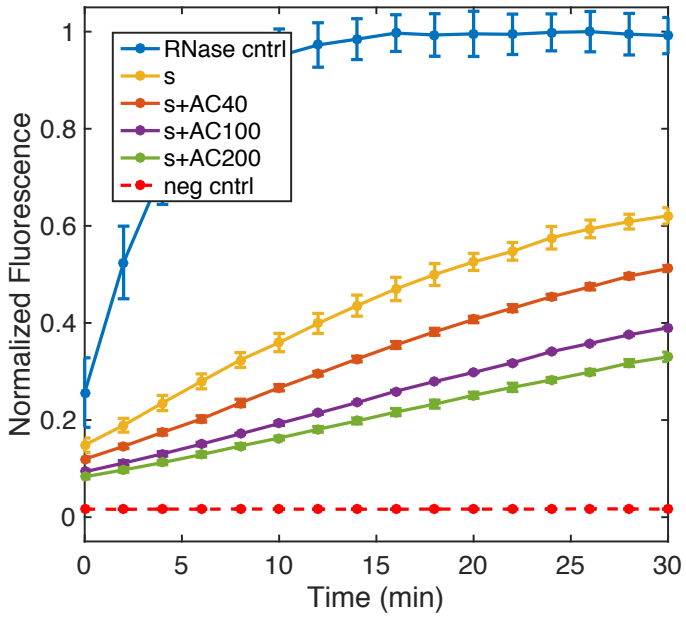

Figure 2-10. Effect of ammonium chloride (40 mM to 200 mM) on RNase activity in serum. The positive controls are RNase A (1.5U/L), and the negative controls are RNase-free water. All data plotted are averaged triplicates (N=3) with error bars of one standard deviation around the mean. Data points where no error bars are visible have errors too small to plot.

Some nucleases require divalent cations to be active and, therefore, can be completely inhibited by chelating agents, such as ethylenediaminetetraacetic acid (EDTA). Many RNases are active in the absence of divalent cations so EDTA is ineffective.[149] Figure 2-11 reports the activity of serum RNases in the presence of EDTA ranging from 10 mM to 100 mM. EDTA appears to

inhibit serum RNases with increasing concentrations, but complete inactivation is not achieved at concentrations up to 100 mM.

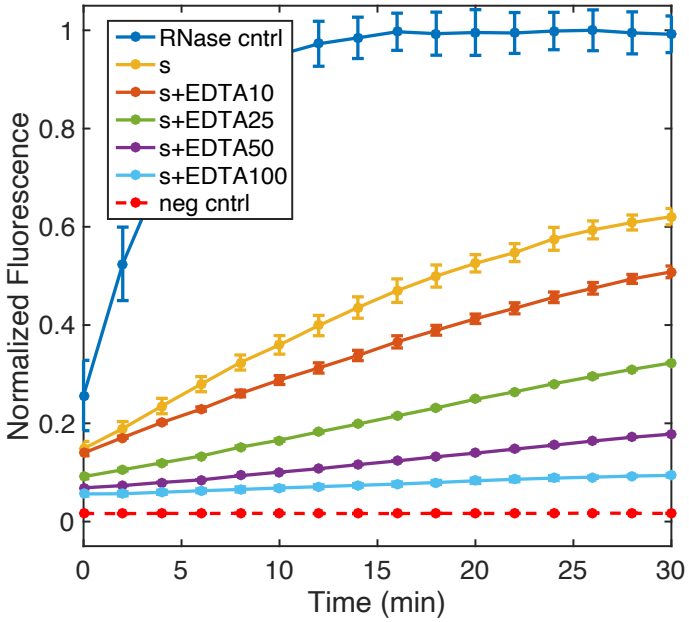

Figure 2-11. Effect of EDTA (10 to 100 mM) on serum RNase activity. The positive controls are RNase A (1.5U/L), and the negative controls are RNase-free water. All data plotted are averaged triplicates (N=3) with error bars of one standard deviation around the mean. Data points where no error bars are visible have errors too small to plot.

2.3.6 *Immediate and irreversible inactivation of serum RNases*

The most effective reagent I identified for RNase inactivation in serum samples is SDS. SDS is a powerful anionic surfactant and protein denaturant commonly used in lysis protocols.[122] Figure 2-12A reports RNase activity in serum samples in the presence of SDS concentrations ranging from 0.1% to 2% w/v. At concentrations of 0.5% and higher, RNase activity could not be detected which suggests the surfactant created fully denaturing conditions. Serum with 0.3% SDS partially inhibited RNases compared to an untreated serum sample. Serum treated with 0.1% SDS resulted in rapid degradation of RNA substrate in the detection assay. This indicates RNA

degradation in serum is more pronounced at low concentrations of SDS where RNases are not fully denatured. I hypothesize this is due to the same phenomenon observed with nonionic surfactants, such as Triton-X. In terms of concentration, I found that SDS is more potent than the gold standard reagent, guanidinium chloride, that must be used at concentrations greater than 4 M to completely prevent RNase activity.

The crucial shortcoming of SDS is it does not irreversibly inactivate serum RNases, which renature once SDS concentration is reduced. This effect is illustrated in Figure 2-12B where an RNaseAlert assay containing serum and 0.5% SDS is diluted 1.66-fold after 15 minutes to a concentration of 0.3%. I observe serum RNases are initially fully inhibited but the dilution of SDS allows RNases to renature and regain activity. Hilz *et al.* reported that SDS reversibly inactivated RNase A and a combination of proteinase K and SDS is needed for irreversible inactivation.[140] I similarly found serum that is digested with 0.5% SDS and 1000 μg/mL proteinase K is irreversibly removed of RNase activity, as shown in Figure 2-12B. Note that the 0.5% SDS in the digested serum is diluted to a final concentration of 0.1% SDS when added to the RNaseAlert assay. For irreversible RNase inactivation by proteolytic digestion with proteinase K, I found SDS must be present in the serum at denaturing concentrations of 0.5% or greater (data not shown).

RNases are reliant on their disulfide bonds for sustained activity, so the reducing agent, DTT, has been shown to irreversibly inactivate RNases, most effectively at elevated temperatures.[128,150] I found that a pretreatment of serum with 0.5% SDS and 75 mM DTT for 30 minutes at 50°C irreversibly inactivated serum RNases. In Figure 2-12B, I demonstrate that this same incubation with SDS and DTT at room temperature does not irreversibly inactivate serum RNases, indicating elevated incubation temperature is crucial. When I attempted to remove serum RNases with solely DTT, the serum firmly coagulated upon heating and could not be manipulated.

The most effective serum pretreatment protocol leveraged a one-hour incubation at 50°C with 0.5% SDS, 1000 µg/mL proteinase K, and 10 mM DTT, which resulted in digested serum with RNase activity indistinguishable from the negative control (as seen in Figure 2-12B). Each reagent disrupts different aspects of protein structure, specifically denaturation, peptide bond cleavage, and disulfide bond reduction, respectively. Individually, the reagents are limited, but in concert, they are able to completely and irreversibly immobilize the diverse and abundant RNases present in human serum. I found this method of RNase inactivation was equally as effective as gold standard guanidinium-based chemistries.

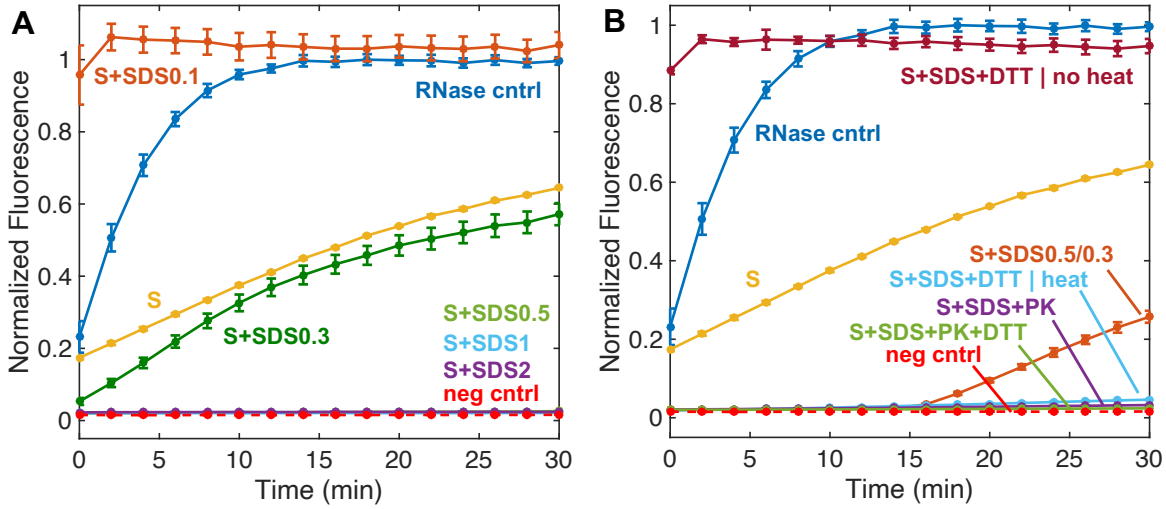

Figure 2-12. (A) Effect of SDS (0.1% to 2% w/v) on serum RNase activity. The positive controls are RNase A (1.5U/L), and the negative controls are RNase-free water. Data for 0.5%, 1%, and 2% SDS are indistinguishable from that of the negative control. (B) Irreversible inactivation of serum RNases using a combination of SDS and proteinase K, DTT, or both. The experimental data labeled 'S+SDS0.5/0.3' monitors serum in the presence of 0.5% SDS for 15 minutes, when a 1.66X dilution of RNase-free water is added to reduce the SDS concentration to 0.3%. I tested serum samples pretreated with a combination of SDS and DTT or proteinase K. 'S+SDS+DTT' is serum pretreated with 0.5% SDS and 75 mM DTT for 30 minutes either at 50°C or room temperature. 'S+SDS+PK' is serum digested with 0.5% SDS and 1000 µg/mL proteinase K at 50°C for one hour. 'S+SDS+PK+DTT' includes 10 mM DTT. Serum samples pretreated or

digested with 0.5% SDS were diluted to a final concentration of 0.1% SDS in the RNaseAlert detection assay.

As I detailed in the introduction section, lysis and RNase inactivation chemistries that avoid high concentrations of guanidinium may not require solid- or liquid-phase extraction for RNA purification. For example, DTT is a common PCR additive and, at low concentrations, does not need to be purified away from target nucleic acids. DTT has been shown to be compatible with multiple reverse transcriptases and polymerases up to 20 mM concentrations.[128] Proteinase K can inhibit nucleic acid amplification assays by digesting polymerases and other necessary enzymes, but it is permanently inactivated by a 5-minute incubation at 95 °C. Proteinase K can also be removed from RNA samples by electrophoretic methods, such as isotachophoresis.[63] SDS is typically incompatible with amplification assays at high concentrations, but the inhibitory effect of SDS can be mitigated using nonionic surfactants, including Triton X and Tween 20.[137] Potassium phosphate may also be used to precipitate SDS out of solution so that PCR can tolerate up to 0.3% w/v SDS.[151] A notable study lysed bacterial cultures with 0.5% SDS and 200 µg/mL proteinase K. The resulting lysate was heated to 95°C to inactivate proteinase K and added directly to a PCR master mix containing Tween 20 for direct amplification and detection of target bacterial DNA.[137] This provides a helpful blueprint for how cumbersome RNA purification may be avoided when using SDS and proteinase K for lysis and RNase inactivation.

2.4 CONCLUSIONS

I investigate alternative methods to the standard guanidinium-based buffers for inactivating endogenous RNases in human serum. I report the use of nonionic surfactants and proteases in blood, as well as two approaches to completely and permanently inactivate serum RNases. I found that degradation of RNA substrate was more pronounced in serum samples treated with common

nonionic surfactant, Triton X-100, than in samples without surfactant. I hypothesize this is due to the surfactants disrupting non-specific ribonucleoprotein complexes in serum that protect RNA from degradation via RNases. I recommend avoiding the use of nonionic detergents in RNase inactivation chemistries as they appear to have deleterious effect, even when used in combination with proteinase K. My results show proteinase K digests RNase A with ease yet is unable to remove all endogenous serum RNases. I found there is an optimum proteinase K concentration of 50 μg/mL for RNase inactivation in serum digestions, with higher and lower concentrations offering significantly worse results. The data suggest there may be certain serum RNase variants that are resistant to proteolytic digestion. This is an unexpected result that contradicts widespread *a priori* assumptions in microbiology that proteinase K eliminates nucleases in biological samples.

I observed that proteinase K is only able to irreversibly inactivate serum RNases in the presence of denaturing concentrations of SDS (i.e. 0.5% or greater). SDS at these higher concentrations immediately inhibits serum RNases, but their activity is regained once the SDS concentration is lowered. Irreversible RNase inactivation by way of SDS requires an incubation combined with proteinase K, DTT, or both. These RNase inactivation techniques use reagents which do not necessitate subsequent solid- or liquid-phase extraction prior to qPCR, simplifying the diagnostic process. It is worth noting that SDS, proteinase K, and DTT are relatively innocuous reagents which allows for safe handling and disposal in resource-limited clinical settings. This is in contrast with solid- or liquid-phase extractions which use hazardous chemicals and flammable organic solvents. Ultimately, my work aims to assist researchers developing simple POC NAATs for bloodborne RNA viruses or other RNA targets.

Chapter 3. HIV DETECTION WITH ITP-BASED RNA EXTRACTION

3.1 INTRODUCTION

The number of people infected with HIV globally continues to steadily increase, with the current total over 36 million.[152] Since the advent of highly effective antiretroviral therapy (ART), almost 20 million HIV-positive people are on treatment, which requires routine viral load monitoring to assess successful viral suppression.[153] Additionally, early infant detection of HIV infections is not possible with typical lateral flow-based antibody tests, so highly sensitive nucleic acid amplification testing (NATs) must be used to detect HIV nucleic acids.[154] The majority of nucleic acid testing for HIV in low- and middle-income countries (LMICs) is carried out on dried blood spots shipped to central laboratories, where expensive automated tests quantitate viral titers.[155] There have been increased efforts to scale-up decentralized HIV molecular testing in LMICs, and several point-of-care (POC) viral load tests have reached market to address this need.[156] Yet effective scale-up efforts have been hampered by the platform and per-test costs, as well as the operational complexity of current viral load tests.

The majority of current commercial HIV POC tests have miniaturized and automated gold-standard approaches to molecular testing of RNA from blood samples.[156] A primary roadblock for simplifying these tests for POC use is sample preparation, which requires removing the salts, proteins, cellular debris, and nucleases present in blood.[19] Endogenous blood RNases are particularly problematic because they are exceptionally stable enzymes and capable of rapidly degrading free RNA in blood in the order of seconds.[20,21] Traditional sample preparation methods for bloodborne RNA targets utilize high concentrations of chaotropic salts (e.g. 6 M guanidinium thiocyanate), toxic disulfide reducing chemicals (e.g. ß-mercaptoethanol), and harsh anionic detergents to lyse virions and inactivate blood RNases.[25,109,157] Highly effective nucleic acid

extraction and purification from the lysate is required to prevent chemicals from interfering with downstream amplification assays. Solid phase extraction is commonly used for purification, but this necessitates repeated buffer exchanges to separate, wash, and elute nucleic acids.[28] For example, a gold standard product for viral RNA extraction is the QIAamp Viral RNA Mini Kit (Qiagen), and it requires 6 manual pipetting steps and 5 centrifugations, totaling 30 minutes to an hour of hands-on time – according to the product handbook. Commercial POC tests automate these steps using robotics, pumps, valves, and other methods for fluidic exchanges.[28] Automating extensive fluidic manipulation requires complicated engineering designs and expensive components. This approach faces a practical barrier to lowering the overall platform costs of molecular testing in blood samples, which has prompted researchers to find new sample preparation approaches for POC use.

Isotachophoresis (ITP) is an electrophoretic separation and concentration technique that has emerged as an attractive alternative to address the need for simplified nucleic acid sample preparation for POC NATs. ITP is capable of extracting nucleic acids from blood samples and removing contaminants, such as various proteins or salts, that inhibit downstream amplification assays.[158] This separation process requires no physical manipulations, buffer exchanges, or other intermediate user steps, but rather automates nucleic acid purification using an applied electric field and simple buffers. ITP leverages a discontinuous buffer system with a leading electrolyte (LE) and trailing electrolyte (TE) to develop an electric field gradient that focuses charged species based on their electrophoretic mobilities.[159] Analytes with mobilities less than the LE and greater than the TE are focused into a concentrated plug at the interface of the two electrolytes. Kondratova et al. were the first to use ITP in agarose gels for DNA extraction from human blood samples, but their work was not well-suited for POC diagnostics because it required lengthy deproteinization

and dialysis pretreatment steps.[46,160] Microchannel-based ITP has since emerged as a promising sample preparation approach for extracting DNA from blood specimens and amplifying with off-chip quantitative polymerase chain reaction (qPCR).[48,161] Notably, Eid et al. detected DNA from *Listeria monocytogenes* cells in 2.5 µL of whole blood using alkaline and proteinase K lysis, microchannel ITP purification, and recombinase polymerase amplification for detection.[162] To my knowledge, the only example of an ITP extraction of RNA from blood samples targeted bacterial rRNA in whole blood and suffered a poor limit of detection due to a low sample volume (~1 nL) and incomplete inactivation of exogenous and endogenous RNases.[163] There have been no reported ITP-based extractions of viral RNA from blood or serum.

In moving towards molecular diagnostics that are appropriate for POC use in LMICs, there are continuing efforts to implement ITP in microfluidic paper-based analytical devices (µPADs). µPADs are well-suited for POC diagnostics due to their wicking properties, ease of reagent deposition and storage, low material cost, and established methods for high-volume manufacturing.[164] There are a number of ITP µPADs that have investigated extraction and concentration of analytes (e.g. fluorophores, DNA, indicator dyes) from pure buffer systems. [165–170] Our group has previously developed an ITP µPAD that extracts free DNA from human blood and amplifies DNA within the ITP plug using recombinase polymerase amplification (RPA). However, sample preparation for POC NAATs for HIV and many other bloodborne infectious diseases requires lysis of the viral envelope, immobilization of harmful blood RNases, and RNA extraction from lysate. I am not aware of any ITP µPADs that addressed these challenges and detected viruses or other molecular targets from blood samples.

In this chapter, I report a method for HIV detection from human serum with an MS2 bacteriophage internal process control using a novel lysis and RNase inactivation method, paper-

based ITP, and duplexed reverse transcription recombinase polymerase amplification (RT-RPA). My previous work studied varied enzymatic and chemical approaches for immobilizing blood RNases.[171] I build on this work to develop a novel 15-minute protocol for off-chip viral lysis, RNase inactivation, and serum protein digestion. I design a unique ITP system to focus RNA into a characteristic ITP plug, while excluding proteinase K and anionic detergent present in the lysate. I determine the limit of detection of the ITP μPAD for RNA extraction by processing digested serum spiked with known RNA concentrations and amplifying with off-chip RT-RPA. I then demonstrate detection of HIV virions and MS2 bacteriophage in human serum within 45-minutes. I seek to address the lack of ITP sample preparation studies for RNA molecular testing, and I propose that ITP μPADs may be employed for low-cost, rapid molecular testing for bloodborne RNA viruses.

3.2 Materials and Methods

3.2.1 *Biological samples*

Human serum used in this study was from pooled blood samples from males with blood type AB (Sigma-Aldrich, St. Louis, MO, USA). According to manufacturer's specifications, pooled blood samples were centrifuged and resulting plasma was clotted via calcium addition. The resulting serum is identical to plasma, with clotting factors removed. Fluorescently labeled DNA was a 70 base pair (bp) double stranded DNA sequence modified with a single Alexa Fluor 488 molecule (Integrated DNA Technologies, Coralville, IA, USA).

Purified HIV RNA was prepared from HIV-1 supernatant as previously detailed by Lillis et al.[68] HIV-1 supernatant (Group M, Subtype A, NCBI accession number: JX140650) was obtained from the External Quality Assurance Program Oversight Laboratory (EQAPOL) at Duke University.[172] Viral RNA was extracted and purified using the QIAamp Viral RNA Mini Kit

(Qiagen, Hilden, Germany) according to the manufacturer's standard protocol. RNA was then quantified with quantitative real-time PCR based on the method described by Rouet et al. using Superscript® III one- step RT-PCR system (Life Technologies, Carlsbad, CA, USA).[173]

Experimental work on HIV virion detection from human serum used a non-infectious HIV strain to reduce laboratory safety risks. HIV detection work employed a cultured HIV-1 subtype B (8E5) virus (SeraCare, Milford, MA, USA). The 8E5 HIV contains a single base addition in its RNA genome at the pol gene, creating a reverse transcription-defective virus with no infectivity. The 8E5 HIV was supplied in a concentrated supernatant and then diluted with serum for experimental work. Bacteriophage MS2 was the internal process control for the HIV assay. The phage was grown and isolated using an established protocol.[174] MS2 stock solution was diluted with phosphate buffered saline and stored at -80 °C.

3.2.2 *Lysis, RNase inactivation, and protein digestion*

I employed a specialized chemistry for combined viral lysis, inactivation of blood RNases, and digestion of serum proteins. This chemistry was based on my previous work investigating various methods for inactivating blood RNases.[171] I incubated serum with a combination of 0.5% sodium dodecyl sulfate (Sigma-Aldrich), 1 mg/mL of proteinase K (Thermo Fisher Scientific, Waltham, MA, USA), and 10 mM dithiothreitol (Sigma-Aldrich). Working stock reagent concentrations were high, such that serum was only diluted 10% (i.e. a 40 µL sample contained 36 µL serum and 4 µL lytic reagents). I conducted a set of experiments extracting HIV RNA from pre-digested serum. For these RNA extraction experiments, I incubated serum with SDS and proteinase K in a water bath for 1 hour at 50 °C. Following this incubation, I spiked known concentrations of purified HIV RNA into the digested serum. For experiments detecting HIV virions in serum, I incubated serum spiked with 8E5 HIV for 15-minutes at 65 °C.

3.2.3 *ITP device construction and buffer composition*

ITP extractions were performed in single-use, disposable ITP μPADs consisting of a plastic petri dish (Thermo Fisher Scientific), acrylic reservoirs, and 22-gauge titanium wire electrodes (McMaster Carr, Elmhurst, IL, USA). Reservoirs were cut with a CO_2 laser cutter (Universal Laser Systems, Scottsdale, AZ, USA) and adhered to the petri dish bases with double-sided tape (3M, Maplewood, MN, USA). The ITP strip spanned the two reservoirs and was constructed Fusion 5 membrane (GE Healthcare, Chicago, IL, USA), which is made with a proprietary method to maximize porosity and minimize adsorption of biomolecules spanning the two reservoirs. Membranes were cut into a teardrop shape (40 mm long with maximum width of 8 mm and minimum width of 3 mm) with an electronic cutter machine (Cameo 3, Silhouette, UT, USA). The membranes were not washed or blocked, and they were stored at room temperature.

The TE buffer consisted of 70 mM Tris (Sigma-Aldrich), 70 mM serine (Sigma-Aldrich), and 0.1% w/v polyvinylpyrrolidone (PVP) (Sigma-Aldrich). The LE buffer in the ITP membrane was 135 mM Tris, 90 mM HCl (Sigma-Aldrich), 50 mM KCl (Sigma-Aldrich), 0.1% w/v PVP (Sigma-Aldrich), and 100 ng/mL poly(A) carrier RNA (GE Healthcare). The LE buffer in the anode reservoir contained 240 mM Tris, 160 mM HCl, 10 mM KCl, and 0.1% PVP. Buffers were prepared with molecular biology grade reagents, RNase-free water (Thermo Fisher Scientific), and PCR-grade microcentrifuge tubes (Eppendorf AG, Hamburg, Germany) to limit introductions of exogenous RNases.

3.2.4 *ITP extraction protocol*

The ITP μPAD processes a 40 μL sample of serum pretreated with proteinase K, SDS, and DTT. Experiments in this work used serum samples with either spiked RNA, spiked HIV, or no analyte. The first step in ITP extraction is pipetting 40 μL of sample onto the porous membrane in

the widened sample region next to the TE reservoir. 1 μL of fluorescently labeled DNA is also added to the sample region for monitoring the location of the ITP during the separation. Then 40 μL of LE buffer is added to wet the remainder of the membrane. 250 μL of LE and TE buffers are added to their respective reservoirs. Initial locations of ITP buffers and sample are depicted in Figure 3-1.

ITP is initiated with a constant 110-volt bias across the ITP strip applied with a source meter (model 2410, Keithley, USA). The ITP plug location is indicated by the fluorescently labeled DNA. I collected fluorescence images of the separation membrane with a microscope (AZ-100, Nikon, USA) equipped with a 0.5X (NA = 0.05) objective. Light supplied by a mercury lamp light source (*exacte*, X-Cite, USA) passed through an epifluorescence filter cube set (Omega Optics, USA) with peak excitation and emission wavelengths of 488 nm and 518 nm, respectively. A 16-bit cooled electron multiplying charge-coupled device camera (Cascade II, Photometrics, Tucson, AZ, USA) collected grayscale images of ITP extractions.

When the ITP plug reaches the center of the narrow extraction zone of the strip, the voltage bias is removed, and this region of the strip is cut out. For RNA extraction experiments, the extraction zone of the paper strip is placed in a 0.5 mL plastic tube with a small hole at the bottom. The 0.5 mL plastic tube is placed inside a 1.5 mL plastic tube and centrifuged, removing the contents of the ITP plug from the paper (~4 μL of eluate). This ITP eluate is pipetted directly into an RT-RPA reaction. For HIV detection experiments from serum, I add the extraction zone of the paper strip directly to an off-chip RT-RPA reaction for duplexed detection of HIV and MS2, as illustrated in Figure 3-1.

3.2.5 *RT-RPA amplification and detection*

The RT-RPA primers and probe for HIV detection were developed by Lillis *et al.* and can be used to amplify HIV-1 RNA across multiple subtypes.[68] The RT-RPA HIV detection assay used a lyophilized pellet solution consists of a lyophilized pellet of RPA reagents from the TwistAmp exo kit (TwistDx, UK), 29.5 µL rehydration buffer, 14 mM magnesium acetate, 540 nM forward primer (Integrated DNA Technologies), 540 nM reverse primer, 120 nM FAM-labeled probe (LGC Biosearch Technologies, Hoddesdon, UK), 0.2 U/µL RNasine RNase Inhibitor (Thermo Fisher), 0.5 U/µL reverse transcriptase (AffinityScript, Agilent, Santa Clara, CA, USA), and 1% w/v Triton X-100 (Sigma-Aldrich). The duplexed RT-RPA assay for HIV and MS2 employed the reagents listed above as well as 216 nM MS2 forward primer, 216 nM MS2 reverse primer, and 48 nM Fluor Red 610-labeled probe.

Experiments examining ITP plug purity used 4 µL of ITP extraction liquid and 2.5 µL of HIV RNA in the RT-RPA reactions. Experiments studying RNA extraction from digested serum used 4 µL of ITP extraction liquid in RT-RPA. For HIV detection experiments, I added the cutout paper ITP extraction zone (containing ~4µL of liquid) directly to RT-RPA reaction tubes. I used RNase-free water to bring all RT-RPA reactions to a total volume of 50 µL per tube. A standalone fluorometer specifically designed for point-of-care testing applications (T16-ISO, Axxin, Australia) heated and measured fluorescence of the RT-RPA reactions. Reaction tubes were removed after 5-minutes of incubation, briefly agitated, and returned to the fluorometer for another 10 minutes. The baseline fluorescence at 3-minutes was subtracted from fluorescence values at all measurement time points for each respective reaction tube. For the HIV assay, I used a threshold of 100 arbitrary fluorescence units in the FAM detection channel to differentiate between

successful and unsuccessful amplification. The MS2 assay fluorescence threshold was 50 arbitrary fluorescence units in the ROX detection channel.

3.2.6 *RNase detection assay*

I employed the RNaseAlert Substrate Detection System (Integrated DNA Technologies) for testing RNase activity in serum samples. I prepared the RNaseAlert experiments in a lidded 96-well plate with black walls and clear bottom (Corning Incorporated, Corning, NY, USA). The total assay volume for each well was 100 µL. Each RNase detection assay contained 10 µL of RNaseAlert substrate, 10 µL of 10X RNaseAlert buffer, 60 µL of RNase-free water, and 20 µL of sample. I used a 12-channel pipette to concurrently add serum samples to each well. The plate was immediately loaded into a plate reader (SpectraMax iD3, Molecular Devices, San Jose, CA, USA). The excitation and emission wavelengths were 485 nm and 535 nm, respectively. The gain was set to "low" with an exposure of 140 ms. The heating block in the plate reader was set to 37 °C. The instrument agitated the plate and measured the fluorescence in the wells every 2 minutes over a 30-minute incubation time.

3.3 Results and Discussion

This HIV detection assay with an MS2 bacteriophage internal control required serum pretreatment, RNA purification with the ITP µPAD, and duplexed RT-RPA. This diagnostic process is illustrated in Figure 3-1. Serum pretreatment is necessary for viral lysis, RNase inactivation, and serum protein degradation. Traditional methods for sample pretreatment in bloodborne pathogen assays leverage high concentrations of guanidine (4 to 6 M), which is a powerful chaotropic agent that denatures proteins.[25] Guanidine-based lysis buffers rapidly destroy viral envelopes and inactivate endogenous blood RNases, and they are easily paired with silica-

based columns or other substrates for solid phase extraction. Unfortunately, guanidine is difficult to pair with ITP systems for nucleic acid purification because high salt samples significantly disrupt the electric field gradient, hindering rapid ITP separation.[158] In this work, I utilize an alternative method for serum pretreatment that uses SDS and proteinase K for combined viral lysis, RNase inactivation, and protein degradation. SDS is a powerful protein denaturant that has long been used in lysis chemistries. Proteinase K is a broad spectrum protease that degrades proteins into a corresponding assortment of polypeptides.[21] Proteolytic digestion is a crucial serum pretreatment step in ITP-based extractions. It has been widely reported that extraction of nucleic acids with ITP is inhibited by nonspecific binding with blood proteins.[47,63,161,162] Extensive protein degradation reduces nucleoprotein complex formation and allows for electromigration of nucleic acids.

I designed the ITP system to separate RNA from inhibitors of downstream RT-RPA and achieve high analyte accumulation in the ITP plug. Both SDS and proteinase K are potent inhibitors of RT-RPA because they inactivate the enzymes and proteins required in the amplification mechanism. SDS is an anionic detergent, so dodecyl sulfate carries the same negative charge as nucleic acids in most buffer conditions. Therefore, it is challenging to electrophoretically separate dodecyl sulfate from nucleic acids using ITP. I instead removed dodecyl sulfate from the lysate with precipitation mediated by a potassium salt, leveraging the very low solubility of potassium dodecyl sulfate (KDS) in water.[175] Potassium salts have previously been shown to remove dodecyl sulfate from nucleic acid samples, enabling direct PCR analysis with no inhibition.[151] I employed potassium chloride in the leading electrolyte in the ITP strip and in the reservoir. Upon application of the electric field, potassium cations migrated from the LE buffer

toward the cathode in the TE reservoir. Potassium cations therefore encountered dodecyl sulfate in this migration path and formed KDS precipitate, as illustrated in Figure 3-1.

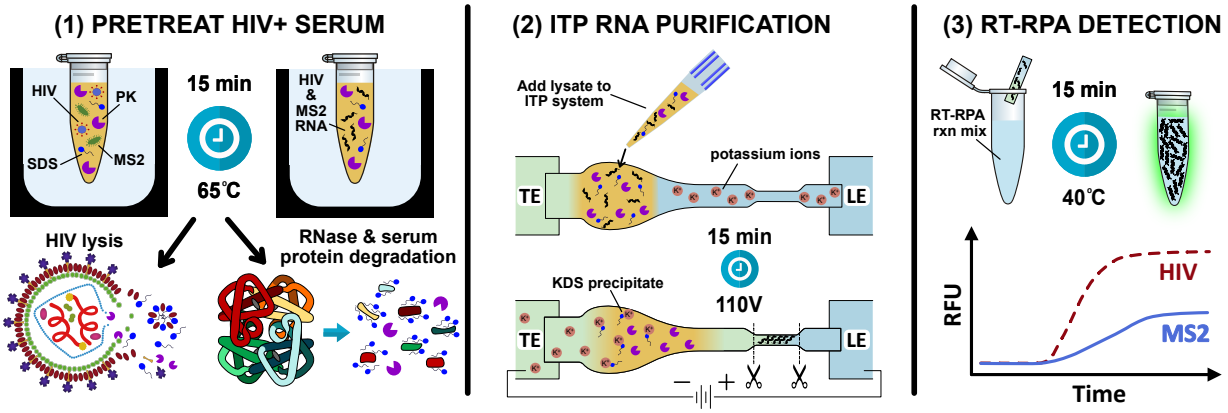

Figure 3-1. Overview of the diagnostic process of HIV+ serum with an internal MS2 control. HIV+ serum spiked with MS2 phage is pretreated with proteinase K, SDS, and DTT at 65°C for 15 minutes. SDS and proteinase K simultaneously lyse HIV and degrade endogenous blood RNases. Free HIV and MS2 RNA are extracted and purified with ITP from serum components, proteinase K, and SDS. Potassium ions in the leading electrolyte precipitate potassium dodecyl sulfate, preventing the anionic detergent from focusing in the ITP plug. A duplexed RT-RPA reaction directly from the cut portion of the paper strip simultaneously amplifies HIV and MS2.

Proteinase K in the serum lysate can be purified away from viral RNA with ITP based on its charge. Proteinase K has an isoelectric point of 8.9 and therefore has a net positive charge in buffers less than pH 8.9.[21] In electrokinetic systems that maintain pH less than 8.9, proteinase K electromigrates in the opposite direction of nucleic acids due to their contrasting charges. ITP systems must be carefully designed because pH gradients can be severe depending on the selection of TE, LE, and buffering counterion. I used numerical simulations to guide my design of the ITP system and select proper electrolytes for purifying and extracting RNA from serum. I used an open source electrophoretic modeling tool, the Stanford Public Release Electrophoretic Separation Solver (SPRESSO), to approximate concentration and pH profiles resulting from various ITP

buffers and plot the simulation outputs in Figure 3-2. I do not go into depth on the equations and assumptions of the simulations here, but details can be found in the original SPRESSO report.[176]

In Figure 3-2A, I show simulated concentration profiles of distinct ionic species for an ITP system with a leading electrolyte comprised of 160 mM HCl and 240 mM tris paired with a trailing electrolyte of 70 mM tris and 70 mM serine. As ITP progresses with an applied electric field, three distinct zones are formed: the original TE zone, the adjusted TE (ATE) zone, and the LE zone. The ATE zone is a region with TE ions which was previously occupied by the LE. As seen in Figure 3-2A, the ATE has increased concentrations of serine and tris compared with the original TE. Figure 3-2B shows that the pH of the ATE in this ITP system is also significantly higher than the TE. I found that using serine as the TE and an LE comprised of HCl with tris as the counterion maintained a pH less than 8.9 in all regions. Therefore, the ITP system was designed for proteinase K to be positively charged and electrophoretically separated from RNA.

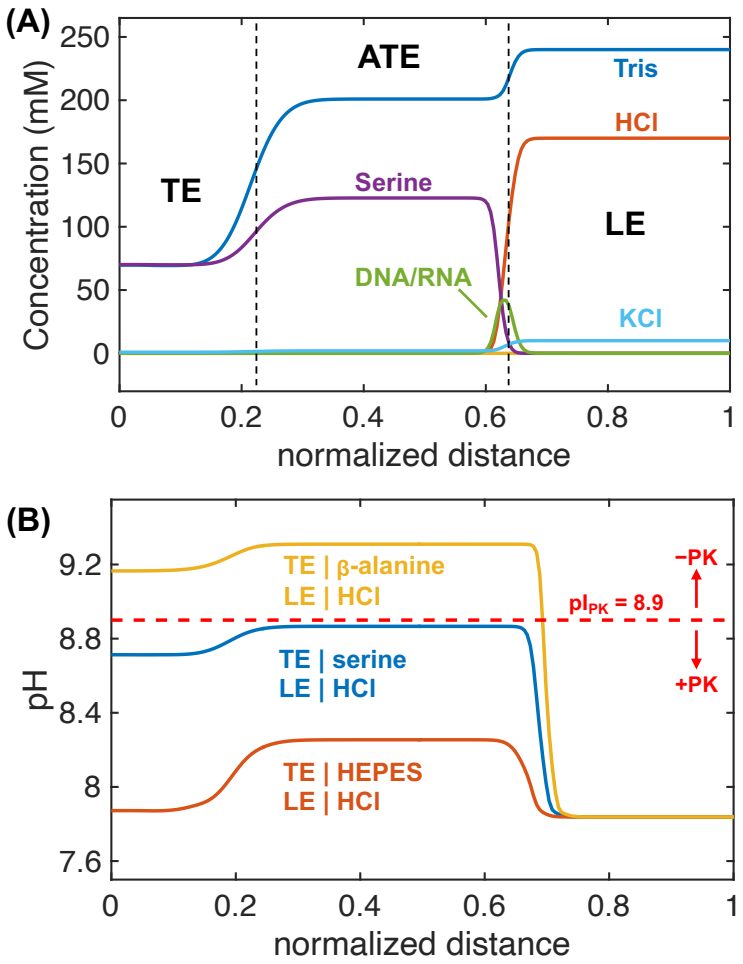

Figure 3-2. Simulations describing the ion concentration and pH profiles of ITP systems. (A) SPRESSO simulation results of concentration profiles with a TE buffer compromised of 70 mM Tris and 70 mM serine and a LE buffer of 240 mM Tris, 160 mM HCl, and 10 mM KCl. As the ITP plug migrates into the region previously containing LE, an adjusted trailing electrolyte (ATE) zone develops directly adjacent to the ITP plug. (B) Simulation results of pH profiles of three different TE selections: HEPES, serine, and ß-alanine. All TE, LE, and counterion concentrations are the same as in (A). The pH of the ATE differs from 8.26 to 9.31 depending on the TE selection. When the pH of the ATE zone is less than 8.9, proteinase K is positively charged and will not electromigrate with negatively charged RNA.

I found that serine (pKa = 9.33, fully ionized electrophoretic mobility of 34.3×10^{-9} m^2 V^{-1} s^{-1}) was a highly effective TE not only for its suitability for proteinase K removal, but also in

maximizing nucleic acid extraction. It has been reported in the literature that lowering the TE conductivity is a key mechanism for increasing analyte accumulation in the ITP plug.[49] Low conductivity creates high electric fields in the TE region of the ITP system, resulting in faster electromigration of analytes in this zone and enhanced accumulation in the ITP plug. I found that under a pH of 9 serine has a very low electrophoretic mobility, resulting in low conductivities in the TE and ATE zones. A majority of the ITP studies on nucleic acid extraction from blood use HEPES (pKa = 7.66, mobility of 21.8×10^{-9} m^2 V^{-1} s^{-1}) as the TE.[158] I demonstrate in Figure 3-2B that HEPES maintains relatively low pH in the system and is well-suited for removing proteinase K. However, HEPES has a higher electrophoretic mobility than serine at pH less than 9, so I found that HEPES could not generate as high of electric field strength in the ATE zone as serine (~0.5x lower). The lower electrophoretic mobility of serine is also useful in focusing HIV RNA that may have reduced mobility in the ITP system due to the tortuosity of the porous membrane and polypeptides that may bind or interact with RNA.[177] There have also been reports of ITP nucleic acid extractions from blood samples using ß-alanine (pKa = 10.24, mobility of 30.8×10^{-9} m^2 V^{-1} s^{-1}) as the TE which offers very high electric field strength in the ATE zone and extraction efficiencies up to 93%.[47,160] However, I found that the high pKa of ß-alanine resulted in a higher alkaline ATE than serine, making it ineffective for proteinase K removal (see Figure 3-2B). I experimented with different counterions, which can be used for pH control, but I found that using tris as the counterion resulted in ITP plugs near pH 8 that were highly compatible with RT-RPA reaction conditions which are also tris-buffered (~pH 8).

In order to ensure simulations were predictive, I experimentally verified SPRESSO simulations predicting the pH profile of an ITP system. I performed ITP in a paper membrane and placed a strip of pH paper on top of the ITP membrane to visualize its approximate pH profile. I

compared these results to simulations of the same ITP system in SPRESSO. I examined an ITP system employing a unique TE consisting of 10 mM tris, 10 mM serine, and 10 mM ß-alanine. The LE contained 120 mM HCl and 180 mM tris. I performed paper-based ITP for 10 minutes at 1 mA constant applied current. In Figure 3-3, I show experimental images of the ITP device with pH paper applied to the ITP membrane both before and after ITP. I observed a two distinct pH zones to the left of the ITP plug. The first zone contains serine ions and the second contains ß-alanine. ß-alanine has a lower electrophoretic mobility than serine in the system. The serine zone is at a significantly higher pH than the ß-alanine zone. I found good agreement between the experimental results and the simulated pH profiles generated by SPRESSO. This suggests that SPRESSO is a useful tool in designing ITP systems, especially for applications where pH control is important.

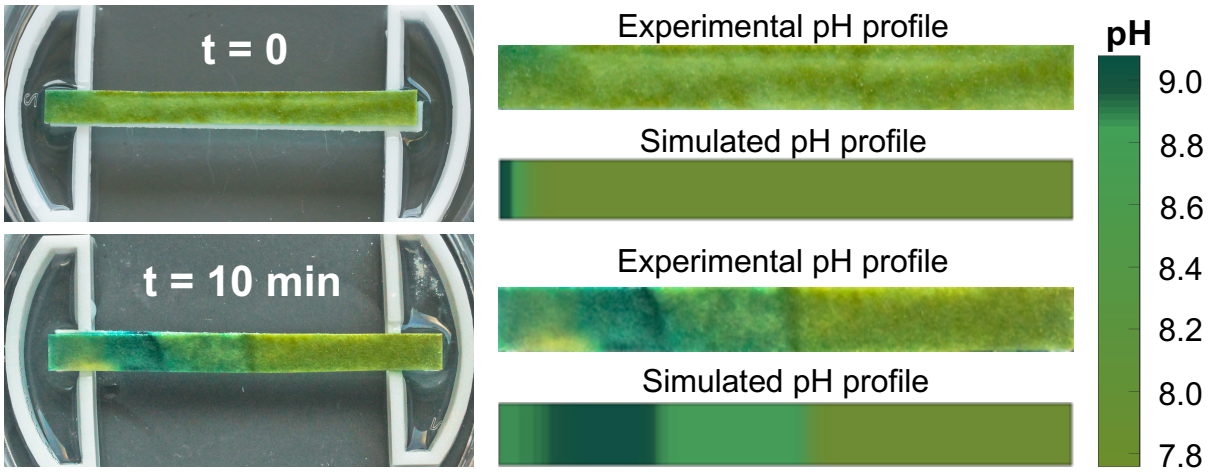

Figure 3-3. Simulations and experiments describing the pH profiles of an ITP system with ß-alanine and serine in the TE buffer. Experimental images of an ITP µPAD with pH paper overlaid on the separation membrane (left side). Images of pH paper were taken at t = 0 and t = 10 mins. Comparisons of SPRESSO simulations and experimental images of pH paper of the ITP system (right side). The ITP system employed a 10 mM Tris, 10 mM ß-alanine, and 10 mM serine TE buffer with 150 mM tris and 100 mM HCl LE buffer. After the LE/TE interfaces migrates 50% of

the strip length, a serine zone with pH ~8.8 develops directly adjacent to the ITP plug, followed by a ß-alanine zone at pH ~9.1.

3.3.1 *Electromigration of nucleic acids through porous membranes*

I screened an assortment of different porous membranes to identify the ideal substrate for minimizing analyte loss during electromigration. Several studies have reported issues with nucleic acid adsorption to substrates or entanglement in porous membranes.[178,179] I use fluorescence imaging of labeled DNA to visualize electromigration of nucleic acids with ITP and identify paper substrates that result in DNA entanglement or adsorption. Figure 3-4 illustrates electromigration of DNA (70 bp) labeled with Alexa Fluor 488 through two different membranes: Fusion 5 (GE Healthcare) and glass fiber (GFCP203000, EMD Millipore). I used a TE buffer consisting of 20 mM tris and 20 mM serine and an LE buffer with 120 mM HCl and 180 mM tris. I used porous membranes cut into straight strips (35 mm by 3 mm). After 15 minutes of ITP in glass fiber, I observe pockets of fluorescence trailing behind the ITP plug. This indicates adsorption or entanglement of DNA occurs during electromigration. Due to this undesirable source of analyte loss, I explored other membranes for use in paper-based ITP. I observed similar DNA adsorption issues in several other glass fiber membranes that are commonly used in lateral flow assays (data not shown). I found that DNA is able to successfully electromigrate through Fusion 5 membrane during ITP with no observable loss of analyte.

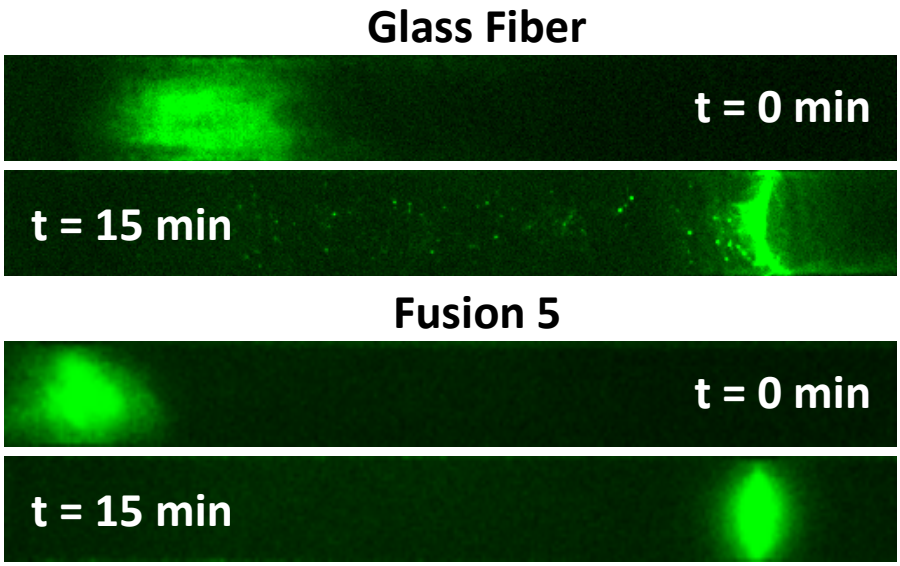

Figure 3-4. Electromigration of fluorescently labeled DNA through porous substrates. I transported DNA labeled with Alexa Fluor 488 across Fusion 5 and glass fiber membranes under identical conditions. Fluorescence images at t = 0 and t = 15 minutes are shown.

Visual observations of DNA transport are useful in designing ITP systems and selecting appropriate membranes, but do not provide information on whether low copies of nucleic acids electromigrate through paper and are viable for amplification. To investigate analyte loss with low copies of nucleic acid, I electromigrated DNA and RNA across porous membranes and detected successful transport with off-chip RPA or RT-RPA. For DNA extractions, I used 200 bp synthetic DNA of a proviral HIV gene and corresponding RPA primers and probe, as previously described.[63] I were able to consistently electromigrate 10 copies of DNA across the length of a Fusion 5 strip and detect them with RPA. Figure 3-5A shows fluorescence measurements over a 20-minute RPA reaction, with fluorescence over 100 arbitrary fluorescence units indicating successful amplification. I also performed experiments electromigrating HIV-1 RNA with an 8,941 bp genome length. I could consistently migrate 50 copies of HIV RNA across the Fusion 5 membrane.

Figure 3-5B shows successful amplification of 50 copies of HIV RNA after ITP extraction (N = 3).

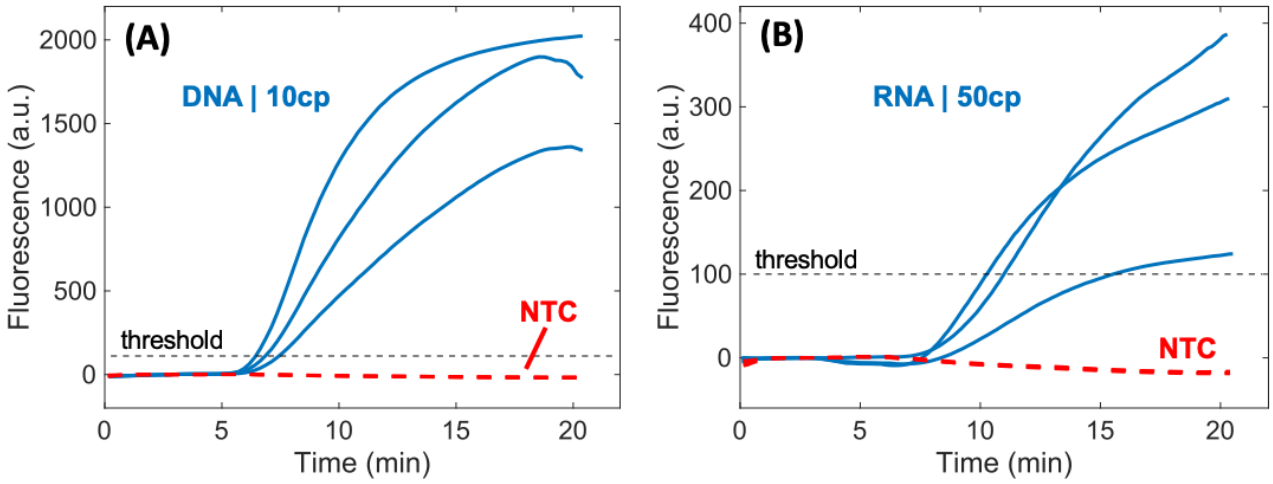

Figure 3-5. Fluorescence measurements of RPA reactions to detect successful electromigration of DNA or RNA across a paper membrane in a pure buffer system. (A) Triplicate experiments of 10 DNA copies extracted with ITP and amplified with RPA. RPA reactions with extracted DNA consistently amplified over the positive/negative threshold of 100 arbitrary fluorescence units. (B) Triplicate experiment of 50 HIV RNA copies extracted and then amplified for detection. Extracted RNA was consistently amplified over the positive/negative threshold. I observed that no template controls (NTCs) for both assays (N = 3 for each) were very consistent and never approached the positive/negative threshold.

3.3.2 *Visualization of DNA Extraction from Serum*

I examined the nucleic acid extraction performance of the ITP µPAD using fluorescence imaging of labeled DNA. I found that labeled DNA was a convenient analyte for optimizing experimental conditions and studying ITP dynamics. The ITP device employs a uniquely shaped porous membrane with a wide sample region that holds a 40 µL volume, as shown in Figure 3-6A. After 15 minutes, nucleic acids are electromigrated into an extraction region containing approximately 4 µL, which can be cut out and added to an RT-RPA reaction. This concentration

step from a large sample volume to a 10-fold smaller extraction volume is advantageous for detecting HIV which may contain less than several hundred RNA copies in 40 μL of serum.

In Figure 3-6B, I present experimental images of an ITP extraction of DNA labeled with Alexa Fluor at a concentration of 100 nM in 40 μL of digested serum. I show images of the early electromigration and focusing into a concentrated plug over the first 10-minutes of ITP. I plot the *y*-averaged intensity as a function of strip length at 0, 5, and 10 minutes. Before the electric field is applied (t=0) the DNA is diffusely distributed over the sample zone with a low average fluorescent intensity. Labeled DNA electromigrate out of the sample zone into the straight region of the strip, forming a concentrated plug between the LE and ATE. After 10 minutes, the DNA has electromigrated across the majority of the strip length, reaching a distance approximately 23 mm from the middle of the sample zone. An additional 5 minutes of migration centers the ITP plug in the extraction region of the strip. I approximated the extraction efficiency of the ITP system by dividing the total fluorescence within the ITP plug by the total fluorescence of 4 picomoles of labeled DNA. I observed extraction efficiencies ranging from 68 to 80% with a 40 μL digested serum sample. I observed improved extraction efficiencies, up to greater than 90%, when processing diluted samples. However, it is reasonable that labeled DNA accumulation within the ITP plug may happen more rapidly and efficiently than with viral RNA targets. HIV RNA is about 10 kilobase pairs in length, and its electrophoretic mobility is likely reduced by the porous media while the labeled DNA (70 bp) is less impeded.

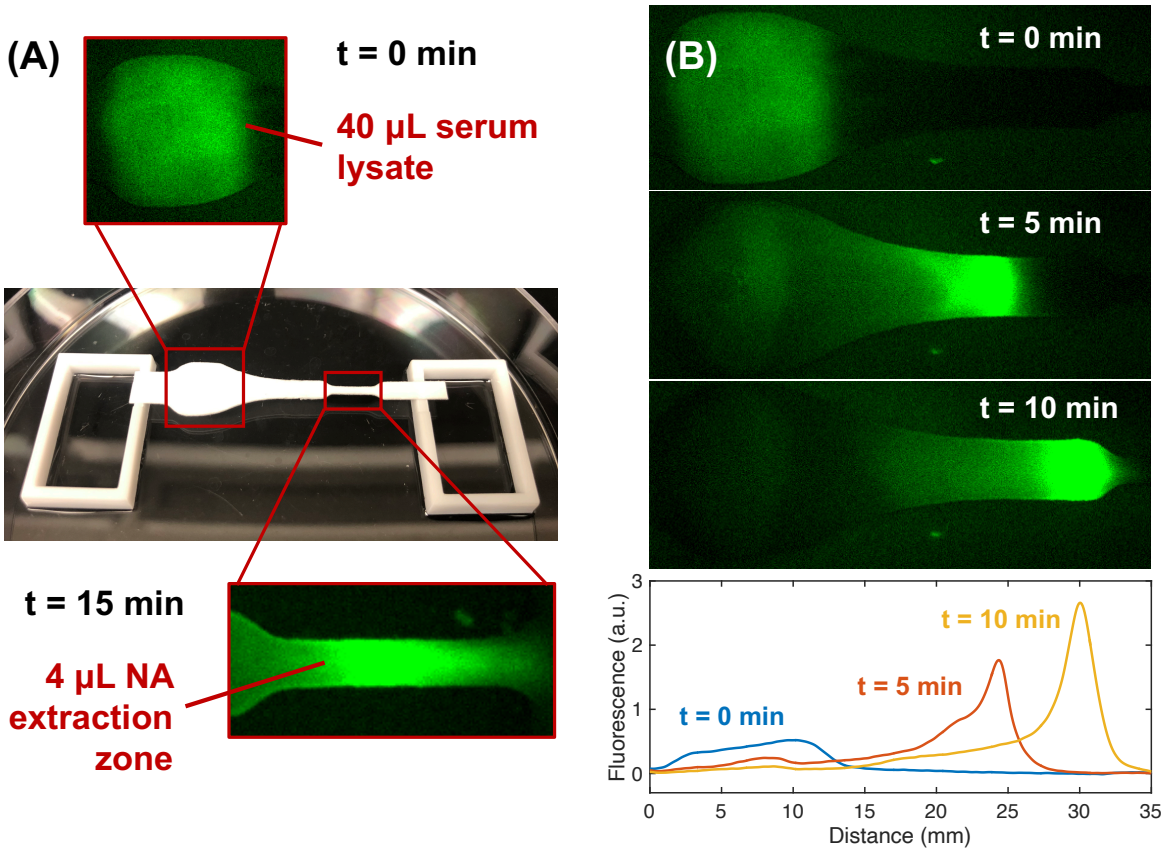

Figure 3-6. Experimental fluorescence images of ITP extraction of labeled DNA from proteolyzed serum. (A) The ITP system consists of a paper strip spanning two acrylic reservoirs within a plastic petri dish. Nucleic acids are extracted from a 40 µL serum lysate into a 4 µL extraction zone. (B) DNA labeled with Alexa Fluor 488 is mixed with digested human serum and is initially located in the wide sample zone of the Fusion 5 membrane. DNA focuses into a concentrated plug in the straight portion of the strip (t=10 min) before entering the extraction zone (~t=15 min). Pixel intensities of the images are y-averaged, creating normalized fluorescence distribution with respect to distance along the membrane for each time point (0, 5, and 10 minutes).

I observe several interesting phenomena in extraction experiments with the ITP µPAD. The data suggest DNA concentration profiles are Gaussian, as predicted by peak-mode ITP literature.[49] I observe electroosmotic flow of the system causes slight dispersion of the plug, widening the DNA distribution and reducing the maximum peak intensity. Electroosmotic dispersion is common in electrokinetics systems and has been extensively studied in

isotachophoresis.[180,181] A region of low-level fluorescence is evident trailing the ITP plug. I hypothesize this fluorescence is from DNA that has formed complexes with polypeptides in the proteolyzed serum proteins, reducing its electrophoretic mobility and preventing stacking. This phenomenon has been previously observed in ITP studies and is supported by the propensity of nucleic acids to nonspecifically interact with proteins in biological samples.[132,161] I also see a small amount of residual fluorescence remain in the sample region of the ITP strip during extraction. I believe this is due to a trace amount of target DNA adsorbing to the porous membrane.

I demonstrate the importance of extensive proteolytic digestion of serum proteins in enabling ITP extraction of nucleic acids. Figure 3-7A shows fluorescence images of DNA extraction from serum digested with 1 mg/mL proteinase K (1 hr incubation at 50 °C), with corresponding y-averaged intensity profiles as a function of strip length. The experiment shown in Figure 3-7B is identical to that of Figure 3-7A, except serum was not proteolyzed with proteinase K. Digestion of serum proteins with proteinase K clearly alters the behavior of ITP-based DNA extraction. Other reports on DNA extraction from serum and plasma have stated that ITP cannot adequately separate DNA without deproteinization of the sample.[46,47] My findings are consistent with these reports. I observe undigested serum hinders the electromigration of DNA through porous membranes, likely due to nucleoprotein complexes that form between serum proteins and DNA. I conclude that thorough digestion of serum proteins is critical to efficient DNA extraction.

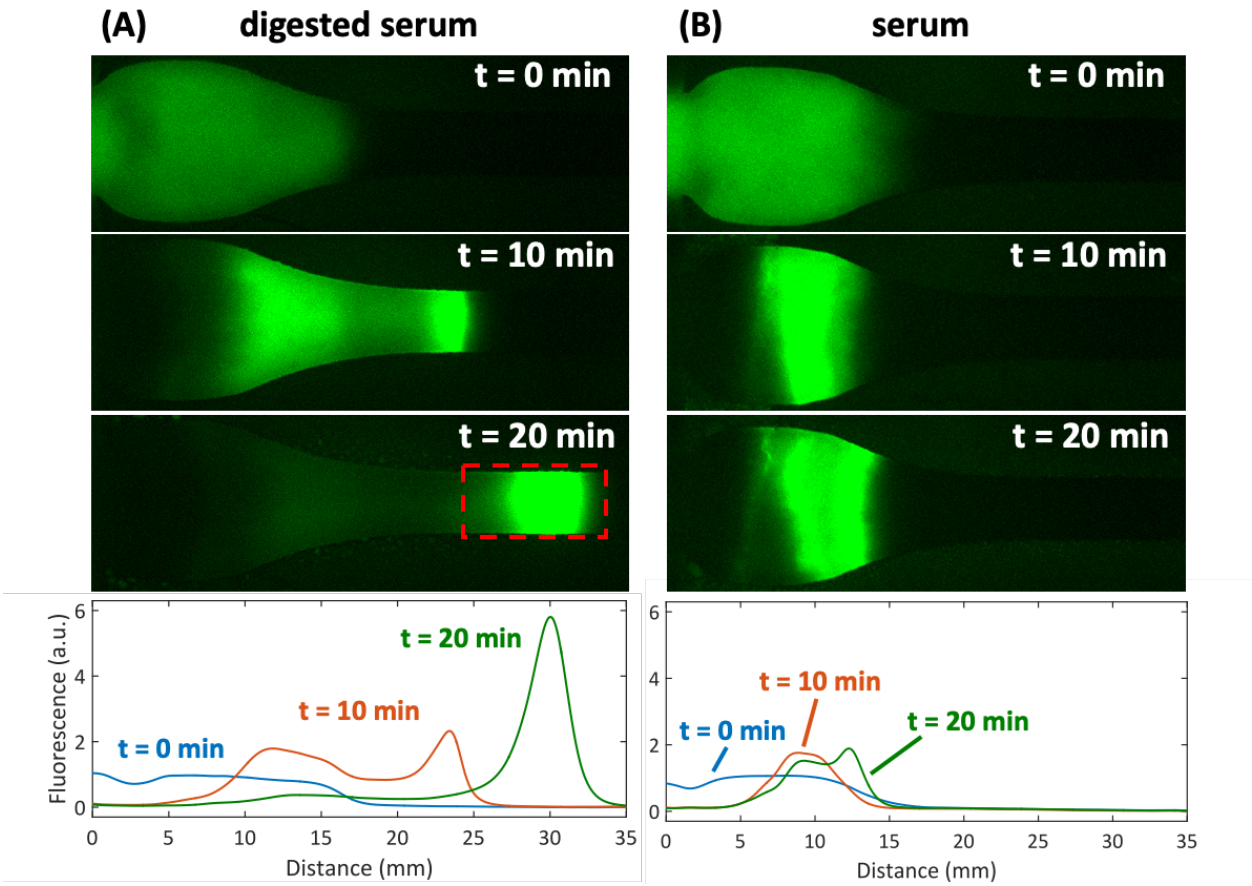

Figure 3-7. Experimental fluorescence images of ITP extraction of nucleic acids from digested serum and untreated serum. (A) DNA labeled with Alexa Fluor 488 is mixed with digested human serum and is initially located in the wide sample zone of the Fusion 5 membrane. After 20 minutes of ITP, DNA focuses into a concentrated plug in the straight portion of the strip. Pixel intensities of the images are y-averaged, creating normalized fluorescence distribution with respect to distance along the membrane for each time point (0, 10, and 20 minutes). (B) ITP extraction of labeled DNA from untreated serum is presented for comparison. Without serum digestion, DNA migration is hindered and does not electromigrate across the length of the strip.

3.3.3 *Extraction of HIV DNA and RNA*

I performed a set of experiments to further assess the purity of the ITP plug by observing its effect on RT-RPA. For these experiments, I processed a 40 µL serum lysate with no added HIV RNA with the ITP system. The extraction zone of the strip was centrifuged to dewater the

membrane. The resulting ITP plug eluate (~4 µL) was added to an RT-RPA reaction with 500 copies of HIV RNA to observe the effect on amplification. Figure 3-8 shows fluorescence amplification curves detecting HIV RNA which indicate the compatibility of ITP plugs with RT-RPA. Positive control reactions with only HIV RNA are provided for comparison. I found that the contents of ITP plugs in extractions including KCl in the LE did not significantly affect RT-RPA performance. In ITP extractions with no KCl, the contents of the ITP plug inhibited RT-RPA such that no amplification was detected. This indicates that the potassium-mediated SDS precipitation removed enough of the anionic detergent to enable RT-RPA. My results also indicate that the ITP system with a serine-based TE was successful in preventing proteinase K from focusing in the ITP plug. This supports simulations of pH conditions that found the ITP system pH was less than the isoelectric point of proteinase K.

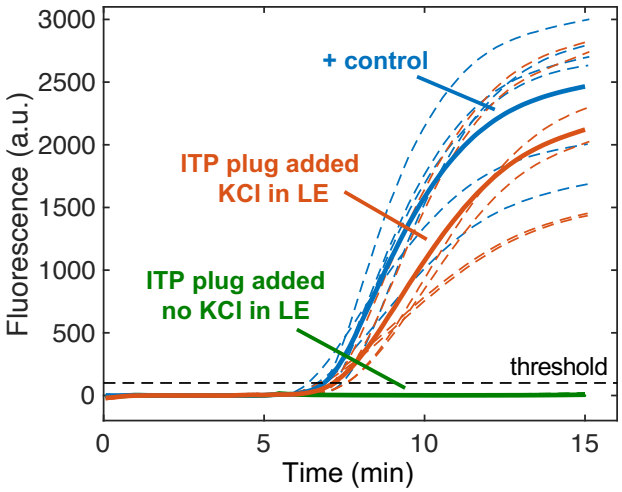

Figure 3-8. Purification of nucleic acids from serum lysates via paper-based ITP. (A) Fluorescence measurements of RPA assays assessing the level of inhibitors present in ITP plugs. Experiments evaluating ITP purification have 500 copies of HIV-1 RNA with 4 µL of ITP plug eluate added into them. Positive control reactions contain only 500 copies of RNA. I plot the replicate amplification curves (N=6 for each) with a dashed line and respective averages with a solid line. Two different ITP systems were evaluated: one containing potassium chloride in the leading

electrolyte to precipitate dodecyl sulfate and the other with no potassium chloride. Positive control experiments (N=3) simply include nuclease free water.

I found that ITP systems with poor TE selections were not able to remove contaminants from the ITP plug. SPRESSO simulations indicated that some TEs resulted in an elevated ATE pH, which leads to proteinase K migrating into the ITP plug along with RNA. In Figure 3-9, I show data for two different ITP systems to demonstrate the importance of TE selection. The first ITP system featured only ß-alanine as the trailing electrolyte. ß-alanine can be a powerful TE for extracting analytes due to its extremely low electrophoretic mobility at most pH levels.[47] However, it is not well-suited for preventing proteinase K from electrophoresing into the plug. The ITP system processed a digested serum sample and the contents of the ITP plug were added to RPA reactions with 1,000 copies of HIV RNA. As expected, these experiments did not amplify because proteinase K was not electrophoretically removed. The second ITP system was designed to remove proteinase K from the ITP plug with a serine TE. This ITP system generated an ITP plug that had minimal effects on the amplification of HIV RNA.

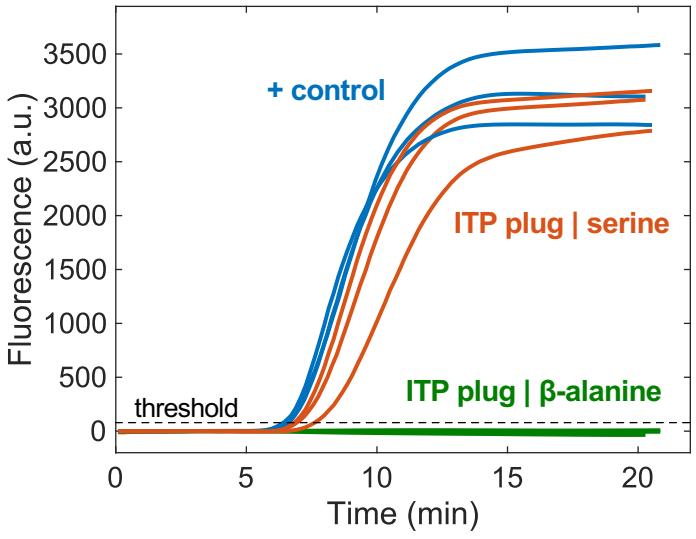

Figure 3-9. Purification of nucleic acids from serum digested with only with proteinase K using different TE selections. I used ITP to process digested serum (no nucleic acids added) with either

serine or ß-alanine TEs. ITP plugs were added to RPA reactions with 1,000 copies of HIV-1 RNA. Fluorescence measurements of RPA indicate the purity of the ITP plugs. Positive control experiments (N = 3) simply include nuclease free water. Serine experiments (N = 3) utilized an ITP chemistry with 10 mM serine. ß-alanine experiments (N = 3) employed a TE buffer with 10 mM ß-alanine.

I analyzed the performance of the ITP μPAD for RNA extraction using pre-digested serum spiked with known concentrations of HIV-1 RNA. Figure 3-10 presents amplification curves for extracted HIV-1 RNA at different input concentrations in serum. The assay could successfully detect 5,000 copies of HIV RNA per mL of serum, corresponding to 200 RNA copies per 40 μL of processed serum. As expected, I found that amplification is much more robust when extracting and detecting higher concentrations of HIV in serum. I found that the sample pretreatment protocol for digesting serum proteins and inactivating endogenous RNases was crucial for subsequent RNA extractions. My early experimental efforts struggled with rapid RNA degradation in serum samples with no RNase control measures, which is consistent with previous reports of extensive RNA degradation in serum on the order of seconds.[20]

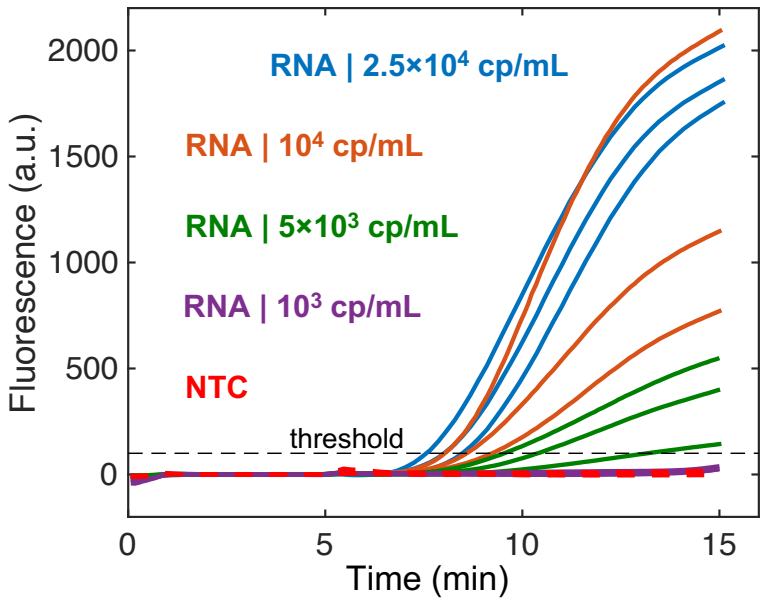

Figure 3-10. Extraction of HIV RNA from digested serum. 5,000 HIV-1 RNA copies per mL of digested serum (200 copies in 40 µL of serum) were consistently extracted and amplified over the threshold fluorescence value with RT-RPA (N=3). No template control (NTC) experiments (N=3 for each assay) did not increase in fluorescence.

In addition to the RNA extractions, I analyzed the performance of the ITP µPAD by extracting DNA from digested serum. Figure 3-11 presents fluorescence amplification curves for extracted DNA and respective triplicate NTCs. The LoD of DNA (200 bp) spiked into digested serum was determined to be 500 copies per mL of serum. This is equivalent to 20 copies in the 40 µL sample volume. The LOD for extracting DNA from digested serum in the ITP µPAD is an order of magnitude better than for extracting RNA. I believe there are multiple reasons for this result. I used synthetic DNA (200 bp length) which is an easier analyte for diagnostics due to the stability of DNA and the low prevalence of harmful DNases in human serum. RNA is much more prone to degradation chemically or due to endogenous RNases. DNA that has a short length is easier for ITP extractions in porous membranes because its electrophoretic mobility is not as hindered as HIV RNA (~9 kb). Further, the RPA assay for DNA used in this work has nearly

single-copy sensitivity, while the RT-RPA assay for HIV has sensitivity down to approximately 30 copies per reaction.[182]

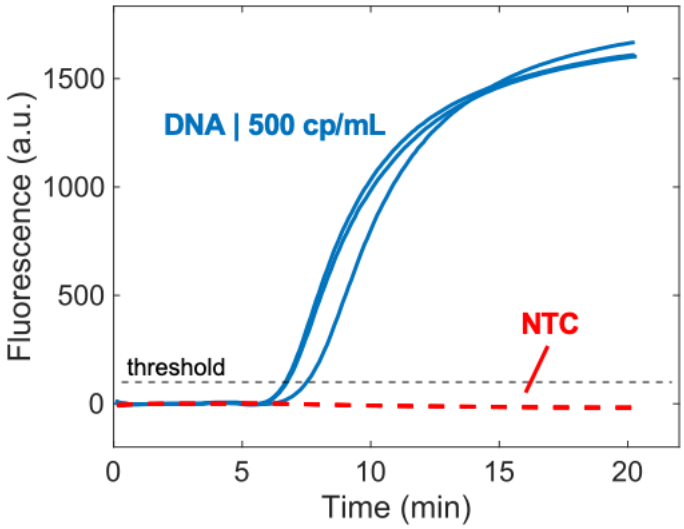

Figure 3-11. Fluorescence measurements for RPA reactions detecting synthetic DNA isotachophoretically extracted from 40 µL samples of digested human serum. (A) DNA at a concentration of 500 copies per mL of serum (20 copies suspended in 40 µL of serum) were extracted and consistently amplified above the positive/negative threshold with RPA (N = 3).

3.4 Detection of HIV-positive Serum

I paired a novel protocol for viral lysis, RNase inactivation, and serum protein digestion with the ITP µPAD to detect HIV virions in human serum. I used a commercial RNase detection assay to evaluate the best serum pretreatment conditions for rapid and complete RNase inactivation and plotted the results in Figure 3-12. I found that the combination of 0.5% SDS and 1 mg/mL proteinase K was able to permanently reduce serum RNase activity to negligible levels when incubated at 65°C for 15-minutes (Figure 3-12). An extended incubation (1 hour) of serum with SDS and proteinase K at a lower temperature (50°C) inactivated RNases to a similar extent. Incubations with either proteinase K or SDS alone were not able to permanently immobilize serum

RNases. The SDS and proteinase K leveraged in the 15-minute RNase inactivation protocol are both potent lytic agents, so I hypothesized that this chemistry would by effective for HIV viral lysis. I pretreated HIV+ serum with the specialized protocol and then extracted RNA from the lysate with the ITP μPAD. Off-chip duplexed RT-RPA detected HIV and MS2 internal control RNA. Similar to HIV, MS2 bacteriophage is a single-stranded RNA virus and consequently acts as an internal process control for viral lysis, RNase inactivation, RNA extraction, reverse transcription, and amplification. I was able to detect HIV in serum at 5×10^4 cp/mL using the assay. Tests with HIV-negative serum did not amplify although the MS2 internal control was still detected. The assay protocol requires 15 minutes for serum pretreatment, 15 minutes for ITP, and 15 minutes for RT-RPA, which totals a 45-minute test runtime.

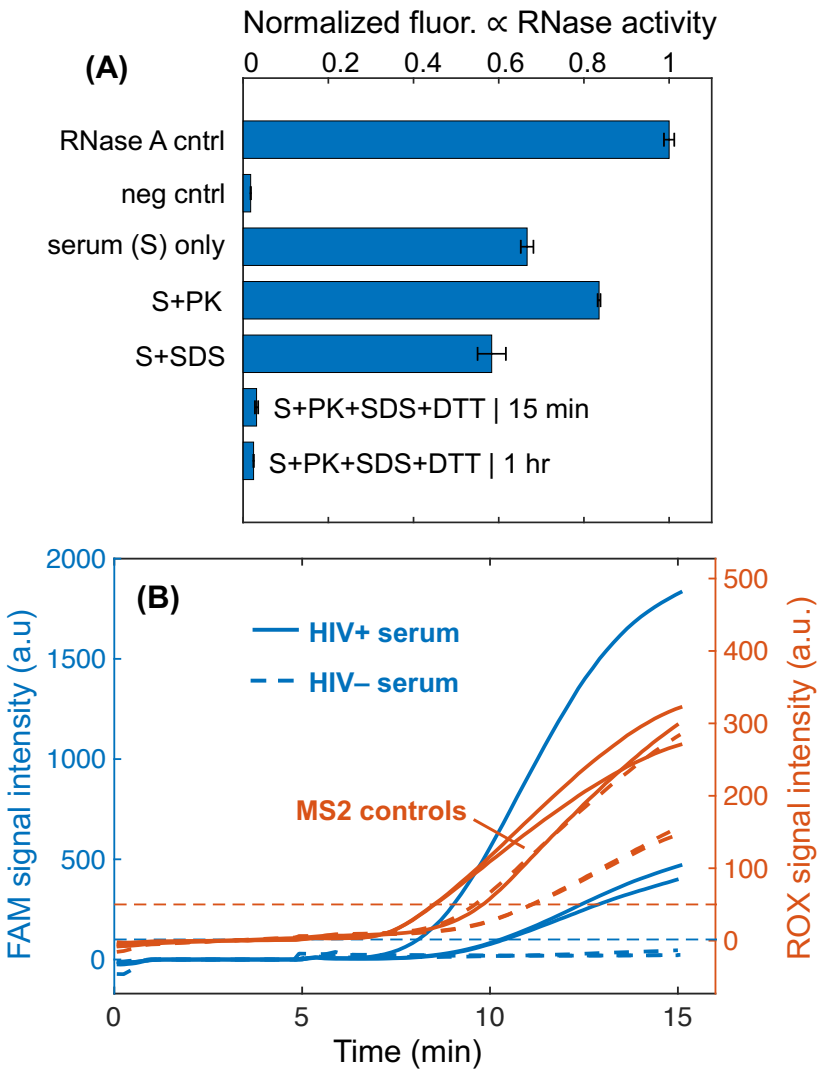

Figure 3-12. (A) RNase activity of serum samples pretreated with proteinase K and/or SDS. A commercial RNase detection assay, RNaseAlert, measures RNase activity by means of fluorescence intensity increase. I found that incubation of serum with 0.5% SDS, 1 mg/mL proteinase K at 65°C for 15 minutes resulted in negligible RNase activity in the lysate. Experiments were run in triplicate and one standard deviation around the mean is plotted for each. RNase A (1.5 U/L) is the positive control and the negative control is RNase-free water add to the RNaseAlert assay. (B) Detection of HIV-1 virions and MS2 phage from human serum. Fluorescence intensities of the two different emission spectra used to simultaneously detect HIV and MS2 amplification. FAM signal intensity indicates successful amplification of target HIV-1, while ROX signal reports amplification of an MS2 region. Experiments with HIV-positive serum

amplify while those with HIV-negative serum do not. All MS2 controls amplify for each respective experiment.

3.5 Conclusions

I report on an alternative assay for HIV detection from human serum within 45-minutes using a novel sample pretreatment chemistry, an ITP μPAD, and RT-RPA. I demonstrate several advancements in the use of ITP for POC nucleic acid-based tests. I identified a protocol for viral lysis, RNase inactivation, and serum protein digestion using a short incubation with proteinase K, SDS, and DTT. This chemistry is unique from previous sample pretreatments in ITP studies which did not adequately address serum RNases. This pretreatment method is also distinct from typical solid phase extraction lysis buffers which rely on high concentrations of guanidinium salts. I designed a specialized ITP μPAD that can directly process 40 μL of serum lysate. This is the largest volume of serum that has been used in ITP nucleic acid extractions, to my knowledge. I controlled the pH of the system to remove proteinase K and leveraged potassium chloride to precipitate SDS in the lysate. I confirmed that the resulting ITP plug was free of inhibitors of RT-RPA and found the ITP μPAD could extract 5,000 copies of HIV RNA per mL of proteolyzed serum. I then demonstrated that the assay can detect HIV in human serum within 45-minutes. The assay features an MS2 bacteriophage for an internal process control of lysis, RNA extraction, reverse transcription, and amplification. This work is the first example of an ITP-based detection assay for RNA viruses in human serum.

My work describes a potential sample preparation method leveraging paper-based ITP that may be used in POC molecular testing for HIV and other bloodborne pathogens. I seek to eliminate the need for highly concentrated chaotropic agents, potent chemicals, and numerous buffer exchanges for viral RNA sample preparation. Lysis buffers with SDS, proteinase K, and DTT are

relatively safe for handling by untrained users and feature easy disposal in resource-limited health care settings. The device features convenient sample addition and low-cost materials, indicating its suitability for point-of-care testing. I demonstrate HIV detection from serum at a viral load of 5×10^4 cp/mL, which is within the clinically relevant range for HIV. Among people living with HIV, there is a significant population who are either not on ART or who have not achieved viral suppression due to adherence issues or a strain of HIV that is resistant to a particular drug regimen. People with unsuppressed HIV infections may have viral loads as high as 10^7 cp/mL.[183] The WHO has recommended that POC tests for viral load monitoring of HIV-positive patients on drug therapies have an limit of detection (LOD) of 1,000 cp/mL in order to maximize treatment failure detection.[184] Ongoing work in the Posner Research Group is focused on improving the system's LOD for HIV virus in blood and on-chip amplification, in moving towards a fully integrated point-of-care HIV viral load monitoring test that is well suited for LMICs.

Chapter 4. SIMULTANEOUS ITP AND RPA

4.1 INTRODUCTION

Diagnostics researchers have investigated varied approaches for integrating sample preparation, amplification, and detection to create POC NAAT devices.[185–189] Paper-based devices are common in the field due to their wicking properties, reagent storage, low cost, and ease of fabrication using minimal equipment. Rodriguez *et al.* developed a paper-based diagnostic for diagnosis of human papillomavirus (HPV) 16 DNA from clinical cervical samples.[190] Sample preparation, amplification, and detection all occurs within the porous network, yet manual buffer exchanges are required. Lafleur *et al*. demonstrated an integrated paper-based device to provide sample-to-result analysis of nasal swab specimens.[191] Their battery-powered approach performs sample lysis, dilution, isothermal amplification, and qualitative colorimetric detection in approximately one hour. Nucleic acid purification was not included in this work, though the presence of inhibiting materials makes this a necessary step for sensitive detection when the target pathogen burden is low. These studies present promising platforms for integrating NAAT operations yet still require further development to process more complex samples and eliminate intermediate user steps.

One of the key challenges facing integrated NAAT diagnostics is the automated exchange of lysis, wash, elution buffers, and/or amplification reagents necessary for sensitive detection of pathogens. Several notable NAAT reports have leveraged ITP for integration of nucleic acid extraction and purification with nucleic acid amplification. Borysiak *et al.* developed an integrated microfluidic diagnostic that employed ITP to purify *E. coli* nucleic acids present in milk, along with heat activated pumps and capillary valves to drive the nucleic acids into a LAMP amplification reaction chamber.[192] In this work, the only user steps were the application of the

electric field and initiating heating for amplification. Eid *et al*. reported a similar assay leveraging ITP and RPA for *L. monocytogenes* detection from whole blood.[193] They extracted nucleic acids into a reservoir using ITP, and then either pipetted target nucleic acids out of the chip into a separate tube or manually added necessary reagents into the chip reservoir for subsequent screening via RPA. Both studies utilized ITP for extraction followed by isothermal amplification in a separate well or chamber. However, there have been no studies to date that use either microchannels or porous substrates to concurrently perform both ITP and amplification—an important development for eliminating intermediate user steps and moving towards developing low cost components for scaled manufacturing.

In this chapter, I present a paper-based NAAT technique that integrates ITP and RPA to simultaneously extract and amplify target nucleic acids from buffer and serum in less than 20 minutes. By applying an electric field, nucleic acids are isolated from the complex sample and focused with RPA reagents within an ITP plug where amplification occurs in a few minutes. A sequence-specific fluorescent probe enables real-time detection and provides sensitive and semi-quantitative results. I first determine the minimum number of copies per reaction required for RPA amplification within an ITP plug in a clean buffer sample. I then report on the limit of detection (LoD) and semi-quantitative results for simultaneous ITP-RPA using human serum. Simultaneous ITP-RPA in the low-cost paper-based device provides rapid results from relatively large sample volumes (20 μL of serum), requiring no user steps in between sample preparation and amplification/detection. I propose that this device can decrease the complexity of traditional laboratory NAATs at a lower cost than POC NAATs that have recently entered the market.

4.2 EXPERIMENTAL SECTION

4.2.1 *Simultaneous ITP-RPA overview and operation*

I conducted experiments with disposable devices that consist of a 30 by 3.5 mm porous glass fiber strip (GFCP203000**,** EMD Millipore, USA) placed between two liquid buffer reservoirs and housed within a sealed 60 mm petri dish (Fisher Scientific, USA), as shown in Figure 4-1A. The glass fiber strip and 3 mm thick acrylic reservoirs were fabricated with a CO_2 laser cutter (Universal Laser Systems, USA). 22-gauge titanium wire electrodes (Unkamen Supplies, USA) are placed in the electrolyte reservoir and connected to a high voltage source meter. I place the device on top of a simple resistive heater plate (Mr. Coffee, USA), maintained at 36 °C using a temperature controller, to aid in heating the reaction and ensure consistency between experiments.

Figure 4-1A shows sterile filtered serum (Sigma-Aldrich, USA) pipetted onto the sample pad region of the glass fiber membrane. To digest proteins that may interfere with the nucleic acid purification or amplification, the sample pad region of the glass fiber strip is pretreated by spotting with 5 µL of 0.05 µg/µL proteinase K (P8107S, New England Biolabs, USA) and 0.1% Triton X-100 (9002-93-1, Sigma-Aldrich, USA) and dried in a desiccator for 20 minutes. I allow 3 minutes for serum protein digestion.

The ITP buffers were developed to separate nucleic acids and RPA reagents from digested serum that is rich with salts, polypeptides, and other biomolecules that inhibit nucleic acid amplification. I employ a finite injection ITP configuration where sample spiked with target synthetic HIV-1 DNA is added directly to the sample pad of the membrane, separating the two ITP buffers: high mobility leading electrolyte (LE) and low mobility trailing electrolyte (TE). Finite injection provides superior nucleic acid extraction efficiency while still allowing adequate separation from amplification inhibitors in the sample.[158]

Commercially-available lyophilized RPA reagents (TwistAmp Exo, TwistDx Ltd., UK) are rehydrated in a solution of LE, RPA primers, and RPA probe. This reaction solution is added to the center of the glass fiber strip, wetting the region between the sample pad and LE reservoir through capillary action as shown in Figure 4-1B. The reservoirs are filled with LE and TE solutions, respectively, and form a fluidic connection through the wetted glass fiber strip (Figure 4-1C). Figure 4-2A shows a schematic depicting the location and concentration of the sample, target, and electrolytes before the experiment is initiated. Note that the RPA reagents are initially spatially separated from the target nucleic acids, which electromigrate to the center of the strip to mix with the RPA reagents and subsequently amplify. The chip is sealed with a plastic lid embedded with titanium electrodes which are positioned into the reservoirs, as shown in Figure 4-1D.

Simultaneous ITP-RPA is initiated by the application of a voltage bias to the electrodes. ITP migrates the nucleic acids from the digested plasma or serum and focuses them with RPA reagents into the ITP plug at the interface of the TE and LE on the porous substrate. The RPA reaction initiates within the plug and target DNA is amplified. RPA-specific amplicons produced in the glass fiber membrane are detected using a sequence-specific fluorescent probe. The signal emanating from the plug is measured using epifluorescence microscopy, as shown in Figure 4-1E. In Figure 4-2, I show concentration profiles of the RPA components and amplified target DNA developed within the ITP plug.

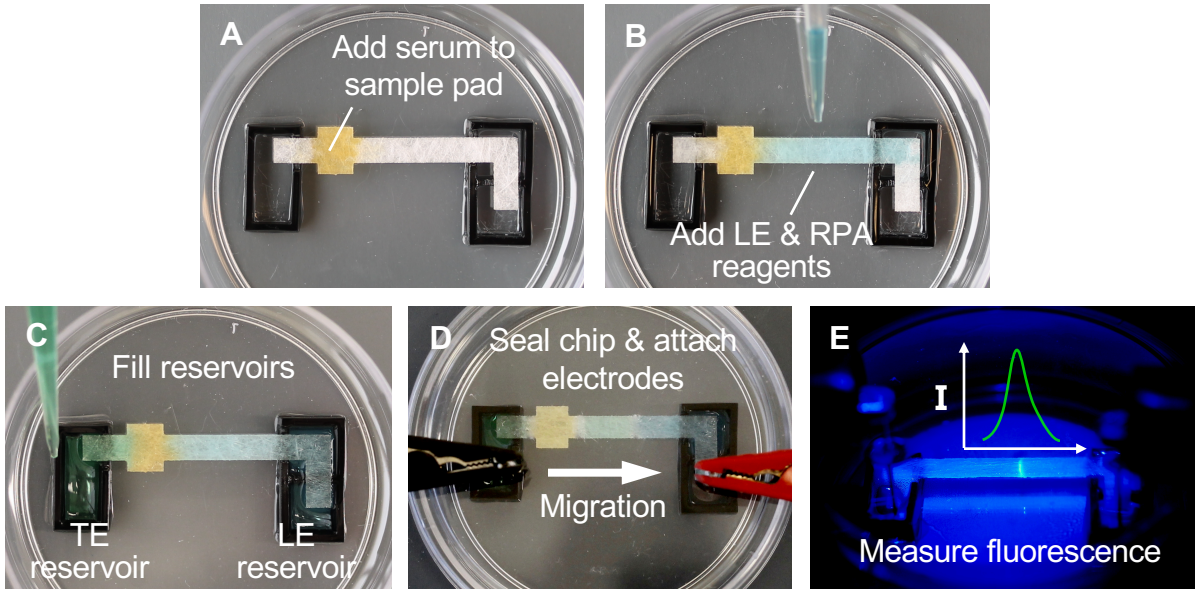

Figure 4-1. Operational steps of simultaneous ITP-RPA from whole blood. (A) Add 20 µL blood serum to the square sample pad region on the left side of the glass fiber strip, which is pretreated with proteinase K. The glass fiber strip is 3.5 mm wide and the square sample region is 4 mm long by 5 mm wide in order to accommodate the whole sample volume. Protein digestion proceeds for 3 minutes within the sample pad. Yellow dye is added to aid visualization of the plasma in these images. (C) Add a mixture of LE and RPA reagents to the center of the glass fiber strip, wetting the region from the sample pad to the LE reservoir. (D) Reservoirs are filled respectively with LE and TE solutions. (E) Seal the chip with a plastic lid embedded with electrodes. The positive electrode is submerged in the LE reservoir and the negative in the TE reservoir. The applied electric field initiates ITP-RPA and extracts nucleic acids from the filtered plasma. (F) A microscope records the fluorescence intensity emanating from the amplification reaction zone in the ITP plug.

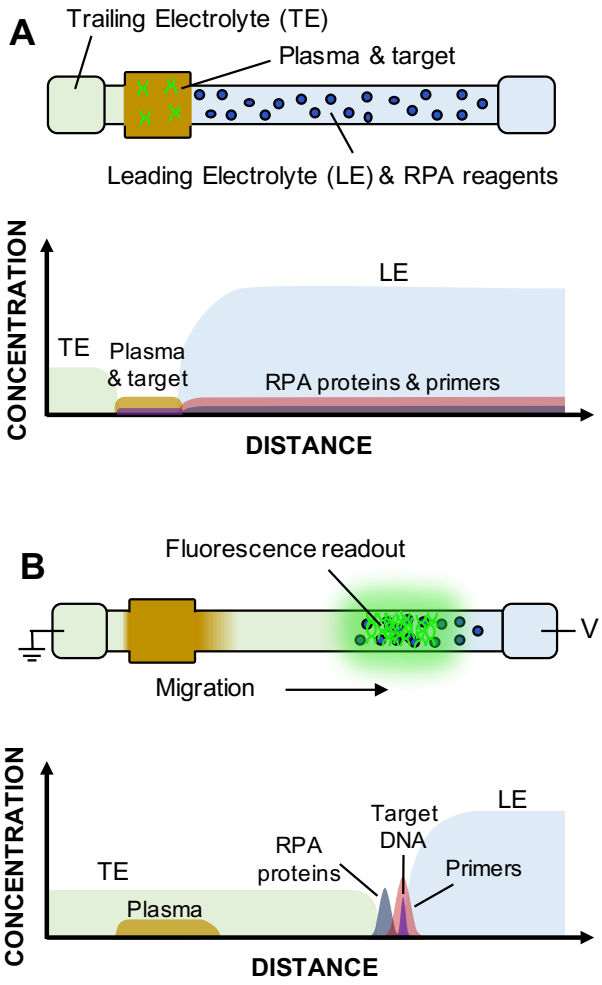

Figure 4-2. Schematic of simultaneous ITP-RPA operation with filtered plasma. I show drawings of the glass fiber strip denoting locations of buffers, reagents, and sample, for the initial (A) and final (B) experimental time points. Approximate concentrations of each constituent are plotted with respect to distance. (A) Following passive filtration of the whole blood, plasma containing target DNA initially wets the sample pad on the left side of strip. LE and RPA reagents are disposed within the glass fiber membrane between the sample region and the LE reservoir. Pure LE and TE solutions reside in respective reservoirs. Initial spatial separation of reaction constituents prevents inhibitors in the sample from interacting with the amplification reagents. (B) Applying an electric field extracts DNA from the sample and focuses it with RPA reagents in the ITP plug. All constituents in the porous membrane electromigrate based on their respective charge and electrophoretic mobility. Nucleic acids and RPA proteins/enzymes speed past components of the plasma to focus at the interface of the LE and TE. The amplification reaction takes place within the concentrated ITP plug to create amplicons and detectable fluorescence.

4.2.2 *ITP and RPA conditions*

The same TE and LE buffers were used for all the experiments. The TE buffer consists of β-alanine (107-95-9, Sigma), Tris (77-86-1, Sigma), polyvinylpyrrolidone (PVP) (9003-39-8, Sigma) and Triton X-100 at pH 8.9–9.1. The LE buffer consists of HCl (7647-01-0, Acros Organics, Belgium), Tris, $MgCl_2$ (7786-30-3, Sigma), polyethylene glycol (PEG) average molecular weight 1,450 (25322-68-3, Sigma), PVP, Triton X-100, and tetramethylammonium chloride (75-57-0, Sigma) at pH 8.1. Reservoirs are filled respectively with 220 µL of LE and 125 µL of TE.

Simultaneous ITP-RPA is performed by applying 150 V with a current compliance of 3.5 mA using a source meter (Model 2410, Keithley, USA). This resulted in 3.5 mA constant current conditions for the first 5 minutes of ITP before transitioning to a constant 150 V with current reducing exponentially to less than 1.0 mA after 15 minutes of electromigration. These relatively high electric currents result from the selected ITP buffers and glass fiber strip's large cross sectional area. Due to the low conductivity of the TE zone, a high electric field develops in this area, resulting in significant Joule heating. I leverage this effect to heat the ITP plug to the optimal temperature for RPA (35–40°C). Different temperature ranges can be achieved depending on the applied voltage, the composition of the ITP buffers, and the dimensions of the glass fiber strip. While this work utilized a resistive heater plate to aid heat control and provide consistency, I observed simultaneous ITP-RPA can be run using solely Joule heating to achieve an appropriate temperature for RPA within the ITP plug.

I developed a custom RPA reaction chemistry that is compatible with amplification in glass fiber membranes and the unique chemical composition required for ITP. The reaction solution consists of an RPA pellet rehydrated with LE solution, 1 µM forward primer, 1 µM reverse primer

(Integrated DNA Technologies, USA), and 250 nM of sequence specific fluorescent probe (Biosearch Technologies, USA). In order to simplify proof-of-concept experiments, I use a synthetic DNA target (200 base pairs) synthesized using the gBlock gene sequence technology (Integrated DNA Technologies, USA). The sequence is adopted from the proviral HIV-1 DNA *pol* gene and contains the complementary sequence for the primers and probe adopted from Boyle *et al*.[194] Full primer, probe, and target sequences are listed in **Table 4-1**.

Table 4-1. Sequences of the target DNA, primers, and sequence specific probe for the RPA assay, as well as the labeled DNA used for extraction-only experiments. bp = nucleotide base pair; FAM = fluorescein amidite; dR = an abasic residue with a fluorophore attached to the ribose via a C-O-C linker; [dSpacer] = abasic site; [T(BHQ-1)] = Black Hole Quencher-1 bound to an internal Thymine residue; Spacer C3 = a moiety that replaces the 3'-OH group preventing nucleotide extension from an intact probe.

Description	**Sequence (5' – 3')**
Abridged HIV-1 *pol* dsDNA (200bp)	AGGCTGAACATCTTAGGACAGCAGTACAAATGGCAGTATTCAT TCACAATTTTAAAAGAAAAGGGGGGATTGGGGGGTACAGAGCA GGGGAAAGAATAGTAGACATAATAGCAACAGACATACAAACTA GAGAACTAGGTTGAGAAATTAGAAAAGTTGAATATGTTAGGGTT TATTACAGGGACAGCAGAGATCCACTT
Forward primer (34bp)	TGGCAGTATTCATTCACAATTTTAAAAGAAAAGG
Reverse primer (34bp)	CCCTAACATATTCAACTTTTCTAATTTCTCAACC
Probe (48bp)	TGCTATTATGTCTACTATTCTTTCCCC[T(FAM)]GC-[dSpacer]C-[T (BHQ1)]GTACCCCCCAATCCCC-SpacerC3

4.2.3 *Data Collection and Analysis*

I perform quantitative epifluorescence imaging (AZ100, Nikon, Japan) with a 0.5X (N=0.05) objective to visualize the fluorescent signal generated by the exonuclease-mediated digestion of the probe bound to RPA amplicons. Using an epifluorescence excitation (488 nm) and emission (518 nm) filter cube set (Omega Optics, USA) and a 16-bit, cooled CCD camera (Cascade 512B, Photometrics, USA), I captured grayscale images of fluorescence at one second intervals over a 15-minute period. The generated data was processed via a custom algorithm (MATLAB, MathWorks, USA) to determine the spatial and temporal fluorescence intensity. The algorithm subtracts the initial background from all images and computes the *y*-average intensity along the length of the strip (*i.e. x*-direction). This results in one-dimensional intensity profiles with respect to the length of the strip for distinct time points. The profiles are integrated over the x-direction to calculate a bulk fluorescence intensity for each time point. I employ a thresholding technique to eliminate some non-specific signal due to probe and enzyme interactions.

The limit of detection (LoD) is the lowest level of analyte that can reliably be measured and is determined according to the Clinical and Laboratory Standards Institute's (CLSI) recommendations for *in vitro* diagnostic tests.[195,196] The LoD is first determined as a signal intensity and then converted into corresponding analyte concentration (*i.e.* copies/mL).[196] The sample intensity LoD is determined as $LoD = \mu_B + 1.645\ \sigma_B + 1.645\ \sigma_S$, where μ_B is the mean intensity of the negative control samples, σ_B is the intensity standard deviation of the negative control samples, σ_S is the intensity sample standard deviation of the low concentration positives. Using these definitions, I have a 5% probability of committing either type I (false positive) or type II (false negative) error at the *LoD*.

4.2.4 *Data Analysis Algorithm*

Fluorescence intensity emanating from the ITP plug indicates successful amplification of target DNA. I collected a grayscale image of the fluorescence from simultaneous ITP-RPA at each second during the course of the reaction (900 seconds for buffer and serum experiments and 780 seconds for whole blood experiments). I developed a MATLAB algorithm to extract RPA amplification curves from the fluorescence images. The algorithm y-averages the intensity of the image, calculates and subtract the background, sets a threshold, and integrates the intensity that exceeds the threshold. Figure 4-3 illustrates this analysis technique for the sample time point of 10 minutes in a positive (1000 cp/rxn) simultaneous ITP-RPA experiment from buffer. The image in Figure 4-3A is y-averaged to create a one-dimensional fluorescence intensity profile with respect to distance across the strip, shown in Figure 4-3C. Additionally, this was performed at the initial time point preceding ITP initiation (t = 0 min) and averaged over 30 seconds, creating a background as shown in Figure 4-3B. This background captured autofluorescence from the glass fiber strip and RPA reagents concentrated near the center of the strip. The background profile was subtracted from each subsequent image to create background subtracted profiles, as shown in Figure 4-3D. For creating amplification curves, I then set a threshold of 114% of the average background signal to exclude non-fluorescent signal from negative experiments (see dashed line in Figure 4-3D). For determining the LoD, I used a threshold of 50% of the average background signal. I integrated the fluorescence signal that exceeds the threshold to determine the intensity value for each experimental time point. For this sample experiment, the bulk intensity with respect to time is plotted in Figure 4-3E.

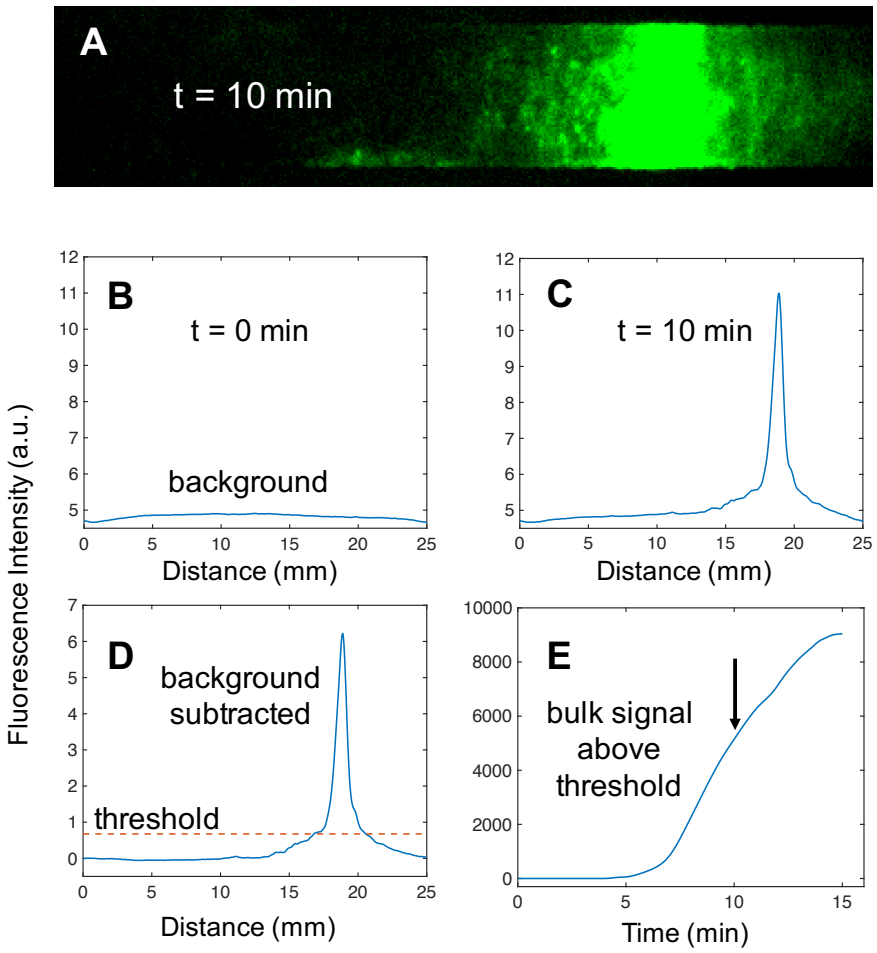

Figure 4-3. Data analysis technique for simultaneous ITP-RPA. I illustrate the methodology using a typical positive experiment. (A) Fluorescence images of the reaction are collected over the course of an experiment. Here I show a sample image at the 10 minute time point. (B) The initial images from the experiment are y-averaged to create a background fluorescence profile. (C) The intensity profile at the 10 minute mark shows signal emanating from the reaction within the ITP plug. Regions of the glass fiber strip far from the plug (e.g. 0 to 10 mm) have similar fluorescence to the background. (D) The background is subtracted from all fluorescence profiles in the experiment. A threshold (orange dashed line) is imposed at 114% of the average background intensity. I integrate the signal that exceeds the threshold to find a single fluorescence value for the 10 minute time point. (E) The arrow indicates the fluorescence value at 10 minutes within the amplification curve of the experiment.

4.3 Results and Discussion

4.3.1 *Simultaneous ITP-RPA in Pure Buffer*

I present a method of amplifying DNA using an RPA reaction that occurs within an ITP plug on a paper substrate to determine the minimum number of copies needed for detectable amplification. These experiments were performed using only buffer as sample and therefore did not require sample preparation. I pipetted HIV-1 DNA suspended in 5 μL of LE onto the middle of the glass fiber strip pre-wetted with LE solution and RPA reagents. Figure 4-4A presents fluorescence images of a positive RPA reaction (10 cp/rxn) as it develops within the plug of the ITP system. When the experiment is initiated (t=0), there is no fluorescence emanating from the strip. Within 5 minutes the DNA, primers, probe, RPA proteins and enzymes focus halfway along the length of the strip, initiating RPA and generating a fluorescence signal. The signal intensity as well as the width of the ITP plug increase as the assay progresses. After 15 minutes the signal reaches its maximum, and the ITP plug nears the LE reservoir, eluting amplified nucleic acids into the reservoir. Trace fluorescence spots remain on the glass fiber in the wake of the reaction plug, possibly due to adsorption or entanglement of RPA amplicons within the fibrous network structure.

Figure 4-4B shows a spatiotemporal intensity map of the positive RPA reaction depicted in Figure 4-4A. This figure represents the y-averaged intensity as a function of space and time, providing insight on the ITP migration dynamics. The map shows that fluorescent products from non-specific enzyme and probe interactions accumulate in the ITP plug and migrate with a constant velocity halfway along the strip (15 mm) in approximately 5 minutes. At this point, the fluorescence intensity within the plug significantly increases due to the amplification of the DNA, while the migration velocity decreases. The reduction in velocity aids the amplification as it increases the accumulation time for necessary RPA reactants to migrate into the plug and ensures

that the plug does not reach the LE reservoir for at least 15 minutes. The ITP plug velocity is a function of the target electrophoretic mobility, local electric field strength, and electroosmotic counter flow.[180,181] After 5 minutes the low conductivity trailing electrolyte has migrated sufficiently far down the strip such that electrical resistance results in the power supply switching from constant current to constant voltage. The net ITP plug migration velocity decreases, due to a combination of electrophoretic migration and electroosmotic flow. Electrophoretic velocity is a linear function of current, so after 5 minutes the current exponentially decreases below the 3.5 mA compliance, reducing the net plug velocity. Previous work on ITP has observed plug trajectories similar to Figure 4-4B.[53,197]

I present the normalized integrated fluorescence intensity of the RPA reporter probe as a function of time for low copy numbers of target DNA in Figure 4-5. The no template control (NTC) is shown as a constant zero intensity over the duration of the experiment (*i.e.* its signal is always below the threshold). When 5 copies of target are introduced, the intensity remains at zero for roughly four minutes where the amplification becomes visible and the intensity increases linearly until 15 minutes where it plateaus. The plateaus may be due to a limiting reagent (*e.g.* ATP required for recombinase functions) or deteriorating reaction conditions in the ITP plug over time (*e.g.* changes in ionic strength, temperature, and pH). Simultaneous ITP and RPA reactions have similar time to detection as compared to tube-based RPA assays.[39,68] While RPA reactions are often exponential when amplifying high initial copies of target DNA, other studies have also reported linear amplification reactions when amplifying low copies of target DNA.[39] The data indicates that simultaneous ITP-RPA can consistently detect 5 to 10 copies per reaction in pure buffer. This suggests that, with ideal nucleic acid purification and extraction, the simultaneous ITP-RPA assay should have similar sensitivity to standard RPA tube assays.[33]

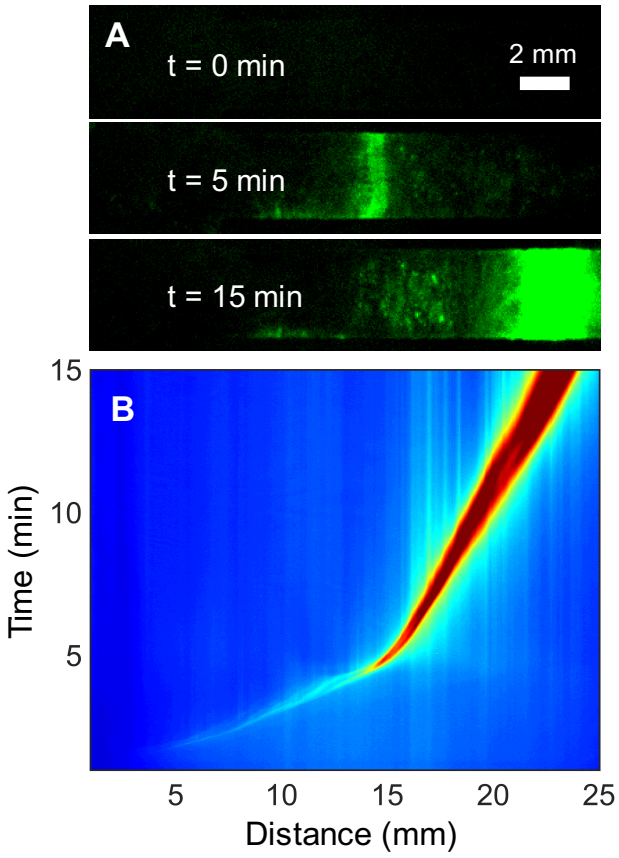

Figure 4-4. Low-copy simultaneous ITP-RPA and real-time detection of target DNA in buffer. DNA is added to the center of the glass fiber strip to demonstrate successful amplification on glass fiber without extraction. (A) Fluorescence images at t=0, 5, 15 minutes of ITP-RPA over the 15-minute experiment. RPA reagents and target DNA initially applied to the glass fiber strip accumulate in the ITP plug. Amplification within the plug initiates after approximately 5 minutes. (B) Spatiotemporal map of a positive (10 cp/rxn) RPA experiment. Red and blue colors denote high and low fluorescence intensity, respectively. The fluorescence intensity of the plug rapidly increases after five minutes and migrating 15 mm down the strip.

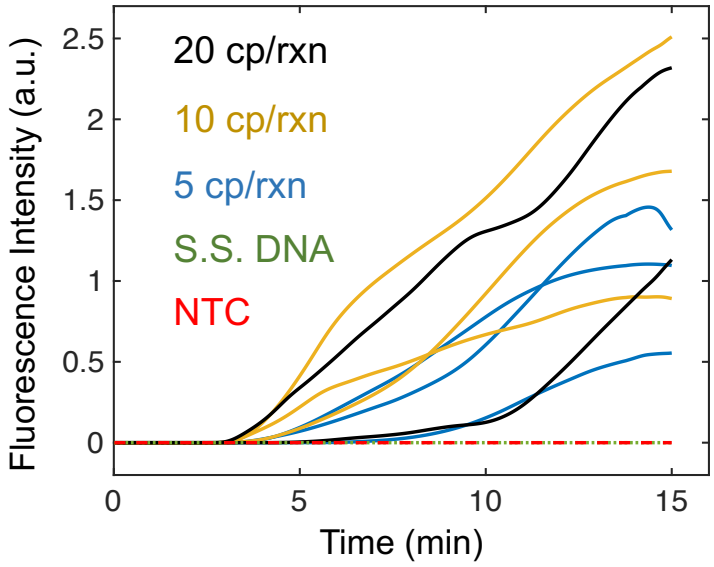

Figure 4-5. Simultaneous ITP-RPA experiments from pure buffer were analyzed to generate fluorescence curves with respect to time for low input DNA copy numbers. I present individual trials for 20 cp/rxn (N=2), 10 cp/rxn (N=3), 5 cp/rxn (N=3), no template control (NTC) (N=3), and 10 pg sheared salmon sperm DNA (N=2). The custom analysis algorithm used a threshold of 114% of the average background signal, so nonspecific signal from the negative controls was negligible.

4.3.2 *Limit of Detection of Simultaneous ITP-RPA*

I conducted experiments to determine the LoD of simultaneous ITP-RPA from sterile-filtered human serum spiked with target DNA. I initially added 20 µL of serum to the sample pad for protein degradation using proteinase K then RPA reagents and ITP buffers were added to the paper and reservoirs. Application of an electric field initiated ITP to simultaneously extract DNA from the serum and focus it with RPA reagents, leading to RPA amplification within the ITP plug. Representative fluorescence images and spatiotemporal maps were similar to those generated with pure DNA (Figure 4-4). I observe an increase in fluorescence trailing the plug that is hypothesized to be a result of proteins found in the serum clogging the fibrous glass fiber network or forming complexes with DNA and impacting the recovery of DNA.[161] DNA bound to undigested serum

proteins have reduced electrophoretic mobility which inhibits its electromigration to the ITP plug. The spatiotemporal map of a typical serum experiment shows a similar change in migration speed as Figure 4-4B. Figure 4-6A shows real-time, normalized integrated fluorescence for NTC and serum samples with target DNA spiked with concentrations ranging from 10^4 copies per mL (cp/mL) (*i.e.* 200 cp/rxn with a 20 μL sample) to 10^7 cp/mL (*i.e.* 2×10^5 cp/rxn). The simultaneous ITP-RPA reactions begin at zero normalized intensity and proceed to amplify in as soon as 5 minutes depending on the input target concentration in the serum.

High-copy experiments amplify in less time, more rapidly (greater slope), and with higher endpoint fluorescence than low-copy experiments, generally plateauing at higher fluorescence values. I hypothesize that endpoint fluorescence is reduced in low-copy samples due to non-specific amplification from primer interactions consuming necessary reagents, such as nucleotides and ATP. Figure 4-6B plots the mean time to the fluorescence threshold inferred from Figure 4-6A with respect to the initial target concentration. The error bars represent the standard deviation of the time to threshold for the triplicates at each concentration. Time to threshold relates to copy number via a power law for concentrations from 10^4 to 10^7 copies/mL. These results are similar to those of Rohrman *et al*. which showed semi-quantitative HIV-1 DNA detection using a tube-based real-time RPA assay.[39] Improvements in extraction efficiency and mitigating adsorption are expected to reduce the LoD and improve the consistency of the test. The observed trend between time to threshold and concentration cannot adequately quantitate input DNA, but it distinguishes high, low, and undetectable levels of target DNA. Therefore I refer to simultaneous ITP-RPA as semi-quantitative, a desirable diagnostic feature in applications such HIV viral load monitoring.[64,198] Using the CLSI definition, I determined the LoD of simultaneous ITP-RPA to be 10^4 cp/mL, equivalent to 200 cp/rxn using a 20 μL sample volume.[195] The LoD calculation

accounted for variations in non-specific fluorescence signal between NTC experiments. This performance is comparable to similar prototypic POC integrated diagnostic platforms.[190,191]

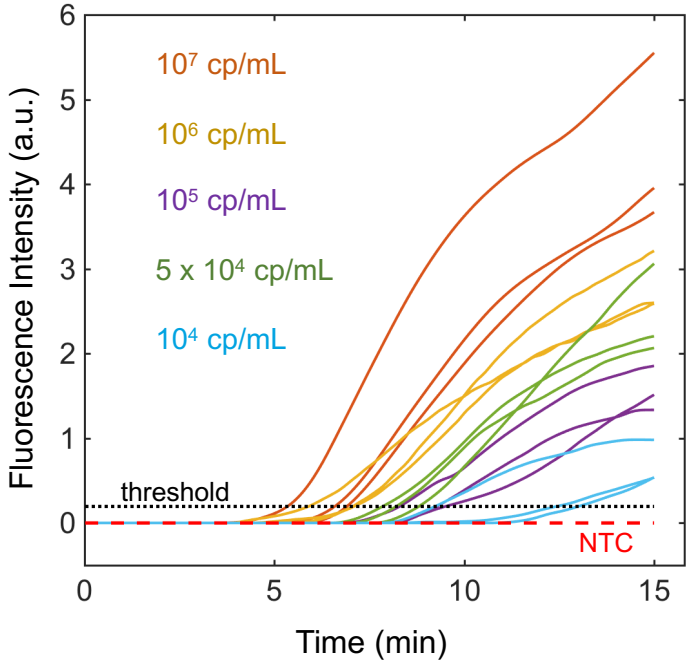

Figure 4-6. Fluorescence intensities from experiments during simultaneous DNA extraction and RPA amplification in human serum spiked with target DNA. (A) Integrated RPA fluorescence intensities plotted with respect to time for a dilution series of DNA concentrations. All replicates (N=3) are shown here. Serum with DNA concentrations less than 10^4 cp/mL did not amplify, so the data is not shown here.

4.4 CONCLUSIONS

The simultaneous ITP-RPA assay has an LoD of 10^4 cp/mL of human serum (*i.e.* equivalent of 200 cp/rxn using a 20 µL serum sample). I demonstrate detection of initial synthetic HIV-1 DNA concentrations of 10^4 cp/mL to 10^7 cp/mL, well within the clinical range for HIV-1 viral loads.[199] I use HIV-1 DNA in this work as a first step towards the goal of viral RNA detection and monitoring. The LoD is comparable to several commercial nucleic acid-based tests for viral

hepatitis B DNA and hepatitis C RNA, both infections where physicians seek quantitative diagnostic information.[200,201] Molecular testing for these bloodborne infectious requires several other technical challenges, including plasma separation, nuclease inactivation, viral lysis, and reverse transcription. I observed 5 copy sensitivity for simultaneous ITP-RPA from buffer which suggests high efficiency isotachophoretic extraction and purification of DNA from serum will dramatically improve the LoD of this test.

Chapter 5. CONCLUSIONS AND RECOMMENDATIONS

5.1 RESEARCH OVERVIEW

Molecular testing of blood samples is the gold-standard diagnostic method for a wide range of applications, such as the detection of infectious diseases, identification of genomic mutations, and quantification of infection severity. In recent years, there have been significant efforts to translate molecular testing procedures from central laboratories to POC settings. For example, POC molecular tests are needed to decentralize HIV viral load monitoring, which enables HIV-positive patients to be rapidly linked to alternative treatment plans if they have not achieved viral suppression.[156] POC nucleic acid amplification testing in low- and middle-income countries (LMICs) is also needed for a number of deadly and prevalent bloodborne infectious diseases, such as hepatitis B, hepatitis C, dengue, Zika, and Ebola viruses. Commercial POC molecular tests have reached the market for some diseases, but their high platform costs, resource demands, and system complexity has limited their widespread adoption in LMICs. These tests automate nucleic acid extraction operations typically done in a central laboratory (e.g. solid phase extraction) via pumps and robotics, driving up platform costs. Further research and development are needed to reduce the complexity and corresponding costs of nucleic acid sample preparation from blood samples.

This dissertation describes novel sample preparation approaches for detecting bloodborne pathogens. I developed paper-based isotachophoresis systems for integrated on-chip detection and specialized nucleic acid purification of DNA and RNA. I also discovered novel chemistries for inactivating endogenous blood RNases and lysing viral envelopes, and I paired these chemistries with isotachophoresis for detecting HIV from human serum. These sample preparation methods use low-cost materials and reagents, and isotachophoresis uses an electric field to automated nucleic acid purification and reduce manual user steps. Ultimately, I believe my innovations may

be used to develop POC nucleic acid amplification tests for bloodborne pathogens in a low-cost format with minimal protocol complexity.

The research in this dissertation was partly motivated by ongoing efforts in the Posner Research Group to develop a POC test for HIV viral load monitoring. The long-term goal of this project is to integrate plasma separation, viral lysis, RNase inactivation, RNA extraction, nucleic acid amplification, and detection within a disposable test cartridge (see renderings of the cartridge and operation in Figure 5-1). The test cartridge may be paired with a mobile phone that can be leveraged for detection and dissemination of diagnostic results. Based on the context of this project, experimental work in this dissertation primarily focused on detecting HIV. HIV is a useful model pathogen from a molecular testing perspective because it has many shared attributes with other common bloodborne viruses. For example, both hepatitis C virus and HIV (1) are bloodborne RNA viruses, (2) are protected by an envelope and capsid, (3) have relatively short genomes (~10kbp), (4) are genetically diverse, (5) have unmet clinical need for POC viral load testing, and (6) require similar testing LoDs (10^3 to 10^4 cp/mL).[79] These two viruses present nearly identical challenges for sample preparation, amplification assays, and detection assays. Therefore, I believe my work on sample preparation for HIV may be easily translated for diagnostics focused on other bloodborne viruses.

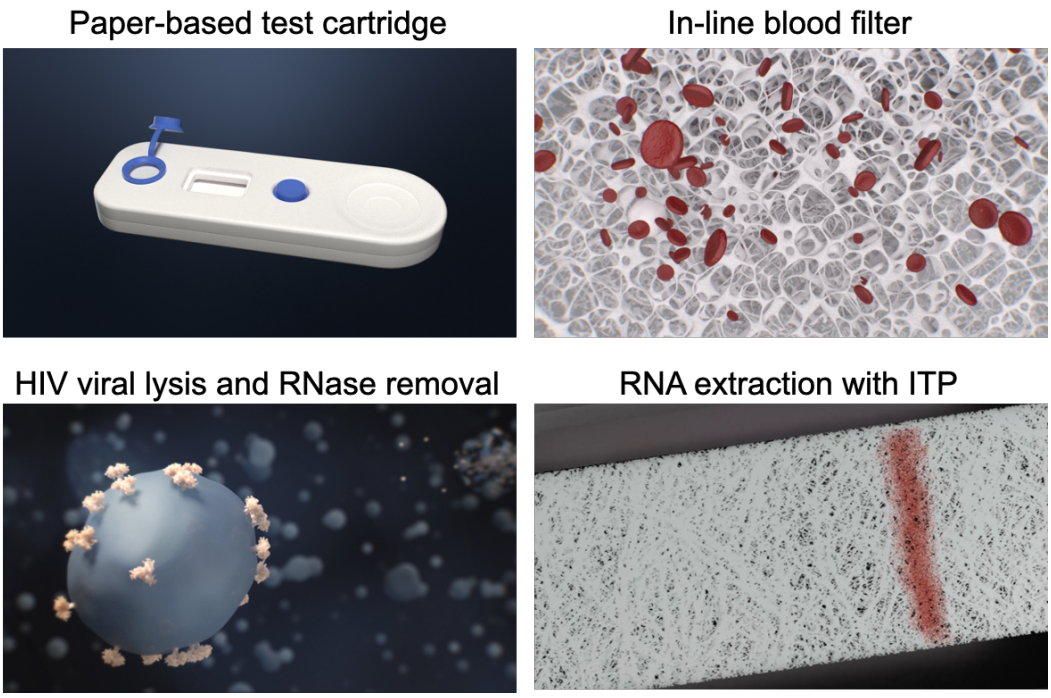

Figure 5-1. Images of a biomedical animation explaining the operation of the envisaged POC HIV viral load test in development by the Posner Research Group. The assay chemistry is all housed with a disposable test cartridge. Blood is added to the inlet port and blood cells are removed using an in-line filter. Proteases and detergents lyse HIV virions and inactive endogenous RNases. An ITP extraction within the paper membrane purifies RNA and enables subsequent recombinase polymerase amplification for HIV detection.

Nucleic acid testing for RNA targets in blood specimens requires sample preparation that inactivates robust blood ribonucleases (RNases) that can rapidly degrade exogenous RNA. Most NAATs rely on decades-old methods that lyse pathogens and inactivate RNases with high concentrations of guanidinium salts. I investigated alternatives to standard guanidinium-based methods for RNase inactivation using an activity assay with an RNA substrate that fluoresces when cleaved. I report on the effects of proteinase K, nonionic surfactants, sodium dodecyl sulfate (SDS), dithiothreitol (DTT), and other additives on RNase activity in human serum. While proteinase K has been widely used in protocols for nuclease inactivation, I found that high

concentrations of proteinase K are unable to eliminate RNase activity in serum, unless used in concert with denaturing concentrations of SDS. I observed that SDS must be combined with proteinase K, DTT, or both for irreversible and complete RNase inactivation in serum. My work provides an alternative chemistry for inactivating endogenous RNases for use in simple, low-cost POC NAATs for bloodborne pathogens.

I detail an assay for HIV detection from human serum with an MS2 bacteriophage internal process control using a novel lysis and RNase inactivation method, paper-based ITP, and duplexed reverse transcription recombinase polymerase amplification (RT-RPA). I leveraged my findings on inactivating blood RNases to develop a novel 15-minute protocol for off-chip viral lysis, RNase inactivation, and serum protein digestion. I design a specialized ITP system to extract RNA from human serum lysate, while excluding harmful proteinase K and anionic detergent. I confirmed that the resulting ITP plug was free of inhibitors of RT-RPA and found the ITP μPAD could extract 5,000 copies of HIV RNA per mL of proteolyzed serum. I then demonstrated that the assay can detect HIV in human serum within 45-minutes. The assay features an MS2 bacteriophage for an internal process control of lysis, RNA extraction, reverse transcription, and amplification.

I developed a novel method for integrating nucleic acid extraction and amplification in a single step using electrokinetics and paper substrates. I used simultaneous isotachophoresis (ITP) and recombinase polymerase amplification (RPA) to rapidly extract, amplify, and detect target nucleic acids from serum in a paper-based format. I demonstrate simultaneous ITP and RPA can consistently detect 5 copies per reaction in buffer and 10,000 copies per milliliter of human serum with no intermediate user steps. The test is rapid (results in less than 20 minutes) and made from low-cost materials, indicating its potential for simplifying POC infectious disease detection in low resource settings. While this work was an elegant solution to integrating nucleic acid extraction

and amplification, it had several practical limitations that hindered its use for detecting bloodborne viruses. First, I employed serum samples spiked with synthetic DNA (a 200bp segment of the HIV proviral genome). I did not perform viral lysis in this work, and synthetic DNA is significantly easier to extract and detect than intact viral nucleic acids. Second, the assay was difficult to troubleshoot. The assay involved a complex biochemical reaction (RPA) occurring within a dynamic electrokinetic system (ITP). I found it difficult to identify reasons for unsuccessful experiments.

5.2 Recommendations on Future Work

The primary innovations of my dissertation are the development of specialized sample preparation chemistries to enable efficient isotachophoretic nucleic acid extraction and isothermal nucleic acid amplification for bloodborne virus detection. There is significant future work needed to implement these chemistries in simple, rapid, low-cost POC molecular tests. The most challenging aspect of my work was lowering the limit of detection of HIV in serum. Target product profiles indicate that POC HIV viral load tests need to be able to detect less than 1,000 copies of HIV RNA per mL of serum.[156] In my work, I achieved detection limits for viral nucleic acids and HIV virions at concentrations 5- to 10-fold higher than the recommended level. There are several areas of future work that would improve the current detection limits. Increasing the volume of blood processed by ITP would introduce more HIV RNA that could be focused in the ITP plug and detected with RT-RPA. Improving the RNA extraction efficiency of ITP would result in higher numbers of purified HIV RNA for downstream detection. Finally, it is crucial to fully inactivate endogenous RNases in serum in order to protect HIV RNA from degradation. I developed a 15-minute protocol for RNase inactivation, but this could use optimization to increase the speed and

extent of RNase removal. Ongoing work by other researchers in the Posner Research Group is focused on integrating all diagnostic operations (i.e. blood filtration, viral lysis, RNase inactivation, RNA extraction, RT-RPA) within a plastic and paper test cartridge. Automating these operations in a single device is extremely challenging and may require years of research and engineering to develop a market-ready test.

5.3 Reflections on the State of POC Molecular Diagnostics

When I started my PhD in the autumn of 2015, POC nucleic acid amplification testing was a vibrant field and largely focused on addressing widespread rapid testing needs in LMICs. Researchers in the field were diverse in background and many published studies focused on individual aspects of the molecular testing (e.g. an isothermal nucleic acid amplification assay for hepatitis B virus DNA or a device for high-efficiency blood fractionation). Years of research has built an extensive collection of literature on aspects of POC molecular testing that will serve as a useful toolbox going forward. Researcher and development of POC diagnostics is split between academic and commercial sources. The dichotomy between academy and commercial labs has, in some ways, slowed the development of novel POC molecular tests. Large biotechnology companies have purchased much of the intellectual property in the nucleic acid amplification space. They are incentivized to hide their trade secrets and bury proprietary assay chemistries in obscure patents. In many areas, academic research labs are left reinventing the wheel in certain circumstances (e.g. developing optimized chemistries for lysis and amplification assays, enzyme selection, membrane selection). Biotechnology companies have sat on their intellectual property and resisted the development of low-cost molecular testing because the market for such tests has largely been restricted to LMICs.

In January 2020, the COVID-19 pandemic accelerated into a devastating worldwide public health emergency and transformed the field of POC molecular diagnostics overnight. Top health experts identified the need to rapidly detect new COVID-19 infections so that infected individuals could self-isolate and rapid contract tracing could take place. POC nucleic acid amplification tests quickly emerged as a leading diagnostic tool due to their superior accuracy and specificity over lateral flow-style antigen tests. Hundreds of companies around the world announced plans to develop POC molecular tests for the SARS-CoV-2 virus that causes COVID-19. Academic groups rapidly shifted focus to developing new molecular testing strategies for the novel coronavirus. In the United States, the NIH announced plans to invest over a billion dollars in POC diagnostics for SARS-CoV-2. Crucially, the FDA began to grant regulatory approval for new POC diagnostics through emergency use authorizations, which offers a significantly quicker path to market for diagnostics. These events catalyzed the research field by injecting enormous amounts of money for new research and establishing easier pathways for POC molecular tests to gain regulatory approval.

As of July 2020, I have witnessed a flurry of new COVID-19 related research activity into POC molecular testing. Many renowned, well-funded research groups in academy and industry alike have entered the diagnostics space and are working on many topics described in this dissertation, such as rapid isothermal nucleic acid assays and methods for inactivating endogenous RNases in clinical specimens. Researchers have been surprisingly transparent about their work and have published detailed protocols on assays in development. It has been interesting time to be in the POC diagnostics field, to put it mildly. I believe the work in this dissertation will be useful for other researchers and aid in the development of next generation diagnostics. I am hopeful that the research investments made towards diagnostics for COVID-19 will bring POC molecular testing

into pharmacies, primary health clinics, and homes across the world. At-home nucleic acid testing for a wide variety of infectious diseases may be a reality in the next decade. This could have transformational health benefits for diagnosing sexually transmitted diseases and curtailing future and ongoing epidemics.

Citations to Previously Published Work

Portions of this dissertation have appeared in the following articles:

Chapter 2

Bender, Andrew T., Benjamin P. Sullivan, Lorraine Lillis, and Jonathan D. Posner. "Enzymatic and chemical-based methods to inactivate endogenous blood ribonucleases for nucleic acid diagnostics." *The Journal of Molecular Diagnostics* (2020).

Chapter 4

Bender, Andrew T., Mark D. Borysiak, Amanda M. Levenson, Lorraine Lillis, David S. Boyle, and Jonathan D. Posner. "Semiquantitative nucleic acid test with simultaneous isotachophoretic extraction and amplification." *Analytical chemistry* 90, no. 12 (2018): 7221-7229.

BIBLIOGRAPHY

(1) Caliendo, A. M.; Gilbert, D. N.; Ginocchio, C. C.; Hanson, K. E.; May, L.; Quinn, T. C.; Tenover, F. C.; Alland, D.; Blaschke, A. J.; Bonomo, R. A.; Carroll, K. C.; Ferraro, M. J.; Hirschhorn, L. R.; Joseph, W. P.; Karchmer, T.; MacIntyre, A. T.; Reller, L. B.; Jackson, A. F.; for the Infectious Diseases Society of America (IDSA). Better Tests, Better Care: Improved Diagnostics for Infectious Diseases. *Clinical Infectious Diseases* **2013**, *57* (suppl 3), S139–S170. https://doi.org/10.1093/cid/cit578.

(2) *Tietz Fundamentals of Clinical Chemistry and Molecular Diagnostics*, Seventh edition.; Burtis, C. A., Bruns, D. E., Sawyer, B. G., Tietz, N. W., Eds.; Elsevier/Saunders: St. Louis, Missouri, 2015.

(3) Olano, J. P.; Walker, D. H. Diagnosing Emerging and Reemerging Infectious Diseases: The Pivotal Role of the Pathologist. *Archives of Pathology & Laboratory Medicine* **2011**, *135* (1), 83–91. https://doi.org/10.1043/2010-0260-RAR.1.

(4) Mothershed, E. A.; Whitney, A. M. Nucleic Acid-Based Methods for the Detection of Bacterial Pathogens: Present and Future Considerations for the Clinical Laboratory. *Clinica Chimica Acta* **2006**, *363* (1–2), 206–220. https://doi.org/10.1016/j.cccn.2005.05.050.

(5) Mackay, I. M. Real-Time PCR in the Microbiology Laboratory. *Clin. Microbiol. Infect.* **2004**, *10* (3), 190–212.

(6) Saag, M. S.; Holodniy, M.; Kuritzkes, D. R.; O'Brien, W. A.; Coombs, R.; Poscher, M. E.; Jacobsen, D. M.; Shaw, G. M.; Richman, D. D.; Volberding, P. A. HIV Viral Load Markers in Clinical Practice. *Nature Medicine* **1996**, *2* (6), 625–629. https://doi.org/10.1038/nm0696-625.

(7) Abe, A.; Inoue, K.; Tanaka, T.; Kato, J.; Kajiyama, N.; Kawaguchi, R.; Tanaka, S.; Yoshiba, M.; Kohara, M. Quantitation of Hepatitis B Virus Genomic DNA by Real-Time Detection PCR. *Journal of Clinical Microbiology* **1999**, *37* (9), 2899–2903.

(8) Gretch, D. R. Diagnostic Tests for Hepatitis C. *Hepatology* **1997**, *26* (S3).

(9) Price, C. P. Regular Review: Point of Care Testing. *BMJ: British Medical Journal* **2001**, *322* (7297), 1285.

(10) Peeling, R. W.; Mabey, D. Point-of-Care Tests for Diagnosing Infections in the Developing World. *Clinical Microbiology and Infection* **2010**, *16* (8), 1062–1069. https://doi.org/10.1111/j.1469-0691.2010.03279.x.

(11) Yager, P.; Domingo, G. J.; Gerdes, J. Point-of-Care Diagnostics for Global Health. *Annual Review of Biomedical Engineering* **2008**, *10* (1), 107–144. https://doi.org/10.1146/annurev.bioeng.10.061807.160524.

(12) Drain, P. K.; Hyle, E. P.; Noubary, F.; Freedberg, K. A.; Wilson, D.; Bishai, W. R.; Rodriguez, W.; Bassett, I. V. Diagnostic Point-of-Care Tests in Resource-Limited Settings. *The Lancet Infectious Diseases* **2014**, *14* (3), 239–249. https://doi.org/10.1016/S1473-3099(13)70250-0.

(13) Chin, C. D.; Linder, V.; Sia, S. K. Lab-on-a-Chip Devices for Global Health: Past Studies and Future Opportunities. *Lab Chip* **2007**, *7* (1), 41–57. https://doi.org/10.1039/B611455E.

(14) Kettler, H.; White, K.; Hawkes, S. J.; others. Mapping the Landscape of Diagnostics for Sexually Transmitted Infections: Key Findings and Recommendations. **2004**.

(15) Abel, G. Current Status and Future Prospects of Point-of-Care Testing around the Globe. *Expert Review of Molecular Diagnostics* **2015**, *15* (7), 853–855. https://doi.org/10.1586/14737159.2015.1060126.

(16) Hsiao, N.; Dunning, L.; Kroon, M.; Myer, L. Laboratory Evaluation of the Alere q Point-of-Care System for Early Infant HIV Diagnosis. *PLoS ONE* **2016**, *11* (3), e0152672. https://doi.org/10.1371/journal.pone.0152672.

(17) Boehme, C. C.; Nabeta, P.; Henostroza, G.; Raqib, R.; Rahim, Z.; Gerhardt, M.; Sanga, E.; Hoelscher, M.; Notomi, T.; Hase, T.; Perkins, M. D. Operational Feasibility of Using Loop-Mediated Isothermal Amplification for Diagnosis of Pulmonary Tuberculosis in Microscopy Centers of Developing Countries. *J. Clin. Microbiol.* **2007**, *45* (6), 1936–1940. https://doi.org/10.1128/JCM.02352-06.

(18) Melchers, W. J. G.; Kuijpers, J.; Sickler, J. J.; Rahamat-Langendoen, J. Lab-in-a-Tube: Real-Time Molecular Point-of-Care Diagnostics for Influenza A and B Using the Cobas® Liat® System. *J. Med. Virol.* **2017**, *89* (8), 1382–1386. https://doi.org/10.1002/jmv.24796.

(19) Niemz, A.; Ferguson, T. M.; Boyle, D. S. Point-of-Care Nucleic Acid Testing for Infectious Diseases. *Trends in Biotechnology* **2011**, *29* (5), 240–250. https://doi.org/10.1016/j.tibtech.2011.01.007.

(20) Tsui, N. B. Y.; Ng, E. K. O.; Lo, Y. M. D. Stability of Endogenous and Added RNA in Blood Specimens, Serum, and Plasma. *Clin. Chem.* **2002**, *48* (10), 1647–1653.

(21) *Enzymes of Molecular Biology*; Burrell, M. M., Ed.; Methods in molecular biology; Humana Press: Totowa, N.J, 1993.

(22) Hermans, J.; Scheraga, H. A. Structural Studies of Ribonuclease. V. Reversible Change of Configuration1-3. *J. Am. Chem. Soc.* **1961**, *83* (15), 3283–3292. https://doi.org/10.1021/ja01476a025.

(23) Zale, S. E.; Klibanov, A. M. On the Role of Reversible Denaturation (Unfolding) in the Irreversible Thermal Inactivation of Enzymes. *Biotechnol. Bioeng.* **1983**, *25* (9), 2221–2230. https://doi.org/10.1002/bit.260250908.

(24) Akasako, A.; Haruki, M.; Oobatake, M.; Kanaya, S. High Resistance of Escherichia Coli Ribonuclease HI Variant with Quintuple Thermostabilizing Mutations to Thermal Denaturation, Acid Denaturation, and Proteolytic Degradation. *Biochemistry* **1995**, *34* (25), 8115–8122. https://doi.org/10.1021/bi00025a018.

(25) Boom, R.; Sol, C. J.; Salimans, M. M.; Jansen, C. L.; Wertheim-van Dillen, P. M.; van der Noordaa, J. Rapid and Simple Method for Purification of Nucleic Acids. *J. Clin. Microbiol.* **1990**, *28* (3), 495–503.

(26) Cox, R. A. [103a] The Use of Guanidinium Chloride in the Isolation of Nucleic Acids. In *Methods in Enzymology*; Nucleic Acids, Part B; Academic Press, 1968; Vol. 12, pp 120–129. https://doi.org/10.1016/0076-6879(67)12123-X.

(27) Thatcher, S. A. DNA/RNA Preparation for Molecular Detection. *Clinical Chemistry* **2015**, *61* (1), 89–99. https://doi.org/10.1373/clinchem.2014.221374.

(28) Ali, N.; Rampazzo, R. de C. P.; Costa, A. D. T.; Krieger, M. A. Current Nucleic Acid Extraction Methods and Their Implications to Point-of-Care Diagnostics. *Biomed Res Int* **2017**, *2017*, 9306564. https://doi.org/10.1155/2017/9306564.

(29) Raizada, N.; Sachdeva, K. S.; Sreenivas, A.; Vadera, B.; Gupta, R. S.; Parmar, M.; Kulsange, S.; Babre, A.; Thakur, R.; Gray, C.; Ramachandran, R.; Alavadi, U.; Ghedia, M.; Vollepore, B.; Dewan, P.; Boehme, C.; Paramsivan, C. N. Feasibility of Decentralised Deployment of Xpert MTB/RIF Test at Lower Level of Health System in India. *PLoS ONE* **2014**, *9* (2), e89301. https://doi.org/10.1371/journal.pone.0089301.

(30) Toley, B. J.; Covelli, I.; Belousov, Y.; Ramachandran, S.; Kline, E.; Scarr, N.; Vermeulen, N.; Mahoney, W.; Lutz, B. R.; Yager, P. Isothermal Strand Displacement Amplification (ISDA): A Rapid and Sensitive Method of Nucleic Acid Amplification for Point-of-Care Diagnosis. *The Analyst* **2015**, *140* (22), 7540–7549. https://doi.org/10.1039/C5AN01632K.

(31) Vincent, M.; Xu, Y.; Kong, H. Helicase-Dependent Isothermal DNA Amplification. *EMBO reports* **2004**, *5* (8), 795–800. https://doi.org/10.1038/sj.embor.7400200.

(32) Notomi, T.; Mori, Y.; Tomita, N.; Kanda, H. Loop-Mediated Isothermal Amplification (LAMP): Principle, Features, and Future Prospects. *Journal of Microbiology* **2015**, *53* (1), 1–5. https://doi.org/10.1007/s12275-015-4656-9.

(33) Piepenburg, O.; Williams, C. H.; Stemple, D. L.; Armes, N. A. DNA Detection Using Recombination Proteins. *PLoS Biology* **2006**, *4* (7), e204. https://doi.org/10.1371/journal.pbio.0040204.

(34) Craw, P.; Balachandran, W. Isothermal Nucleic Acid Amplification Technologies for Point-of-Care Diagnostics: A Critical Review. *Lab on a Chip* **2012**, *12* (14), 2469. https://doi.org/10.1039/c2lc40100b.

(35) Lillis, L.; Lehman, D.; Singhal, M. C.; Cantera, J.; Singleton, J.; Labarre, P.; Toyama, A.; Piepenburg, O.; Parker, M.; Wood, R.; Overbaugh, J.; Boyle, D. S. Non-Instrumented Incubation of a Recombinase Polymerase Amplification Assay for the Rapid and Sensitive Detection of Proviral HIV-1 DNA. *PLoS ONE* **2014**, *9* (9), e108189. https://doi.org/10.1371/journal.pone.0108189.

(36) Niemz, A.; Ferguson, T. M.; Boyle, D. S. Point-of-Care Nucleic Acid Testing for Infectious Diseases. *Trends in Biotechnology* **2011**, *29* (5), 240–250. https://doi.org/10.1016/j.tibtech.2011.01.007.

(37) Euler, M.; Wang, Y.; Nentwich, O.; Piepenburg, O.; Hufert, F. T.; Weidmann, M. Recombinase Polymerase Amplification Assay for Rapid Detection of Rift Valley Fever Virus. *Journal of Clinical Virology* **2012**, *54* (4), 308–312. https://doi.org/10.1016/j.jcv.2012.05.006.

(38) Rohrman, B.; Richards-Kortum, R. Inhibition of Recombinase Polymerase Amplification by Background DNA: A Lateral Flow-Based Method for Enriching Target DNA. *Analytical Chemistry* **2015**, *87* (3), 1963–1967. https://doi.org/10.1021/ac504365v.

(39) Crannell, Z. A.; Rohrman, B.; Richards-Kortum, R. Quantification of HIV-1 DNA Using Real-Time Recombinase Polymerase Amplification. *Analytical Chemistry* **2014**, *86* (12), 5615–5619. https://doi.org/10.1021/ac5011298.

(40) Bocek, P.; Deml, M.; Gebauer, P.; Dolnik, V. *Analytical Isotachophoresis*; VCH, Weinheim, 1988.

(41) Kohlrausch, F. Uber Concentrations-Verschiebungen Durch Elektrolyse Im Inneren von Losungen Und Losungsgemischen. *Ann. Phys. Chem. (Leipzig)* **1897**, *62*, 209–239.

(42) Hruška, V.; Gaš, B. Kohlrausch Regulating Function and Other Conservation Laws in Electrophoresis. *Electrophoresis* **2007**, *28* (1–2), 3–14. https://doi.org/10.1002/elps.200600513.

(43) Kendall, J.; Crittenden, E. D. The Separation of Isotopes. *Proc Natl Acad Sci U S A* **1923**, *9* (3), 75–78.

(44) Pospichal, J.; Gebauer, P.; Bocek, P. Measurement of Mobilities and Dissociation Constants by Capillary Isotachophoresis. *Chemical Reviews* **1989**, *89* (2), 419–430.

(45) Kondratova, V.; Serd'uk, O.; Shelepov, V.; Lichtenstein, A. Concentration and Isolation of DNA from Biological Fluids by Agarose Gel Isotachophoresis. *BioTechniques* **2005**, *39* (5), 695–699. https://doi.org/10.2144/000112020.

(46) Kondratova, V. N.; Botezatu, I. V.; Shelepov, V. P.; Lichtenstein, A. V. Isotachophoresis of Nucleic Acids in Agarose Gel Rods. *Biochemistry (Moscow)* **2009**, *74* (11), 1285–1288. https://doi.org/10.1134/S0006297909110169.

(47) Kondratova, V. N.; Botezatu, I. V.; Shelepov, V. P.; Lichtenstein, A. V. Tube Gel Isotachophoresis: A Method for Quantitative Isolation of Nucleic Acids from Diluted Solutions. *Analytical Biochemistry* **2011**, *408* (2), 304–308. https://doi.org/10.1016/j.ab.2010.09.004.

(48) Marshall, L. A.; Rogacs, A.; Meinhart, C. D.; Santiago, J. G. An Injection Molded Microchip for Nucleic Acid Purification from 25 Microliter Samples Using Isotachophoresis. *Journal of Chromatography A* **2014**, *1331*, 139–142. https://doi.org/10.1016/j.chroma.2014.01.036.

(49) Khurana, T. K.; Santiago, J. G. Sample Zone Dynamics in Peak Mode Isotachophoresis. *Analytical Chemistry* **2008**, *80* (16), 6300–6307. https://doi.org/10.1021/ac800792g.

(50) Persat, A.; Chambers, R. D.; Santiago, J. G. Basic Principles of Electrolyte Chemistry for Microfluidic Electrokinetics. Part I: Acid–Base Equilibria and PH Buffers. *Lab on a Chip* **2009**, *9* (17), 2437–2453. https://doi.org/10.1039/b906465f.

(51) Persat, A.; Suss, M. E.; Santiago, J. G. Basic Principles of Electrolyte Chemistry for Microfluidic Electrokinetics. Part II: Coupling between Ion Mobility, Electrolysis, and Acid–Base Equilibria. *Lab Chip* **2009**, *9* (17), 2454–2469. https://doi.org/10.1039/B906468K.

(52) Garcia-Schwarz, G.; Bercovici, M.; Marshall, L. A.; Santiago, J. G. Sample Dispersion in Isotachophoresis. *Journal of Fluid Mechanics* **2011**, *679*, 455–475. https://doi.org/10.1017/jfm.2011.139.

(53) Moghadam, B. Y.; Connelly, K. T.; Posner, J. D. Isotachophoretic Preconcenetration on Paper-Based Microfluidic Devices. *Analytical Chemistry* **2014**, *86* (12), 5829–5837. https://doi.org/10.1021/ac500780w.

(54) Rosenfeld, T.; Bercovici, M. 1000-Fold Sample Focusing on Paper-Based Microfluidic Devices. *Lab Chip* **2014**, *14* (23), 4465–4474. https://doi.org/10.1039/C4LC00734D.

(55) Li, X.; Luo, L.; Crooks, R. M. Low-Voltage Paper Isotachophoresis Device for DNA Focusing. *Lab Chip* **2015**, *15* (20), 4090–4098. https://doi.org/10.1039/C5LC00875A.

(56) Antiretroviral Therapy Cohort Collaboration. Survival of HIV-Positive Patients Starting Antiretroviral Therapy between 1996 and 2013: A Collaborative Analysis of Cohort Studies. *Lancet HIV* **2017**, *4* (8), e349–e356. https://doi.org/10.1016/S2352-3018(17)30066-8.

(57) U=U | United States | Prevention Access Campaign https://www.preventionaccess.org/ (accessed Nov 15, 2018).

(58) Singh, R. P.; Dilworth, A. D.; Singh, M.; McLaren, D. L. Evaluation of a Simple Membrane-Based Nucleic Acid Preparation Protocol for RT-PCR Detection of Potato Viruses from Aphid and Plant Tissues. *J. Virol. Methods* **2004**, *121* (2), 163–170. https://doi.org/10.1016/j.jviromet.2004.06.012.

(59) Puren, A.; Gerlach, J. L.; Weigl, B. H.; Kelso, D. M.; Domingo, G. J. Laboratory Operations, Specimen Processing, and Handling for Viral Load Testing and Surveillance. *J Infect Dis* **2010**, *201* (Supplement_1), S27–S36. https://doi.org/10.1086/650390.

(60) Rodriguez, N. M.; Linnes, J. C.; Fan, A.; Ellenson, C. K.; Pollock, N. R.; Klapperich, C. M. Paper-Based RNA Extraction, *in Situ* Isothermal Amplification, and Lateral Flow Detection for Low-Cost, Rapid Diagnosis of Influenza A (H1N1) from Clinical Specimens. *Analytical Chemistry* **2015**, *87* (15), 7872–7879. https://doi.org/10.1021/acs.analchem.5b01594.

(61) Chen, X.; Cui, D.-F.; Liu, C.-C.; Li, H. Microfabrication and Characterization of Porous Channels for DNA Purification. *J. Micromech. Microeng.* **2007**, *17* (1), 68. https://doi.org/10.1088/0960-1317/17/1/009.

(62) Byrnes, S. A.; Bishop, J. D.; Lafleur, L.; Buser, J. R.; Lutz, B.; Yager, P. One-Step Purification and Concentration of DNA in Porous Membranes for Point-of-Care Applications. *Lab Chip* **2015**, *15* (12), 2647–2659. https://doi.org/10.1039/C5LC00317B.

(63) Bender, A. T.; Borysiak, M. D.; Levenson, A. M.; Lillis, L.; Boyle, D. S.; Posner, J. D. Semiquantitative Nucleic Acid Test with Simultaneous Isotachophoretic Extraction and

Amplification. *Analytical Chemistry* **2018**, *90* (12), 7221–7229. https://doi.org/10.1021/acs.analchem.8b00185.

(64) Luft, L. M.; Gill, M. J.; Church, D. L. HIV-1 Viral Diversity and Its Implications for Viral Load Testing: Review of Current Platforms. *International Journal of Infectious Diseases* **2011**, *15* (10), e661–e670. https://doi.org/10.1016/j.ijid.2011.05.013.

(65) Curtis, K. A.; Rudolph, D. L.; Nejad, I.; Singleton, J.; Beddoe, A.; Weigl, B.; LaBarre, P.; Owen, S. M. Isothermal Amplification Using a Chemical Heating Device for Point-of-Care Detection of HIV-1. *PLoS ONE* **2012**, *7* (2), e31432. https://doi.org/10.1371/journal.pone.0031432.

(66) Ocwieja, K. E.; Sherrill-Mix, S.; Liu, C.; Song, J.; Bau, H.; Bushman, F. D. A Reverse Transcription Loop-Mediated Isothermal Amplification Assay Optimized to Detect Multiple HIV Subtypes. *PLOS ONE* **2015**, *10* (2), e0117852. https://doi.org/10.1371/journal.pone.0117852.

(67) Tang, W.; Chow, W. H. A.; Li, Y.; Kong, H.; Tang, Y.; Lemieux, B. Nucleic Acid Assay System for Tier II Laboratories and Moderately Complex Clinics to Detect HIV in Low-Resource Settings. *The Journal of Infectious Diseases* **2010**, *201* (s1), S46–S51. https://doi.org/10.1086/650388.

(68) Lillis, L.; Lehman, D. A.; Siverson, J. B.; Weis, J.; Cantera, J.; Parker, M.; Piepenburg, O.; Overbaugh, J.; Boyle, D. S. Cross-Subtype Detection of HIV-1 Using Reverse Transcription and Recombinase Polymerase Amplification. *Journal of Virological Methods* **2016**, *230*, 28–35. https://doi.org/10.1016/j.jviromet.2016.01.010.

(69) Crannell, Z. A.; Rohrman, B.; Richards-Kortum, R. Quantification of HIV-1 DNA Using Real-Time Recombinase Polymerase Amplification. *Analytical Chemistry* **2014**, *86* (12), 5615–5619. https://doi.org/10.1021/ac5011298.

(70) Gurrala, R.; Lang, Z.; Shepherd, L.; Davidson, D.; Harrison, E.; McClure, M.; Kaye, S.; Toumazou, C.; Cooke, G. S. Novel PH Sensing Semiconductor for Point-of-Care Detection of HIV-1 Viremia. *Scientific Reports* **2016**, *6* (1). https://doi.org/10.1038/srep36000.

(71) Lecossier, D. Hypermutation of HIV-1 DNA in the Absence of the Vif Protein. *Science* **2003**, *300* (5622), 1112–1112. https://doi.org/10.1126/science.1083338.

(72) Gueudin, M.; Baron, A.; Alessandri-Gradt, E.; Lemée, V.; Mourez, T.; Etienne, M.; Plantier, J.-C. Performance Evaluation of the New HIV-1 Quantification Assay, Xpert HIV-1 Viral Load, on a Wide Panel of HIV-1 Variants. *J. Acquir. Immune Defic. Syndr.* **2016**, *72* (5), 521–526. https://doi.org/10.1097/QAI.0000000000001003.

(73) Swanson, P.; Mendoza, C. de; Joshi, Y.; Golden, A.; Hodinka, R. L.; Soriano, V.; Devare, S. G.; Hackett, J. Impact of Human Immunodeficiency Virus Type 1 (HIV-1) Genetic Diversity on Performance of Four Commercial Viral Load Assays: LCx HIV RNA Quantitative, AMPLICOR HIV-1 MONITOR v1.5, VERSANT HIV-1 RNA 3.0, and NucliSens HIV-1 QT. *J. Clin. Microbiol.* **2005**, *43* (8), 3860–3868. https://doi.org/10.1128/JCM.43.8.3860-3868.2005.

(74) Ritchie, A. V.; Goel, N.; Sembongi, H.; Lehga, J.; Farleigh, L. E.; Edemaga, D.; Wisniewski, C. A.; Lee, H. H. Performance Evaluation of the Point-of-Care SAMBA I and II HIV-1 Qual Whole Blood Tests. *Journal of Virological Methods* **2016**, *237*, 143–149. https://doi.org/10.1016/j.jviromet.2016.08.017.

(75) Malmsten, A. Reverse Transcriptase Activity Assays for Retrovirus Quantitation and Characterization, Uppsala University, Uppsala, 2005.

(76) Shafiee, H.; Lidstone, E. A.; Jahangir, M.; Inci, F.; Hanhauser, E.; Henrich, T. J.; Kuritzkes, D. R.; Cunningham, B. T.; Demirci, U. Nanostructured Optical Photonic Crystal Biosensor for HIV Viral Load Measurement. *Sci Rep* **2014**, *4*, 4116. https://doi.org/10.1038/srep04116.

(77) World Health Organization; World Health Organization; Global Hepatitis Programme. *Global Hepatitis Report, 2017*; 2017.

(78) Terrault, N. A.; Lok, A. S. F.; McMahon, B. J.; Chang, K.-M.; Hwang, J. P.; Jonas, M. M.; Brown, R. S.; Bzowej, N. H.; Wong, J. B. Update on Prevention, Diagnosis, and Treatment of Chronic Hepatitis B: AASLD 2018 Hepatitis B Guidance. *Hepatology* **2018**, *67* (4), 1560–1599. https://doi.org/10.1002/hep.29800.

(79) World Health Organization; Global Hepatitis Programme. *WHO Guidelines on Hepatitis B and C Testing.*; 2017.

(80) Mendy, M. E.; Welzel, T.; Lesi, O. A.; Hainaut, P.; Hall, A. J.; Kuniholm, M. H.; McConkey, S.; Goedert, J. J.; Kaye, S.; Rowland-Jones, S.; Whittle, H.; Kirk, G. D. Hepatitis B Viral Load and Risk for Liver Cirrhosis and Hepatocellular Carcinoma in The Gambia, West Africa. *J Viral Hepat* **2010**, *17* (2), 115–122. https://doi.org/10.1111/j.1365-2893.2009.01168.x.

(81) Echevarría, J. M.; Avellón, A. Hepatitis B Virus Genetic Diversity. *Journal of Medical Virology* **2006**, *78* (S1), S36–S42. https://doi.org/10.1002/jmv.20605.

(82) Norder, H.; Couroucé, A.-M.; Coursaget, P.; Echevarria, J. M.; Lee, S.-D.; Mushahwar, I. K.; Robertson, B. H.; Locarnini, S.; Magnius, L. O. Genetic Diversity of Hepatitis B Virus

Strains Derived Worldwide: Genotypes, Subgenotypes, and HBsAg Subtypes. *Intervirology* **2004**, *47* (6), 289–309. https://doi.org/10.1159/000080872.

(83) Kourtis, A. P.; Bulterys, M.; Hu, D. J.; Jamieson, D. J. HIV–HBV Coinfection — A Global Challenge. *New England Journal of Medicine* **2012**, *366* (19), 1749–1752. https://doi.org/10.1056/NEJMp1201796.

(84) Pol, S.; Corouge, M.; Vallet-Pichard, A. Daclatasvir-Sofosbuvir Combination Therapy with or without Ribavirin for Hepatitis C Virus Infection: From the Clinical Trials to Real Life. *Hepat Med* **2016**, *8*, 21–26. https://doi.org/10.2147/HMER.S62014.

(85) Hill, A.; Simmons, B.; Gotham, D.; Fortunak, J. Rapid Reductions in Prices for Generic Sofosbuvir and Daclatasvir to Treat Hepatitis C. *J Virus Erad 2* (1), 28–31.

(86) Ivanova Reipold, E.; Easterbrook, P.; Trianni, A.; Panneer, N.; Krakower, D.; Ongarello, S.; Roberts, T.; Miller, V.; Denkinger, C. Optimising Diagnosis of Viraemic Hepatitis C Infection: The Development of a Target Product Profile. *BMC Infectious Diseases* **2017**, *17* (S1). https://doi.org/10.1186/s12879-017-2770-5.

(87) Reipold, E. I.; Trianni, A.; Krakower, D.; Ongarello, S.; Roberts, T.; Easterbrook, P.; Denkinger, C. Values, Preferences and Current Hepatitis B and C Testing Practices in Low- and Middle-Income Countries: Results of a Survey of End Users and Implementers. *BMC Infect Dis* **2017**, *17* (Suppl 1). https://doi.org/10.1186/s12879-017-2769-y.

(88) Llibre, A.; Shimakawa, Y.; Mottez, E.; Ainsworth, S.; Buivan, T.-P.; Firth, R.; Harrison, E.; Rosenberg, A. R.; Meritet, J.-F.; Fontanet, A.; Castan, P.; Madejón, A.; Laverick, M.; Glass, A.; Viana, R.; Pol, S.; McClure, C. P.; Irving, W. L.; Miele, G.; Albert, M. L.; Duffy, D. Development and Clinical Validation of the Genedrive Point-of-Care Test for Qualitative Detection of Hepatitis C Virus. *Gut* **2018**, *67* (11), 2017–2024. https://doi.org/10.1136/gutjnl-2017-315783.

(89) Neto, M. F.; Butzler, M. A.; Reed, J. L.; Rui, X.; Fisher, M. J.; Kelso, D. M.; McFall, S. M. Immiscible Phase Filter Extraction and Equivalent Amplification of Genotypes 1–6 of Hepatitis C RNA: The Building Blocks for Point-of-Care Diagnosis. *Journal of Virological Methods* **2017**, *248*, 107–115. https://doi.org/10.1016/j.jviromet.2017.06.016.

(90) Simmonds, P. Genetic Diversity and Evolution of Hepatitis C Virus – 15 Years On. *Journal of General Virology* **2004**, *85* (11), 3173–3188. https://doi.org/10.1099/vir.0.80401-0.

(91) Bhatt, S.; Gething, P. W.; Brady, O. J.; Messina, J. P.; Farlow, A. W.; Moyes, C. L.; Drake, J. M.; Brownstein, J. S.; Hoen, A. G.; Sankoh, O.; Myers, M. F.; George, D. B.; Jaenisch, T.; Wint, G. R. W.; Simmons, C. P.; Scott, T. W.; Farrar, J. J.; Hay, S. I. The

Global Distribution and Burden of Dengue. *Nature* **2013**, *496* (7446), 504–507. https://doi.org/10.1038/nature12060.

(92) World Health Organization. *Global Strategy for Dengue Prevention and Control, 2012-2020.*; World Health Organization: Geneva, Switzerland, 2012.

(93) Organization, W. H. *Dengue: Guidelines for Diagnosis, Treatment, Prevention and Control*; World Health Organization, 2009.

(94) Laboratory Guidance and Diagnostic Testing | Dengue | CDC https://www.cdc.gov/dengue/clinicallab/laboratory.html (accessed Nov 15, 2018).

(95) Bai, Z.; Liu, L.; Tu, Z.; Yao, L.; Liu, J.; Xu, B.; Tang, B.; Liu, J.; Wan, Y.; Fang, M.; Chen, W. Real-Time PCR for Detecting Circulating Dengue Virus in the Guangdong Province of China in 2006. *Journal of Medical Microbiology* **2008**, *57* (12), 1547–1552. https://doi.org/10.1099/jmm.0.2008/003418-0.

(96) Singh, R. K.; Dhama, K.; Karthik, K.; Tiwari, R.; Khandia, R.; Munjal, A.; Iqbal, H. M. N.; Malik, Y. S.; Bueno-Marí, R. Advances in Diagnosis, Surveillance, and Monitoring of Zika Virus: An Update. *Front Microbiol* **2018**, *8*. https://doi.org/10.3389/fmicb.2017.02677.

(97) Zika Virus https://www.cdc.gov/zika/hc-providers/testing-guidance.html (accessed Nov 15, 2018).

(98) Theel, E. S.; Hata, D. J. Diagnostic Testing for Zika Virus: A Postoutbreak Update. *J Clin Microbiol* **2018**, *56* (4). https://doi.org/10.1128/JCM.01972-17.

(99) Ebola Situation Report - 15 July 2015 | Ebola http://apps.who.int/ebola/current-situation/ebola-situation-report-15-july-2015 (accessed Nov 15, 2018).

(100) Broadhurst, M. J.; Brooks, T. J. G.; Pollock, N. R. Diagnosis of Ebola Virus Disease: Past, Present, and Future. *Clinical Microbiology Reviews* **2016**, *29* (4), 773–793. https://doi.org/10.1128/CMR.00003-16.

(101) Schieffelin, J. S.; Shaffer, J. G.; Goba, A.; Gbakie, M.; Gire, S. K.; Colubri, A.; Sealfon, R. S. G.; Kanneh, L.; Moigboi, A.; Momoh, M.; Fullah, M.; Moses, L. M.; Brown, B. L.; Andersen, K. G.; Winnicki, S.; Schaffner, S. F.; Park, D. J.; Yozwiak, N. L.; Jiang, P.-P.; Kargbo, D.; Jalloh, S.; Fonnie, M.; Sinnah, V.; French, I.; Kovoma, A.; Kamara, F. K.; Tucker, V.; Konuwa, E.; Sellu, J.; Mustapha, I.; Foday, M.; Yillah, M.; Kanneh, F.; Saffa, S.; Massally, J. L. B.; Boisen, M. L.; Branco, L. M.; Vandi, M. A.; Grant, D. S.; Happi, C.; Gevao, S. M.; Fletcher, T. E.; Fowler, R. A.; Bausch, D. G.; Sabeti, P. C.; Khan, S. H.; Garry, R. F.; KGH Lassa Fever Program; Viral Hemorrhagic Fever Consortium; WHO

Clinical Response Team. Clinical Illness and Outcomes in Patients with Ebola in Sierra Leone. *N. Engl. J. Med.* **2014**, *371* (22), 2092–2100. https://doi.org/10.1056/NEJMoa1411680.

(102) Yager, P.; Domingo, G. J.; Gerdes, J. Point-of-Care Diagnostics for Global Health. *Annual Review of Biomedical Engineering* **2008**, *10* (1), 107–144. https://doi.org/10.1146/annurev.bioeng.10.061807.160524.

(103) Dyer, K. D.; Rosenberg, H. F. The RNase a Superfamily: Generation of Diversity and Innate Host Defense. *Mol Divers* **2006**, *10* (4), 585–597. https://doi.org/10.1007/s11030-006-9028-2.

(104) Klink, T. A.; Woycechowsky, K. J.; Taylor, K. M.; Raines, R. T. Contribution of Disulfide Bonds to the Conformational Stability and Catalytic Activity of Ribonuclease A. *European Journal of Biochemistry* **2000**, *267* (2), 566–572. https://doi.org/10.1046/j.1432-1327.2000.01037.x.

(105) Resnick, H.; Carter, J. R.; Kalnitsky, G. The Relationship of Disulfide Bonds and Activity in Ribonuclease. *The Journal of biological chemistry* **1959**, *234* (7), 1711–1713.

(106) Sorrentino, S. The Eight Human "Canonical" Ribonucleases: Molecular Diversity, Catalytic Properties, and Special Biological Actions of the Enzyme Proteins. *FEBS Letters* **2010**, *584* (11), 2194–2200. https://doi.org/10.1016/j.febslet.2010.04.018.

(107) Akagi, K.; Murai, K.; Hirao, N.; Yamanaka, M. Purification and Properties of Alkaline Ribonuclease from Human Serum. *Biochimica et Biophysica Acta (BBA) - Nucleic Acids and Protein Synthesis* **1976**, *442* (3), 368–378. https://doi.org/10.1016/0005-2787(76)90311-7.

(108) Kim, Y.; Han, M.-S.; Kim, J.; Kwon, A.; Lee, K.-A. Evaluation of Three Automated Nucleic Acid Extraction Systems for Identification of Respiratory Viruses in Clinical Specimens by Multiplex Real-Time PCR. *Biomed Res Int* **2014**, *2014*, 430650. https://doi.org/10.1155/2014/430650.

(109) Chomczynski, P.; Sacchi, N. Single-Step Method of RNA Isolation by Acid Guanidinium Thiocyanate-Phenol-Chloroform Extraction. *Anal. Biochem.* **1987**, *162* (1), 156–159. https://doi.org/10.1006/abio.1987.9999.

(110) Gong, M. M.; Nosrati, R.; San Gabriel, M. C.; Zini, A.; Sinton, D. Direct DNA Analysis with Paper-Based Ion Concentration Polarization. *J. Am. Chem. Soc.* **2015**, *137* (43), 13913–13919. https://doi.org/10.1021/jacs.5b08523.

(111) Kenyon, S. M.; Meighan, M. M.; Hayes, M. A. Recent Developments in Electrophoretic Separations on Microfluidic Devices. *ELECTROPHORESIS* **2011**, *32* (5), 482–493. https://doi.org/10.1002/elps.201000469.

(112) Marshall, L. A.; Rogacs, A.; Meinhart, C. D.; Santiago, J. G. An Injection Molded Microchip for Nucleic Acid Purification from 25 Microliter Samples Using Isotachophoresis. *Journal of Chromatography A*. https://doi.org/10.1016/j.chroma.2014.01.036.

(113) Hall, A. T.; Zovanyi, A. M.; Christensen, D. R.; Koehler, J. W.; Minogue, T. D. Evaluation of Inhibitor-Resistant Real-Time PCR Methods for Diagnostics in Clinical and Environmental Samples. *PLOS ONE* **2013**, *8* (9), e73845. https://doi.org/10.1371/journal.pone.0073845.

(114) Zhang, Z.; Kermekchiev, M. B.; Barnes, W. M. Direct DNA Amplification from Crude Clinical Samples Using a PCR Enhancer Cocktail and Novel Mutants of Taq. *J Mol Diagn* **2010**, *12* (2), 152–161. https://doi.org/10.2353/jmoldx.2010.090070.

(115) Cai, D.; Behrmann, O.; Hufert, F.; Dame, G.; Urban, G. Direct DNA and RNA Detection from Large Volumes of Whole Human Blood. *Sci Rep* **2018**, *8* (1), 1–9. https://doi.org/10.1038/s41598-018-21224-0.

(116) Manage, D. P.; Morrissey, Y. C.; Stickel, A. J.; Lauzon, J.; Atrazhev, A.; Acker, J. P.; Pilarski, L. M. On-Chip PCR Amplification of Genomic and Viral Templates in Unprocessed Whole Blood. *Microfluidics and Nanofluidics* **2011**, *10* (3), 697–702. https://doi.org/10.1007/s10404-010-0702-4.

(117) Pastorino, B.; Bessaud, M.; Grandadam, M.; Murri, S.; Tolou, H. J.; Peyrefitte, C. N. Development of a TaqMan® RT-PCR Assay without RNA Extraction Step for the Detection and Quantification of African Chikungunya Viruses. *Journal of Virological Methods* **2005**, *124* (1), 65–71. https://doi.org/10.1016/j.jviromet.2004.11.002.

(118) Craw, P.; Balachandran, W. Isothermal Nucleic Acid Amplification Technologies for Point-of-Care Diagnostics: A Critical Review. *Lab on a Chip* **2012**, *12* (14), 2469. https://doi.org/10.1039/c2lc40100b.

(119) Curtis, K. A.; Rudolph, D. L.; Owen, S. M. Sequence-Specific Detection Method for Reverse Transcription, Loop-Mediated Isothermal Amplification of HIV-1. *Journal of Medical Virology* **2009**, *81* (6), 966–972. https://doi.org/10.1002/jmv.21490.

(120) Shehadul Islam, M.; Aryasomayajula, A.; Selvaganapathy, P. R. A Review on Macroscale and Microscale Cell Lysis Methods. *Micromachines (Basel)* **2017**, *8* (3), 83. https://doi.org/10.3390/mi8030083.

(121) Innis, M. A.; Gelfand, D. H.; Sninsky, J. J.; White, T. J. *PCR Protocols: A Guide to Methods and Applications*; Academic Press, 2012.

(122) Johnson, M. Detergents: Triton X-100, Tween-20, and More. *Mater Methods* **2013**, *3* (1), 163.

(123) Yoon, J.; Yoon, Y.-J.; Lee, T. Y.; Park, M. K.; Chung, J.; Shin, Y. A Disposable Lab-on-a-Chip Platform for Highly Efficient RNA Isolation. *Sensors and Actuators B: Chemical* **2018**, *255*, 1491–1499. https://doi.org/10.1016/j.snb.2017.08.157.

(124) McGookin, R. RNA Extraction by the Proteinase k Method. *Methods Mol. Biol.* **1985**, *2*, 109–112. https://doi.org/10.1385/0-89603-064-4:109.

(125) Wiegers, U.; Hilz, H. A New Method Using 'Proteinase K'to Prevent MRNA Degradation during Isolation from HeLa Cells. *Biochemical and biophysical research communications* **1971**, *44* (2), 513–519.

(126) Jones, M. N.; Skinner, H. A.; Tipping, E.; Wilkinson, A. The Interaction between Ribonuclease A and Surfactants. *Biochemical Journal* **1973**, *135* (1), 231–236. https://doi.org/10.1042/bj1350231.

(127) Mendelsohn, S. L.; Young, D. A. Inhibition of Ribonuclease Efficacy of Sodium Dodecyl Sulfate, Diethyl Pyrocarbonate, Proteinase K and Heparin Using a Sensitive Ribonuclease Assay. *Biochimica et Biophysica Acta (BBA) - Nucleic Acids and Protein Synthesis* **1978**, *519* (2), 461–473. https://doi.org/10.1016/0005-2787(78)90099-0.

(128) Pasloske, B. L.; Wu, W. Method and Reagents for Inactivating Ribonucleases RNase A, RNase I and RNase T1. US6777210B1, August 17, 2004.

(129) Räuber, N. R. K.; Jany, K.-D.; Pfleiderer, G. Ribonuclease A Digestion by Proteinase K. *Zeitschrift für Naturforschung C* **1978**, *33* (9–10), 660–663. https://doi.org/10.1515/znc-1978-9-1009.

(130) Wilson, C. W. A Rapid Staining Technique for Detection of RNase after Polyacrylamide Gel Electrophoresis. *Analytical Biochemistry* **1969**, *31*, 506–511. https://doi.org/10.1016/0003-2697(69)90294-2.

(131) Kunitz, M. A Spectrophotometric Method for the Measurement of Ribonuclease Activity. *J. Biol. Chem.* **1946**, *164* (2), 563–568.

(132) Jankowsky, E.; Harris, M. E. Specificity and Non-Specificity in RNA–Protein Interactions. *Nat Rev Mol Cell Biol* **2015**, *16* (9), 533–544. https://doi.org/10.1038/nrm4032.

(133) Reddi, K. K.; Holland, J. F. Elevated Serum Ribonuclease in Patients with Pancreatic Cancer. *Proc Natl Acad Sci U S A* **1976**, *73* (7), 2308–2310.

(134) Hartmann, R. K.; Bindereif, A.; Schön, A.; Westhof, E. Handbook of RNA Biochemistry. 201.

(135) Jha, S. K.; Marqusee, S. Kinetic Evidence for a Two-Stage Mechanism of Protein Denaturation by Guanidinium Chloride. *Proceedings of the National Academy of Sciences* **2014**, *111* (13), 4856–4861. https://doi.org/10.1073/pnas.1315453111.

(136) Thompson, R. E.; Duncan, G.; McCord, B. R. An Investigation of PCR Inhibition Using Plexor®-Based Quantitative PCR and Short Tandem Repeat Amplification. *Journal of Forensic Sciences* **2014**, *59* (6), 1517–1529. https://doi.org/10.1111/1556-4029.12556.

(137) Goldenberger, D.; Ritzler, M.; Altwegg, M. A Simple "Universal" DNA Extraction Procedure Using SDS and Proteinase K Is Compatible with Direct PCR Amplification. 4.

(138) Choi, N.-S.; Hahm, J.-H.; Maeng, P.-J.; Kim, S.-H. Comparative Study of Enzyme Activity and Stability of Bovine and Human Plasmins in Electrophoretic Reagents, β-Mercaptoethanol, DTT, SDS, Triton X-100, and Urea. *BMB Reports* **2005**, *38* (2), 177–181. https://doi.org/10.5483/BMBRep.2005.38.2.177.

(139) Sidstedt, M.; Hedman, J.; Romsos, E. L.; Waitara, L.; Wadsö, L.; Steffen, C. R.; Vallone, P. M.; Rådström, P. Inhibition Mechanisms of Hemoglobin, Immunoglobulin G, and Whole Blood in Digital and Real-Time PCR. *Analytical and Bioanalytical Chemistry* **2018**, *410* (10), 2569–2583. https://doi.org/10.1007/s00216-018-0931-z.

(140) Hilz, H.; Wiegers, U.; Adamietz, P. Stimulation of Proteinase K Action by Denaturing Agents: Application to the Isolation of Nucleic Acids and the Degradation of 'Masked' Proteins. *European Journal of Biochemistry* **1975**, *56* (1), 103–108. https://doi.org/10.1111/j.1432-1033.1975.tb02211.x.

(141) Simpson, A. M.; Bakalara, N.; Simpson, L. A Ribonuclease Activity Is Activated by Heparin or by Digestion with Proteinase K in Mitochondrial Extracts of Leishmania Tarentolae. *J. Biol. Chem.* **1992**, *267* (10), 6782–6788.

(142) Proc, J. L.; Kuzyk, M. A.; Hardie, D. B.; Yang, J.; Smith, D. S.; Jackson, A. M.; Parker, C. E.; Borchers, C. H. A Quantitative Study of the Effects of Chaotropic Agents, Surfactants,

and Solvents on the Digestion Efficiency of Human Plasma Proteins by Trypsin. *J. Proteome Res.* **2010**, *9* (10), 5422–5437. https://doi.org/10.1021/pr100656u.

(143) Doumas, B. T.; Peters, T. Serum and Urine Albumin: A Progress Report on Their Measurement and Clinical Significance. *Clinica Chimica Acta* **1997**, *258* (1), 3–20. https://doi.org/10.1016/S0009-8981(96)06446-7.

(144) Hellman, L. M.; Fried, M. G. Electrophoretic Mobility Shift Assay (EMSA) for Detecting Protein-Nucleic Acid Interactions. *Nat Protoc* **2007**, *2* (8), 1849–1861. https://doi.org/10.1038/nprot.2007.249.

(145) Rogacs, A.; Santiago, J. G. Method of Preparing RNA from Ribonuclease-Rich Sources. US9057673B2, June 16, 2015.

(146) Rogacs, A.; Qu, Y.; Santiago, J. G. Bacterial RNA Extraction and Purification from Whole Human Blood Using Isotachophoresis. *Analytical Chemistry* **2012**, *84* (14), 5858–5863. https://doi.org/10.1021/ac301021d.

(147) Curtis, K. A.; Rudolph, D. L.; Owen, S. M. Sequence-specific detection method for reverse transcription, loop-mediated isothermal amplification of HIV-1 https://onlinelibrary.wiley.com/doi/abs/10.1002/jmv.21490 (accessed Jun 27, 2019). https://doi.org/10.1002/jmv.21490.

(148) Curtis, K. A.; Morrison, D.; Rudolph, D. L.; Shankar, A.; Bloomfield, L. S. P.; Switzer, W. M.; Owen, S. M. A Multiplexed RT-LAMP Assay for Detection of Group M HIV-1 in Plasma or Whole Blood. *Journal of Virological Methods* **2018**, *255*, 91–97. https://doi.org/10.1016/j.jviromet.2018.02.012.

(149) Zhu, L. Q.; Gangopadhyay, T.; Padmanabha, K. P.; Deutscher, M. P. Escherichia Coli Rna Gene Encoding RNase I: Cloning, Overexpression, Subcellular Distribution of the Enzyme, and Use of an Rna Deletion to Identify Additional RNases. *Journal of Bacteriology* **1990**, *172* (6), 3146–3151. https://doi.org/10.1128/jb.172.6.3146-3151.1990.

(150) Chen, Z.; Ling, J.; Gallie, D. R. RNase Activity Requires Formation of Disulfide Bonds and Is Regulated by the Redox State. *Plant Mol. Biol.* **2004**, *55* (1), 83–96. https://doi.org/10.1007/s11103-004-0438-1.

(151) Boiso, L.; Hedman, J. Overcoming Sodium Dodecyl Sulfate Induced PCR Inhibition. *Forensic Science International: Genetics* **2017**, *29*, e16–e18. https://doi.org/10.1016/j.fsigen.2017.03.020.

(152) WHO | Data and statistics http://www.who.int/hiv/data/en/ (accessed Mar 11, 2020).

(153) World Health Organization (WHO). Guideline on when to start antiretroviral therapy and on pre-exposure prophylaxis for HIV http://apps.who.int/iris/bitstream/10665/186275/1/9789241509565_eng.pdf.

(154) World Health Organization; World Health Organization; Department of HIV/AIDS. *WHO Recommendations on the Diagnosis of HIV Infection in Infants and Children.*; 2010.

(155) Roberts, T.; Cohn, J.; Bonner, K.; Hargreaves, S. Scale-up of Routine Viral Load Testing in Resource-Poor Settings: Current and Future Implementation Challenges. *Clin Infect Dis* **2016**, *62* (8), 1043–1048. https://doi.org/10.1093/cid/ciw001.

(156) Drain, P. K.; Dorward, J.; Bender, A.; Lillis, L.; Marinucci, F.; Sacks, J.; Bershteyn, A.; Boyle, D. S.; Posner, J. D.; Garrett, N. Point-of-Care HIV Viral Load Testing: An Essential Tool for a Sustainable Global HIV/AIDS Response. *Clinical Microbiology Reviews* **2019**, *32* (3), 25.

(157) Wood, E. J. Molecular Cloning. A Laboratory Manual by T Maniatis, E F Fritsch and J Sambrook. Pp 545. Cold Spring Harbor Laboratory, New York. 1982. $48 ISBN 0-87969-136-0. *Biochemical Education* **1983**, *11* (2), 82–82. https://doi.org/10.1016/0307-4412(83)90068-7.

(158) Rogacs, A.; Marshall, L. A.; Santiago, J. G. Purification of Nucleic Acids Using Isotachophoresis. *Journal of Chromatography A* **2014**, *1335*, 105–120. https://doi.org/10.1016/j.chroma.2013.12.027.

(159) Longsworth, L. G. Diffusion Measurements, at 25°, of Aqueous Solutions of Amino Acids, Peptides and Sugars. *J. Am. Chem. Soc.* **1953**, *75* (22), 5705–5709. https://doi.org/10.1021/ja01118a065.

(160) Kondratova, V.; Serd'uk, O.; Shelepov, V.; Lichtenstein, A. Concentration and Isolation of DNA from Biological Fluids by Agarose Gel Isotachophoresis. *BioTechniques* **2005**, *39* (5), 695–699. https://doi.org/10.2144/000112020.

(161) Persat, A.; Marshall, L. A.; Santiago, J. G. Purification of Nucleic Acids from Whole Blood Using Isotachophoresis. *Anal. Chem.* **2009**, *81* (22), 9507–9511. https://doi.org/10.1021/ac901965v.

(162) Eid, C.; G. Santiago, J. Assay for Listeria Monocytogenes Cells in Whole Blood Using Isotachophoresis and Recombinase Polymerase Amplification. *Analyst* **2017**, *142* (1), 48–54. https://doi.org/10.1039/C6AN02119K.

(163) Rogacs, A.; Qu, Y.; Santiago, J. G. Bacterial RNA Extraction and Purification from Whole Human Blood Using Isotachophoresis. *Anal. Chem.* **2012**, *84* (14), 5858–5863. https://doi.org/10.1021/ac301021d.

(164) Gong, M. M.; Sinton, D. Turning the Page: Advancing Paper-Based Microfluidics for Broad Diagnostic Application. *Chem. Rev.* **2017**, *117* (12), 8447–8480. https://doi.org/10.1021/acs.chemrev.7b00024.

(165) Moghadam, B. Y.; Connelly, K. T.; Posner, J. D. Isotachophoretic Preconcenetration on Paper-Based Microfluidic Devices. *Anal. Chem.* **2014**, *86* (12), 5829–5837. https://doi.org/10.1021/ac500780w.

(166) Li, X.; Luo, L.; Crooks, R. M. Low-Voltage Paper Isotachophoresis Device for DNA Focusing. *Lab Chip* **2015**, *15* (20), 4090–4098. https://doi.org/10.1039/C5LC00875A.

(167) Schaumburg, F.; Kler, P. A.; Carrell, C. S.; Berli, C. L. A.; Henry, C. S. USB Powered Microfluidic Paper-Based Analytical Devices. *Electrophoresis* **2019**. https://doi.org/10.1002/elps.201900273.

(168) Rosenfeld, T.; Bercovici, M. Amplification-Free Detection of DNA in a Paper-Based Microfluidic Device Using Electroosmotically Balanced Isotachophoresis. *Lab on a Chip* **2018**, *18* (6), 861–868. https://doi.org/10.1039/C7LC01250K.

(169) Moghadam, B. Y.; Connelly, K. T.; Posner, J. D. Two Orders of Magnitude Improvement in Detection Limit of Lateral Flow Assays Using Isotachophoresis. *Anal. Chem.* **2015**, *87* (2), 1009–1017. https://doi.org/10.1021/ac504552r.

(170) Rosenfeld, T.; Bercovici, M. 1,000-Fold Sample Focusing on Paper-Based Microfluidic Devices. *Lab Chip* **2014**. https://doi.org/10.1039/C4LC00734D.

(171) Bender, A. T.; Sullivan, B. P.; Lillis, L.; Posner, J. D. Enzymatic and Chemical-Based Methods to Inactivate Endogenous Blood Ribonucleases for Nucleic Acid Diagnostics. *The Journal of Molecular Diagnostics* **2020**. https://doi.org/10.1016/j.jmoldx.2020.04.211.

(172) Sanchez, A. M.; DeMarco, C. T.; Hora, B.; Keinonen, S.; Chen, Y.; Brinkley, C.; Stone, M.; Tobler, L.; Keating, S.; Schito, M.; Busch, M. P.; Gao, F.; Denny, T. N. Development of a Contemporary Globally Diverse HIV Viral Panel by the EQAPOL Program. *J. Immunol. Methods* **2014**, *409*, 117–130. https://doi.org/10.1016/j.jim.2014.01.004.

(173) Rouet, F.; Chaix, M.-L.; Nerrienet, E.; Ngo-Giang-Huong, N.; Plantier, J.-C.; Burgard, M.; Peeters, M.; Damond, F.; Ekouevi, D. K.; Msellati, P.; Ferradini, L.; Rukobo, S.; Maréchal, V.; Schvachsa, N.; Wakrim, L.; Rafalimanana, C.; Rakotoambinina, B.; Viard, J.-P.; Seigneurin, J.-M.; Rouzioux, C.; Groups, for the A. N. de R. sur le S. A. W. Impact

of HIV-1 Genetic Diversity on Plasma HIV-1 RNA Quantification: Usefulness of the Agence Nationale de Recherches Sur Le SIDA Second-Generation Long Terminal Repeat-Based Real-Time Reverse Transcriptase Polymerase Chain Reaction Test. *JAIDS Journal of Acquired Immune Deficiency Syndromes* **2007**, *45* (4), 380–388. https://doi.org/10.1097/QAI.0b013e3180640cf5.

(174) Dreier, J.; Störmer, M.; Kleesiek, K. Use of Bacteriophage MS2 as an Internal Control in Viral Reverse Transcription-PCR Assays. *Journal of Clinical Microbiology* **2005**, *43* (9), 4551–4557. https://doi.org/10.1128/JCM.43.9.4551-4557.2005.

(175) Suzuki, H.; Terada, T. Removal of Dodecyl Sulfate from Protein Solution. *Analytical Biochemistry* **1988**, *172* (1), 259–263. https://doi.org/10.1016/0003-2697(88)90440-X.

(176) Bercovici, M.; Lele, S. K.; Santiago, J. G. Open Source Simulation Tool for Electrophoretic Stacking, Focusing, and Separation. *Journal of Chromatography A* **2009**, *1216* (6), 1008–1018. https://doi.org/10.1016/j.chroma.2008.12.022.

(177) Stellwagen, N. C.; Stellwagen, E. Effect of the Matrix on DNA Electrophoretic Mobility. *J Chromatogr A* **2009**, *1216* (10), 1917–1929. https://doi.org/10.1016/j.chroma.2008.11.090.

(178) Lafleur, L. K.; Bishop, J. D.; Heiniger, E. K.; Gallagher, R. P.; Wheeler, M. D.; Kauffman, P.; Zhang, X.; Kline, E. C.; Buser, J. R.; Kumar, S.; Byrnes, S. A.; Vermeulen, N. M. J.; Scarr, N. K.; Belousov, Y.; Mahoney, W.; Toley, B. J.; Ladd, P. D.; Lutz, B. R.; Yager, P. A Rapid, Instrument-Free, Sample-to-Result Nucleic Acid Amplification Test. *Lab Chip* **2016**, *16* (19), 3777–3787. https://doi.org/10.1039/C6LC00677A.

(179) Byrnes, S. A.; Bishop, J. D.; Yager, P. Enabling Lateral Transport of Genomic DNA through Porous Membranes for Point-of-Care Applications. *Analytical Methods* **2017**, *9* (23), 3450–3463. https://doi.org/10.1039/C7AY00293A.

(180) Bhattacharyya, S.; Gopmandal, P. P.; Baier, T.; Hardt, S. Sample Dispersion in Isotachophoresis with Poiseuille Counterflow. *Physics of Fluids* **2013**, *25* (2), 022001. https://doi.org/10.1063/1.4789967.

(181) Garcia-Schwarz, G.; Bercovici, M.; Marshall, L. A.; Santiago, J. G. Sample Dispersion in Isotachophoresis. *Journal of Fluid Mechanics* **2011**, *679*, 455–475. https://doi.org/10.1017/jfm.2011.139.

(182) Lillis, L.; Lehman, D. A.; Siverson, J. B.; Weis, J.; Cantera, J.; Parker, M.; Piepenburg, O.; Overbaugh, J.; Boyle, D. S. Cross-Subtype Detection of HIV-1 Using Reverse Transcription and Recombinase Polymerase Amplification. *J. Virol. Methods* **2016**, *230*, 28–35. https://doi.org/10.1016/j.jviromet.2016.01.010.

(183) Pilcher, C. D.; Joaki, G.; Hoffman, I. F.; Martinson, F. E.; Mapanje, C.; Stewart, P. W.; Powers, K. A.; Galvin, S.; Chilongozi, D.; Gama, S.; Price, M. A.; Fiscus, S. A.; Cohen, M. S.; for the UNC Project, M. Amplified Transmission of HIV-1: Comparison of HIV-1 Concentrations in Semen and Blood during Acute and Chronic Infection. *AIDS* **2007**, *21* (13), 1723–1730. https://doi.org/10.1097/QAD.0b013e3281532c82.

(184) World Health Organization. *Consolidated Guidelines on the Use of Antiretroviral Drugs for Treating and Preventing HIV Infection: Recommendations for a Public Health Approach.*; 2016.

(185) Kloke, A.; Fiebach, A. R.; Zhang, S.; Drechsel, L.; Niekrawietz, S.; Hoehl, M. M.; Kneusel, R.; Panthel, K.; Steigert, J.; von Stetten, F.; Zengerle, R.; Paust, N. The LabTube – a Novel Microfluidic Platform for Assay Automation in Laboratory Centrifuges. *Lab on a Chip* **2014**, *14* (9), 1527. https://doi.org/10.1039/c3lc51261d.

(186) Connelly, J. T.; Rolland, J. P.; Whitesides, G. M. "Paper Machine" for Molecular Diagnostics. *Analytical Chemistry* **2015**, *87* (15), 7595–7601. https://doi.org/10.1021/acs.analchem.5b00411.

(187) Ferguson, T. M.; Weigel, K. M.; Lakey Becker, A.; Ontengco, D.; Narita, M.; Tolstorukov, I.; Doebler, R.; Cangelosi, G. A.; Niemz, A. Pilot Study of a Rapid and Minimally Instrumented Sputum Sample Preparation Method for Molecular Diagnosis of Tuberculosis. *Scientific Reports* **2016**, *6*, 19541. https://doi.org/10.1038/srep19541.

(188) Liu, C.; Mauk, M. G.; Hart, R.; Qiu, X.; Bau, H. H. A Self-Heating Cartridge for Molecular Diagnostics. *Lab Chip* **2011**, *11* (16), 2686–2692. https://doi.org/10.1039/C1LC20345B.

(189) Roskos, K.; Hickerson, A. I.; Lu, H.-W.; Ferguson, T. M.; Shinde, D. N.; Klaue, Y.; Niemz, A. Simple System for Isothermal DNA Amplification Coupled to Lateral Flow Detection. *PLOS ONE* **2013**, *8* (7), e69355. https://doi.org/10.1371/journal.pone.0069355.

(190) Rodriguez, N. M.; Wong, W. S.; Liu, L.; Dewar, R.; Klapperich, C. M. A Fully Integrated Paperfluidic Molecular Diagnostic Chip for the Extraction, Amplification, and Detection of Nucleic Acids from Clinical Samples. *Lab Chip* **2016**, *16* (4), 753–763. https://doi.org/10.1039/C5LC01392E.

(191) Lafleur, L. K.; Bishop, J. D.; Heiniger, E. K.; Gallagher, R. P.; Wheeler, M. D.; Kauffman, P.; Zhang, X.; Kline, E. C.; Buser, J. R.; Kumar, S.; Byrnes, S. A.; Vermeulen, N. M. J.; Scarr, N. K.; Belousov, Y.; Mahoney, W.; Toley, B. J.; Ladd, P. D.; Lutz, B. R.; Yager, P. A Rapid, Instrument-Free, Sample-to-Result Nucleic Acid Amplification Test. *Lab Chip* **2016**, *16* (19), 3777–3787. https://doi.org/10.1039/C6LC00677A.

(192) Borysiak, M. D.; Kimura, K. W.; Posner, J. D. NAIL: Nucleic Acid Detection Using Isotachophoresis and Loop-Mediated Isothermal Amplification. *Lab Chip* **2015**, *15* (7), 1697–1707. https://doi.org/10.1039/C4LC01479K.

(193) Eid, C.; Santiago, J. G. Assay for Listeria Monocytogenes Cells in Whole Blood Using Isotachophoresis and Recombinase Polymerase Amplification. *The Analyst* **2017**, *142* (1), 48–54. https://doi.org/10.1039/C6AN02119K.

(194) Boyle, D. S.; Lehman, D. A.; Lillis, L.; Peterson, D.; Singhal, M.; Armes, N.; Parker, M.; Piepenburg, O.; Overbaugh, J. Rapid Detection of HIV-1 Proviral DNA for Early Infant Diagnosis Using Recombinase Polymerase Amplification. *MBio* **2013**, *4* (2). https://doi.org/10.1128/mBio.00135-13.

(195) Tholen, D. W. *Protocols for Determination of Limits of Detection and Limits of Quantitation: Approved Guideline*; NCCLS: Wayne, Pa., 2004.

(196) Borysiak, M. D.; Thompson, M. J.; Posner, J. D. Translating Diagnostic Assays from the Laboratory to the Clinic: Analytical and Clinical Metrics for Device Development and Evaluation. *Lab Chip* **2016**, *16* (8), 1293–1313. https://doi.org/10.1039/C6LC00015K.

(197) Khurana, T. K.; Santiago, J. G. Effects of Carbon Dioxide on Peak Mode Isotachophoresis: Simultaneous Preconcentration and Separation. *Lab on a Chip* **2009**, *9* (10), 1377. https://doi.org/10.1039/b815460k.

(198) Ritchie, A. V.; Ushiro-Lumb, I.; Edemaga, D.; Joshi, H. A.; De Ruiter, A.; Szumilin, E.; Jendrulek, I.; McGuire, M.; Goel, N.; Sharma, P. I.; Allain, J.-P.; Lee, H. H. SAMBA HIV Semiquantitative Test, a New Point-of-Care Viral-Load-Monitoring Assay for Resource-Limited Settings. *Journal of Clinical Microbiology* **2014**, *52* (9), 3377–3383. https://doi.org/10.1128/JCM.00593-14.

(199) Kersting, S.; Rausch, V.; Bier, F. F.; von Nickisch-Rosenegk, M. Rapid Detection of Plasmodium Falciparum with Isothermal Recombinase Polymerase Amplification and Lateral Flow Analysis. *Malaria journal* **2014**, *13* (1), 99.

(200) Pawlotsky, J.-M. Molecular Diagnosis of Viral Hepatitis. *Gastroenterology* **2002**, *122* (6), 1554–1568. https://doi.org/10.1053/gast.2002.33428.

(201) Krajden, M.; McNabb, G.; Petric, M. The Laboratory Diagnosis of Hepatitis B Virus. *Can J Infect Dis Med Microbiol* **2005**, *16* (2), 65–72.